# Neural and Behavioural Mechanisms of Olfactory Matching

विद्या वाचस्पति की उपाधि की अपेक्षाओं की आंशिक पूरर्त में परस्तुत शोध परबंध

A thesis submitted in partial fulfillment of the requirements of the degree of Doctor of Philosophy

वारा / By राजदीप भौमिक / Rajdeep Bhowmik

पंजीकरण सं. / Registration No. 20172007 शोध परबंध पर्रवेक्षक / Thesis Supervisor

निक्सन एम. अब्राहम / Nixon M. Abraham



भारतीय विज्ञान शिक्षा एवं अनुसंधान संस्थान पुणे INDIAN INSTITUTE OF SCIENCE EDUCATION AND RESEARCH PUNE

#### CERTIFICATE

Certified that the work incorporated in the thesis entitled 'Neural and Behavioural Mechanisms of Olfactory Matching', submitted by Rajdeep Bhowmik, was carried out by the candidate, under my supervision. The work presented here or any part of it has not been included in any other thesis submitted previously for the award of any degree or diploma from any other University or institution.

(Dr. Nixon M. Abraham)

Date:08/04/2025

#### **Declaration by Student**

Name of Student: Rajdeep Bhowmik

Reg. No.: 20172007

Thesis Supervisor(s): Dr. Nixon M. Abraham

Department: Biology

Date of joining program: August 2017

Date of Pre-Synopsis Seminar: 26th September 2024

Title of Thesis: Neural and Behavioural Mechanisms of Olfactory Matching

I declare that this written submission represents my idea in my own words and where others' ideas have been included; I have adequately cited and referenced the original sources. I declare that I have acknowledged collaborative work and discussions wherever such work has been included. I also declare that I have adhered to all principles of academic honesty and integrity and have not misrepresented or fabricated or falsified any idea/data/fact/source in my submission. I understand that violation of the above will be cause for disciplinary action by the Institute and can also evoke penal action from the sources which have thus not been properly cited or from whom proper permission has not been taken when needed.

The work reported in this thesis is the original work done by me under the guidance of

Nixon M. Abraham Dr./Prof.\_\_\_ 08/04/2025

Righer Bharmile

Date:

Signature of the student (Rajdeep Bhowmik)

# Table of contents

Abstract		I	
Synopsis		III	
Acknowledg	ements	IX	
Chapter 1 In	troduction	1	
1.1.	Introduction to working memory	2	
1.2.	Components of working memory across		
	sensory modalities	4 7	
1.3.	Molecular correlates of working memory		
1.4.	A brief introduction to olfactory working memory	9	
1.5.	A brief introduction to the mammalian olfactory system	10	
1.6.	Probing olfaction: Past and Present	13	
1.7.	Neural basis of working memory	15	
1.8.	Attentional control and working memory	17	
1.9.	Evolution of working memory: the emergence	18	
1.10.	of cognitive trade-off Working memory impairment and disease	10	
1.10.	: A special look at olfaction	20	
Chapter 2 M	1aterials and Methods		
Chapter 2 P	iateriats and Methods		
2.1.	Olfactory matching paradigm in humans	22	
	2.1.1. Study Population	22	
	2.1.2. Inclusion and exclusion criteria	22	
	2.1.3. Ethics committee guidelines	22	
	2.1.4. Study location	22	
	2.1.5. Olfactory detection task	23	
	2.1.6. Olfactory Matching Paradigm	23	
	2.1.7. Simple odor matching task	23	
	2.1.8. Complex Odor matching		
	2.1.8.1. 60-40 binary mixtures	24	
	2.1.8.2. 80-20 binary mixtures	24	
	2.1.9. Apparatus	o :	
2.2	2.1.9.1. Olfactory-action meter	24	
2.2.	Odors used in the experiment	00	
0.0	2.2.1. Odor Preparation	26	
2.3.	Modified olfactory-action meter for probing cognitive	28	
	health in patients		

	2.3.2.	2.3.2. Detection task				
	2.3.3.	. Odor matching task				
	2.3.4.	Olfactory	learning across sessions	31		
2.4.	Olfactory behaviour in mice					
	2.4.1.	Olfactory	behavioural training using odor			
		matching paradigm		31		
	2.4.2.	Behaviou	ral training in freely moving mice			
		2.4.2.1.	Apparatus	32		
		2.4.2.2.	Habituation and pre-training	32		
		2.4.2.3.	Training with olfactory matching paradigm	33		
	2.4.3.	Measurer	nent of behavioural parameters	34		
		2.4.3.1.	Learning curve	34		
		2.4.3.2.	Sample pattern	34		
		2.4.3.3.	Lick pattern	35		
		2.4.3.4.	Olfactory matching time (OMT)	35		
2.5.	Gener	ation of co	nditional knockout mice	36		
	2.5.1. Confirmation of stereotactic coordinates					
		using fluo	rescent dye	36		
	2.5.2.	Surgical ir	njection of Cre-viral particles	37		
	2.5.3.	Habituati	on and pre-training	37		
	2.5.4.	Measurer	nent of olfactory matching time	38		
	2.5.5.	Immunoh	istochemistry	38		
	2.5.6.	Protein es	stimation	39		
Chapter 3 Ur	ncertain	ity revealed	d by delayed responses during olfactory matc	hing		
3.1. Intro	oductio	n		41		
3.2. Mat	erials a	nd method	S	43		
	3.2.1.	Chemicals	s used in the experiment	43		
	3.2.2.	Study Pop	ulation	43		
	3.2.3. Inclusion and Exclusion Criteria					
	3.2.4. Ethics Committee Guidelines					
	3.2.5. Study Location					
	3.2.6. Odor Preparation					
	3.2.7.	Complex	odor matching task			
		3.2.7.1.6	0-40 binary mixtures	45		
		3.2.7.2.8	0-20 binary mixtures	45		
	3.2.8.	Olfactory-	Action meter	45		
	3.2.9.	Olfactory	detection task	46		
	3.2.10	). Olfactory	Matching Paradigm	46		
		3.2.10.1.	Simple odor matching task	47		

28

2.3.1. Apparatus

3.2.10.2. Complex Odor matching	47		
3.2.11. Detectability index calculation	48		
3.2.12. Calculation of chance level	48		
3.2.13. Data and statistical analysis	49		
3.3. Results			
3.3.1. Development of the Olfactory-action			
meter for assessing the sensory and cognitive			
behavioural correlates in humans	49		
3.3.2. Faster response time correlates to more			
accurate matching performance	53		
3.3.3. Matching accuracy declines for complex			
odor matching	56		
3.4. Discussion	59		
Chapter 4 Persistent neurocognitive deficits during and post-SARS CoV-	-2 infection		
4.1 latraduction	00		
4.1. Introduction	63		
4.2. Materials and Methods	65		
4.2.1. Study population	66		
4.2.2. Inclusion/Exclusion criteria	67		
4.2.3. Sample size calculation	69		
4.2.4. Ethics committee approval information	69		
4.2.5. Study location	69		
4.2.6. Design of the Olfactory-action meter	70		
4.2.7. Odors	71		
4.2.8. Paradigm of Olfactory function test	71		
4.2.9. Olfactory detectability measurement	71		
4.2.10. Measurement of Olfactory function score	73		
4.2.11. Statistical analyses	73		
4.3. Results	74		
4.3.1. Symptomatic patients of COVID-19 show	7.4		
impaired odor detection	74		
4.3.2. Symptomatic patients and recovered participants			
of COVID-19 infection show impaired olfactory learning	79		
4.3.3. Symptomatic COVID-19 patients show			
significantly less severe olfactory impairment in			
comparison to asymptomatic carriers	81		
4.3.4. Confounding variables do not affect the			
experimental parameters	83		
4.4. Discussion	85		

# **Chapter 5** Bidirectional modulation of E/I balance in the olfactory bulb regulates olfactory working memory

5.1. Introduction		
5.2. Materials and methods		
5.2.1. Olfactory matching paradigm		
in freely moving mice	91	
5.2.2. Apparatus	92	
5.2.3. Habituation and pre-training	93	
5.2.4. Olfactory matching paradigm	93	
5.2.5. Measurement of behavioural parameters		
5.2.5.1. Learning curve	94	
5.2.5.2. Sample pattern	94	
5.2.5.3. Lick pattern	94	
5.2.5.4. Calculation of		
Olfactory matching time (OMT)	95	
5.2.6. Generation of conditional knockout mice	95	
5.2.7. Habituation and pre-training	95	
5.2.8. Immunohistochemistry	95	
5.2.9. Protein level quantification	95	
5.3. Results		
5.3.1. Mice learn to perform odor matching		
with high delay periods	96	
5.3.2. Odor matching activity undergoes refinement		
with progression of training	98	
5.3.3. Increased inhibition on projection neurons in		
mouse olfactory bulb improves odor matching	101	
5.3.4. Decreased inhibition on projection neurons in		
mouse olfactory bulb improves odor matching	103	
5.4. Discussion	105	
References	108	
General Discussion		
List of Publications		

#### Abstract

Matching sensory stimuli involves different decision processes such as detection and discrimination, along with holding the perceived information. Therefore, it provides a combined readout of sensory and cognitive fitness. In the context of increasing reports of brain disorders where olfactory system's functions are hampered, establishing precise methods for quantifying olfactory fitness has become an emerging need. We have developed a novel olfactory matching paradigm to probe sensory and cognitive functions involving olfactory system, using an automated custom-built olfactory-action meter. In over 300 healthy subjects, with a mean detection accuracy of around 90%, we observed significantly better olfactory matching performance for simple odors, in comparison to complex odor mixtures. Olfactory matching accuracy remained unaltered across varying inter-stimulus intervals. However, the olfactory matching time shown by the subjects for correct responses was significantly lower than the incorrect responses. We further studied symptomatic COVID-19 patients' behavioural readouts, and found olfactory and cognitive deficits. These deficits were shown to be persistent in certain subjects even after the recovery.2 To investigate the neural mechanisms of olfactory matching, we performed a delayed odor matching task in freely-moving mice. We gradually increased the stimulus delay from 2s up to 52s by training the same batch of animals for many weeks. With the gradual increase in delay period, mice successfully performed odor matching tasks with high accuracy even for long stimulus delays, on extensive training. As after-odor representation in the olfactory bulb (OB) controls olfactory memory (unpublished data from the lab), we studied the role of OB circuits in modulating olfactory working memory. The inhibitory interneurons of OB directly modulate the activity of projection neurons, mitral and tufted cells, and refine the output from OB. Using conditional knockout mouse lines of GluA2 (AMPA receptor subunit), and NR1 (NMDA receptor subunit), we generated granule cell layer-specific (inhibitory interneurons) knockouts (KOs) by delivering Cre through the viral vectors. Knocking out the GluA2 subunit of AMPA receptors on inhibitory interneurons can enhance the inhibition on projection neurons. Conversely, the deletion of NR1 subunit renders NMDA receptors non-functional, resulting in reduced inhibition on the projection neurons.3 As these two groups were trained for three different stimulus delays with their respective control groups, GluA2 KO mice showed significantly improved performance in comparison to control mice, whereas the NR1 KO group exhibited a slower learning pace compared to control animals. These results indicate the potential role of OB inhibitory circuits in modulating olfactory matching readouts, where working memory is involved.

- 1. R. Bhowmik et al., Uncertainty revealed by delayed responses during olfactory matching. bioRxiv, 2022.2009.2011.507462 (2022).
- 2. R. Bhowmik et al., Persistent olfactory learning deficits during and post-COVID-19 infection. Curr Res Neurobiol 4, 100081 (2023).
- 3. N. M. Abraham et al., Synaptic Inhibition in the Olfactory Bulb Accelerates Odor Discrimination in Mice. Neuron 65, 399-411 (2010).

#### Synopsis

Sensation and perception play a critical role in the survival, foraging, and mating across most species in the animal kingdom. Recognizing a predatory cue in a lightning-quick sniff or being able to identify a novel odor that might provide an alternative food source, may decide life or death in the wild. Animals, including humans, have relied on sensory and associated memory systems for time immemorial, paving the path for the evolution of highly specialized and complex neurocognitive systems. For our daily activities, we heavily rely on a kind of memory system that does not need to hold too much information for too long. Such capacity limited system that holds small amount of information while allowing the ability to manipulate sensory data based on knowledge and past experiences, forms the basis of working memory.

The flourishing advent of memory research that started with the studying of patient H.M.<sup>3</sup>, opened new doors for neuroscience and the understanding of information storage in the brain. H.M., who had undergone a bilateral medial temporal lobectomy, was comfortable holding information for short periods of time while completely incapable of forming long-term memories. This along with other provocative cases like patient K.F.,<sup>4</sup> who had almost the opposite behavioural phenotype that of patient H.M., shifted the scientific perspective from a unitary long-term memory (LTM) system to being composed of two distinctly separate ones.

There were abundance of doubt and misconceptions, very characteristic of emerging scientific fields, regarding how this new kind of memory system stores information, what purpose does it serve, if and how does it interact with LTM and so on. Soon, in 1974, Baddeley and Hitch proposed that this memory system is not only able to store information temporarily but can, in conjunction with other cognitive components of the brain, process and manipulate it. They popularized the term working memory (WM) to identify this memory system. In their three-component model, Baddeley and Hitch, hypothesized three distinct components namely the phonological loop, the visuospatial sketchpad and the central executive. As the names of the components themselves are sufficiently suggestive, the phonological loop is primarily concerned with semantic

understanding<sup>6</sup> and the visuospatial sketchpad helps in formation and willful alteration of mental imagery, planning as well as processing spatial and textural information.<sup>7</sup> The central executive, on the other hand, was thought to be tasked with managing and coordinating between these two sub-systems providing attentional supervision.

Meanwhile, attempts have been made to find neural correlates of working memory with occasional success.<sup>8</sup> But how LTM and WM interact has remained largely unclear. To accommodate a mediator between these two-memory system, Baddeley introduced a fourth component to the existing model, namely the episodic buffer.<sup>9</sup> This component was proposed to be actively involved in the buffering short- and long-term stores.

Over the years, a systems level understanding of WM had started to take shape. Discovery of persistent firing of neurons that are thought to sustain transient memory traces<sup>10</sup> to cortical areas actively involved working memory-related task has greatly consolidated our understanding of the phenomena.<sup>11,12</sup> But for various reasons, some sensory modalities were studied much more frequently than others. The sensory modality of olfaction is of the latter kind. Moreover, the unique anatomical and functional complexities of different sensory systems provide enough modality-specific specialization to essentially prevent generalization beyond a certain level.<sup>13</sup> Neural correlates of olfactory working memory (OWM), therefore, remain largely unknown.

Recent years have tragically highlighted the importance of olfaction and related cognitive functioning. <sup>14,15</sup> Not too long ago, the COVID-19 pandemic that brought the world to a stand-still, symptomatically manifested itself largely through sensory loss of smell. <sup>16</sup> Probing olfactory fitness has been shown to sieve out even asymptomatic COVID-19 carriers with high precision. <sup>17</sup> Long-known are reports of olfactory loss predating neurodegenerative conditions like Parkinson's and Alzheimer's. <sup>18–20</sup> OWM-related task has been shown to identify persistent neurocognitive deficit in recovered COVID-19 patients as well. <sup>21</sup> Therefore, under the light of recent research and emerging diagnostic potential in the context of neurocognitive well-being, investigating neural correlates of OWM withhold great potential, both scientifically and clinically.

In the subsequent chapters, we delve into investigating OWM in healthy humans and under diseased conditions. We employed a delayed matching task, termed Olfactory Matching (OM), using a custom-built olfactory-action meter (OAM) that had been modified as the situations had necessitated. Each trial in the OM task involved delivering one odor stimulus to the nostrils of the participant followed by an interval. Once the interval is over, a second odor stimulus is delivered to the subject and the subject had to match the two stimuli, i.e., whether the two stimuli were same or different. For carrying out the OM task, we employed a pseudorandomized automated odor delivery system using our custom-built OAM that could deliver odorized air with high temporal precision to the nostrils of the participants without any interference from the experimenter. We employed separate cohorts of subjects performing simple (monomolecular) odor matching and matching of binary odor mixtures. Healthy participants performed a session of 20 odor matching trials in one session, upon which their matching accuracy and reaction times were recorded. The delay period was varied across sessions, 2.5s, 5s, 7.5s and 10s for simple OM task and 5s and 10s for complex OM task, but was kept constant during one session.

A total of 180 subjects participated in the simple OM task whereas 107 participants were part of the complex odor matching task. Our findings show that the odor matching performance significantly declined with increase in odor complexity. The effect of stimulus complexity on OM performance was also evident when odor matching time (OMT), i.e., reaction times recorded for each trial, was seen to be significantly higher for complex OM in comparison to matching of simple odors. Our analysis also revealed an interesting positive correlation between faster decisions and accuracy.<sup>22</sup>

With the outbreak of COVID-19, we further employed a modified version of the OAM in probing olfactory-based neurocognitive fitness in symptomatic COVID-19 patients. Our findings show striking loss of olfactory detectability and matching performance in comparison to healthy controls. We also had symptomatic, healthy and recovered subjects perform odor detection and consecutive matching task that spanned up to five days. Our results revealed persistent olfactory learning deficit in recovered subjects at least 12 weeks since recovery while their odor detectability was comparable to controls.<sup>21</sup>

To investigate the neural correlates of OWM, we optimized the delayed matching paradigm for freely moving mice. To probe the odor memory capacity, we initially trained mice with 2s delay and once trained, gradually increased the delay to up to 52s. Our data show that mice can learn to perform with high accuracy for long delays, however, confounding effects of prolonged training period cannot be undermined.

Interestingly, most of our existing understanding of OWM involves higher cortical areas, whereas, the role of pre-cortical circuit, especially the olfactory bulb remains elusive. We therefore decided to perturb the excitation-inhibition balance of the OB via conditional KOs and observe how it affects OWM performance. Based on previously published work<sup>23</sup>, we generated GluA2 KO and NR1KO GCL-specific KO animals. GluA2 and NR1 are subunits of AMPA and NMDA receptors respectively. GluA2 KO AMPA receptors, being more permeable to Ca<sup>2+</sup> ions<sup>24</sup>, impart increased inhibition on the projection neurons, namely the mitral and tufted (M/T) cells. Whereas NR1 KO would in turn limit cation entry<sup>25</sup> in the granule cells, thereby, decreasing inhibition on the M/T cells.<sup>23,26</sup> As we trained the two group of KO animals with their respective sham group, GluA2 KO group showed significantly faster learning in comparison to the sham animals. Whereas, the NR1KO mice show significantly slower learning. Our findings thus highlights interesting role the E/I balance plays at the level of olfactory bulb that can directly affect OWM performance.

Our findings, thus, demonstrate that performance in odor matching tasks is sensitive to odor complexity in healthy humans and faster matching times correlate with higher accuracy. Moreover, OM tasks showed great potential in probing long-term neurocognitive deficits in COVID-19 patients. This opens a promising avenue for potential therapeutic applications. Apart from these, alluring findings with the animals studies underline the crucial roles of E/I balance at the pre-cortical level in modulating odor matching performance. Our work as a whole shows great promise for dissecting neural underpinnings of OWM and, at the same time, serve important diagnostic applications.

#### References

- 1. Thomas-Danguin, T. *et al.* The perception of odor objects in everyday life: a review on the processing of odor mixtures. *Front Psychol* **5**, (2014).
- 2. Baddeley, A. Working memory: Looking back and looking forward. *Nat Rev Neurosci* **4**, 829–839 (2003).
- 3. Milner, B. Amnesia following operation on the temporal lobes. in *Amnesia* (eds. Whitty, C. W. M. & Zangwill, O. L.) (London: Butterworth, 1966).
- 4. Shallice, T. & Warrington, E. K. Independent Functioning of Verbal Memory Stores: A Neuropsychological Study. *Quarterly Journal of Experimental Psychology* **22**, 261–273 (1970).
- 5. Baddeley, A. D. & Hitch, G. Working Memory. in *Psychology of Learning and Motivation* (ed. Bower, G. H.) vol. 8 47–89 (Academic Press, 1974).
- 6. Vallar, G. & Baddeley, A. Phonological short-term store and sentence processing. *Cogn Neuropsychol* **4**, 417–438 (1987).
- 7. Logie, R. H. *Visuo-Spatial Working Memory*. (Hove, East Sussex; Hillsdale [N.J.]: L. Erlbaum Associates, 1995).
- 8. Goldman-Rakic, P. S. Architecture of the Prefrontal Cortex and the Central Executive. *Ann N Y Acad Sci* **769**, 71–84 (1995).
- 9. Baddeley, A. The episodic buffer: a new component of working memory? *Trends Cogn Sci* **4**, 417–423 (2000).
- 10. Curtis, C. E. & D'Esposito, M. Persistent activity in the prefrontal cortex during working memory. *Trends in Cognitive Sciences* vol. 7 415–423 Preprint at https://doi.org/10.1016/S1364-6613(03)00197-9 (2003).
- 11. Zhang, X. *et al.* Active information maintenance in working memory by a sensory cortex. *Elife* **8**, (2019).
- 12. Yang, A. I. *et al.* The what and when of olfactory working memory in humans. *Current Biology* **31**, 4499-4511.e8 (2021).
- 13. Mori, K. & Sakano, H. Olfactory Circuitry and Behavioral Decisions. *Annu Rev Physiol* **83**, 231–256 (2021).
- 14. Ponsen, M. M. *et al.* Idiopathic hyposmia as a preclinical sign of Parkinson's disease. *Ann Neurol* **56**, 173–181 (2004).
- 15. Rebholz, H. *et al.* Loss of Olfactory Function—Early Indicator for Covid-19, Other Viral Infections and Neurodegenerative Disorders. *Frontiers in Neurology* vol. 11 Preprint at https://doi.org/10.3389/fneur.2020.569333 (2020).
- 16. Gerkin, R. C. *et al.* Recent smell loss is the best predictor of COVID-19 among individuals with recent respiratory symptoms. (2020).
- 17. Bhattacharjee, A. S., Joshi, S. V., Naik, S., Sangle, S. & Abraham, N. M. Quantitative assessment of olfactory dysfunction accurately detects asymptomatic COVID-19 carriers. *EClinicalMedicine* **28**, 100575 (2020).
- 18. Doty, R. L. Olfactory dysfunction in Parkinson disease. *Nat Rev Neurol* **8**, 329–339 (2012).
- 19. Djordjevic, J., Jones-Gotman, M., De Sousa, K. & Chertkow, H. Olfaction in patients with mild cognitive impairment and Alzheimer's disease. *Neurobiol Aging* **29**, 693–706 (2008).

- 20. Pandey, S., Bapat, V., Abraham, J. N. & Abraham, N. M. Long COVID: From olfactory dysfunctions to viral Parkinsonism. *World J Otorhinolaryngol Head Neck Surg* (2024) doi:10.1002/wjo2.175.
- 21. Bhowmik, R. *et al.* Persistent olfactory learning deficits during and post-COVID-19 infection. *Current Research in Neurobiology* **4**, 100081 (2023).
- 22. Bhowmik, R. *et al.* Uncertainty revealed by delayed responses during olfactory matching. *bioRxiv* 2022.09.11.507462 (2022) doi:10.1101/2022.09.11.507462.
- 23. Abraham, N. M. *et al.* Synaptic Inhibition in the Olfactory Bulb Accelerates Odor Discrimination in Mice. *Neuron* **65**, 399–411 (2010).
- 24. Cull-Candy, S., Brickley, S. & Farrant, M. NMDA receptor subunits: diversity, development and disease. *Curr Opin Neurobiol* **11**, 327–335 (2001).
- 25. Cui, Z. *et al.* Inducible and Reversible NR1 Knockout Reveals Crucial Role of the NMDA Receptor in Preserving Remote Memories in the Brain. *Neuron* **41**, 781–793 (2004).
- 26. Gschwend, O. *et al.* Neuronal pattern separation in the olfactory bulb improves odor discrimination learning. *Nat Neurosci* **18**, 1474–1482 (2015).

# Acknowledgements

I would like to express my gratitude to all those who have supported me throughout my PhD journey. Firstly, I would like to sincerely thank my supervisor, Dr. Nixon M. Abraham, for his scientific guidance, mentorship and encouragement all these years. His deep knowledge, constructive criticism and patient guidance have been pivotal in completing my thesis and in shaping me as a researcher.

I would like to thank my RAC members, Prof. Aurnab Ghose, Dr. Raghav Rajan and Prof. Girish Ratnaparkhi for their timely guidance in the annual meetings.

I would like to thank LNCB lab members both past and present. Special thanks to Anindya, Sarang and Meenakshi for helping me during the initial years of my PhD. I would also like to pay my respects to Late Sasank Konakamchi. He was a good mentor.

I would like to thank my parents, Ratul Bhowmik and Dipu Deb, for being my strength throughout my doctoral studies as well as life. I would like to thank my sisters Titli and Tip who have been a constant source of comfort and joy. I feel gifted to have Deep and Shouvik as my friends without whom life would not have made sense. I thank Vandana for her companionship, understanding and shared laughter. I lost a great friend with the untimely passing of Ashish. He lives on in my memory. I am indebted to Somya for being there all these the years as a sincere friend and helping me out with several experimental hurdles.

There are several other faculty members who have made my PhD years fulfilling. I would like to thank Suhita and Collins for all the warmth, Nishad for all the musical moments, Prof. Subhedar who never fell short of encouraging me and Satyajit for giving me a glimpse of what exceptional mentoring looks like. I would like to thank IISER Pune Animal House facility, the Academic Office (especially Sayalee and Swapnil), Microscopy facility (Santosh and Vijay), the housekeeping staff (especially Somnath) and all the security personnel who made life at IISER Pune enthralling. Finally, I thank IISER Pune and CSIR for funding.

# Chapter 1

#### Introduction

Memory is an essential component of our survival. Nothing, from multicellular organisms evading predatory cues to the evolution of highly complex life forms to the continuing saga of human civilization, would have been possible without retaining and preservation of sensory information. Some would argue that the reason we, and many other organisms, perceive time is because of memory. Without memory, there is no time. 1 Now, one may ask how fundamental memory systems for a species are. Is it possible to be conscious without memory? Some say, it might be.<sup>2</sup> So, what is memory? On a rudimentary level, memory is nothing but storage of information that can be retrieved as and when needed.<sup>3</sup> But why is it mentioned as a system? The trick (or maybe trouble) with biological phenomena is that (almost) nothing comes in an isolated form, like a one-off incident controlled by one particular molecule, gene or cells for that matter. Storing information by itself hardly serves any purpose unless there is an accompanying mechanism for rapid, virtually instantaneous, retrieval. One way to tackle this mutual inclusivity of two different components of a memory system is to directly link physiological or cellular responses of an organism to its environmental stimuli.<sup>4</sup> Also, for organisms that can be classified as simpler in traditional sense, memory systems need to enhance survivability by aiding in avoiding predators. But as such systems evolve into more complex multi-component phenomena, this no longer remains limited to only evading predatory cues.<sup>5</sup>

Most things we are capable as humans are either made possible or somehow enhanced by the presence of an extremely well-developed memory system. To broadly classify, but not claiming to be universal, the memory systems are categorized primarily based on how long the information can be stored. This approach has led to two different memory systems, namely, short-term and long-term memory. As the names make it obvious, short-term memory (STM) systems allow information storage only for short amount of time, usually tens of seconds, whereas long-term memory system allows for storage of memories indefinitely, often months or years. Given that both the memory systems are concerned with storing information, short term memory has been, mistakenly, thought of as a subsystem of long-term memory. But emerging studies in

the recent decades had implicated a much more diffused systemic arrangement with distinct mechanisms exclusive to STM.8 Everyday life hardly runs exclusively on any of these sub-systems. Rather, a sophisticated, rapid and probabilistic mechanism<sup>9,10</sup> that takes in sensory information, stores it temporarily and allows mental manipulation based on the interplay among episodic long-term store, reasoning and imagination allows for the complex and multidimensional daily functioning.<sup>11</sup> We term this system as working memory.

Historically, a plethora of paradigms have been employed to investigate various aspects of working memory. 12,13 The age-old delayed match to sample involved matching two stimuli, presented one after the other, usually with an interval. 14-16 This paradigm has been greatly successful across animal species and sensory modalities. Cognitive neuroscientists have also employed relatively simpler tasks like n-back tasks to often quantify working memory capacity. Unlike DMS task, the subject needs to match a stimuli with one presented 'n' steps earlier. 16 Due to its ease of execution and inexpensive experimental setup, this paradigm has been greatly popular for human cognitive experiments including many fMRI studies. 17,18 For rodents and flies, particularly, Radial maze, T-maze or Y-maze alternation tasks has been heavily relied upon over the years. 19-21 Training the animals to alternate between maze-arms on successive trials, mostly under the pretext of a reward, researchers could probe phenomena like working memory and navigation. Sternberg task offers another variation to the n-back task where participants need to decide whether a probe item (or stimuli) is part of a short list of items (stimuli) presented before. <sup>22,23</sup> A recent variation of this task in the context of the olfactory sensory modality, comes the odor span task where the animals are required identify novel odor among previously encountered odorants across the training session.<sup>24</sup> Of these array of various paradigms, DMS tasks has proven to be one of the most useful and widely used paradigms when it comes to investigating neural mechanisms of working memory.<sup>25</sup>

#### 1.1. Introduction to working memory

In the simplest of terms, working memory (WM), is often defined as an allencompassing cognitive process that involves STM and its (mental) manipulation of information in order to perform both trivial and complex cognitive tasks.<sup>26</sup> Perhaps the most relatable example of WM in today's life would be memorizing a one-time-password for a bank transaction for a couple of seconds, only to be oblivious of it a few minutes later. As mentioned, WM possesses in its definition the concept of manipulation of information.<sup>27</sup> This distinguishes the phenomena from STM, which is primarily characterized by and limited to temporary storage of information. Now the concept of information storage and retrieval is complemented with complex criterion of processing.

Conceptual evolution regarding non-unitary form of memory systems started to take shape in the early 1960s when several clinical studies indicated different types of memory architecture in place.<sup>26</sup> One of the pioneering studies came from the patient Henry Molaison (Patient H.M.).<sup>28</sup> Henry had undergone a bilateral medial temporal lobectomy, following which he was unable to form new memories. And yet, he had virtually no problem in remembering information for short periods of time. Milner's pioneering research is sometimes regarded as the most convincing evidence for the dichotomy of two largely independent memory systems.<sup>26</sup> This received further reinforcement, when another study reported a case where the opposite set of systems were affected in stark contrast to Patient H.M. In this case study, Shallice and Warrington (1970), reported a patient (K.F.), with 'profound repetition defect' (neurologically termed as conduction aphasia).<sup>29</sup> The patient showed a digit, and a letter span no more than two items while his performance in long-term memory tests remained indistinguishable than controls. This landmark study coupled with several other findings<sup>30</sup>, many of which were clinical case studies of classic amnesic syndrome, outlined one of the most widely accepted views of memory today. The current idea of memory system divides it broadly into two categories, namely the long-term memory (LTM) and short-term memory (STM), as mentioned earlier.

One of the most influential models of the late 1960s, proposed by Atkinsons and Shiffrin (1968)<sup>31</sup>, assumed flow of information from the sensory stimuli to a temporary, capacity-limited short-term store (Figure 1.1). A subset of this information was further stored for longer period in LTM. And what would make the cut for LTM would be determined by the depth of processing, as proposed by Craik and Lockhart (1972).<sup>32</sup>

The proposal was quite intuitive in the sense that information that was better contextualized and connected to existing knowledge had a much better chance of retention. Despite patients strongly reported a dissociation between LTM and STM, Atkinsons and Shiffrin's model assumed STM to be essential for long-term learning. <sup>26</sup> In an attempt to resolve this conflict, a series of experiments conducted by Baddeley and Hitch suggested the independent and yet inter-twined nature of STM and LTM. <sup>27</sup> Though the idea of a memory system, termed as working memory, that helps in 'execution of plans' had been aired much earlier<sup>33</sup>, it lacked any substantial theoretical footing for over a decade. In 1974, Baddeley and Hitch replaced the idea of a solitary system of STM with a model of working memory that comprised of a complex, multi-component functional unit of cognitive processing and storage. <sup>27</sup>

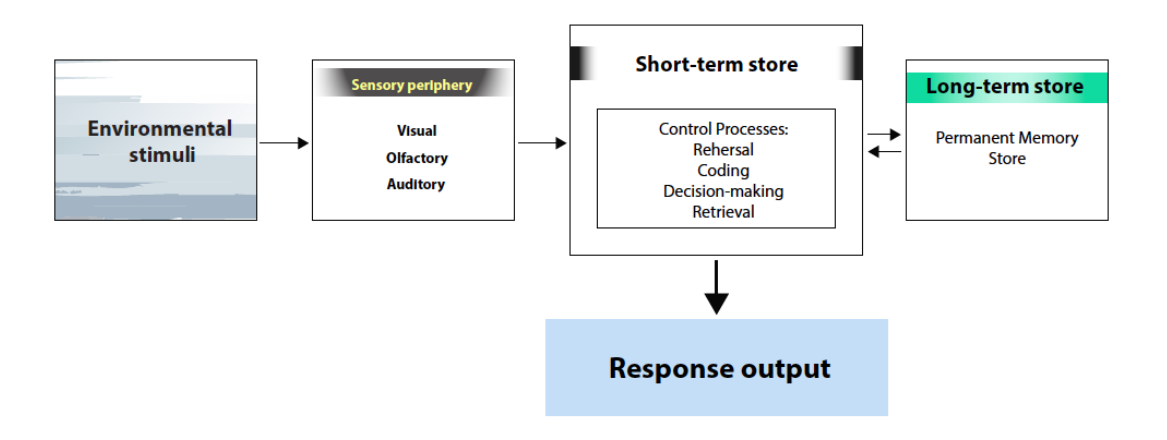


Figure 1.1. The model of human memory proposed by Atkinson & Shiffrin (1968). (Adapted and modified from The Psychology of Memory by A. Baddeley, 2002)

#### 1.2. Components of working memory across sensory modalities

The model proposed by Baddeley and Hitch, had three functional units: the Central Executive, the Visuo-spatial sketchpad and the Phonological loop (Figure 1.2). The central executive is thought of as a center of attentional supervision of cognitive processes involving short-term memory.<sup>27</sup> This component of WM has also been thought to have selective attentional control over perceptual information. The visuo-spatial sketchpad had been thought of to be able to store and manipulate information regarding visual and spatial cues.<sup>34</sup> It helps in retention and manipulation of essential

visual and spatial information including physical features like size, shape, texture, movement etc. <sup>27</sup> It has also been proposed to play a crucial role in planning movement and serve as a rehearsal phase for visual enactment. <sup>34</sup> The phonological loop exists as a separate sub-system that was characterized by a sub-vocal rehearsal phase coupled with a limited information storage capacity. <sup>35</sup> The latter two sub-systems acted mostly as subordinate components under the supervisory activity of the former. The phonological loop relied on verbal auditory stimuli or internally generated codes for non-auditory stimuli. <sup>36</sup> Information in the store largely depleted over a few seconds if not rehearsed. <sup>37</sup> These three components interacted in a manner that allowed a complex and often iterative interaction with the environment.



Figure 1.2. The Baddeley and Hitch Model of Working memory (1974).

Until this point, the field of working memory still lacked a significant breakthrough in terms empirical evidence concerning the proposed sub-systems. One of the first breakthroughs came in 1984<sup>38</sup>, when Vallar and Baddeley reported a case-study of a patient in Milan. This patient, Patient PV, showed conditions consistent with impairment of phonological loop following a stroke. This case allowed for an empirically convincing peek into the functioning of this sub-system. Earlier psycholinguistic approaches<sup>39</sup> have suggested language comprehension necessitates withholding linguistic information in the STM while it is being analyzed semantically and syntactically. The authors, therefore, expected a Contrary to the authors' initial hypothesis, Patient PV did not show any deficit in tests evaluating language comprehension except for highly non-trivial or artificial sentences.<sup>40</sup> On the contrary, the patient showed impairment in semantic coding-dependent phonological learning.<sup>41</sup> Children with Specific Language Impairment (SLI) have been shown to have highly

compromised phonological WM<sup>36</sup> which have been suspected to be caused by poor phonological loop capacity.<sup>42</sup> Further research in neuropsychological patients as well as healthy adults and children, helped emerge the role of phonological loop as an integral part in learning of language.<sup>42,43</sup>

For several decades, STM and LTM have been thought to be two separate systems. It was obvious that these systems interact extensively, but the details of this interaction were not clear. One of the phenomena that has prompted the idea of an intermediary between the long- and short-term systems, was chunking of information.<sup>26</sup> This refers to clubbing of information in WM based on prior memory in the LTM. To accommodate for such an intermediary, Baddeley introduced the concept of episodic buffer in 2000.<sup>44</sup> But there is debate over the reorganization roles once the concept of episodic buffer is introduced. Some researchers now argue for a pivotal role of episodic buffer in language acquisition and acquisition of intricate cognitive abilities during childhood years, which was previously thought to be the role of central executive.<sup>45</sup>

Several other models<sup>46,47</sup> have been proposed over the years, while parallel efforts have been made in finding the neural correlates of proposed models. Despite enabling an extensive push and rejuvenated interest in WM research, leading theoretical models are having a hard time explaining the ever-growing empirical dissociations of WM sub-systems. Different components of each sensory modality seem to have their own dissociable signature, which has proved hard for the WM model to cope up with. 48 The leading model of working memory takes into account sensory information gathered mostly via visual and auditory modalities<sup>11</sup>, whether the same sub-systems equally contribute to other sensory modalities remains unclear. Visuospatial WM tasks still dominate the field. This may have been because of the choice of experimental animals or paradigms. Also, some features, like working memory capacity, may be easily dissociable for certain sensory modalities. For example, visual memory capacity has been shown to be limited to about four colours or orientation in visual WM store. 49 Similar estimates are proposed for verbal WM as well. 50 But for other sensory modalities, such specificity may not be easily achievable. Potentially for these reasons, olfaction and other sensory systems remain poorly studied in the context of WM. But that does not mean that these under-studied modalities do not hold the

potential for exciting new direction in WM and clinical research. One good example for this comes from the study of tactile stimulus. Tactile WM is one of the earliest sensory systems to be studied for WM. <sup>51</sup> Humans have been shown to be able to hold tactile information for many seconds, but they performed best when at a shorter delay of no more than 5s. Beyond that a decline is seen in performance, but this deterioration is progressive but remains relatively stable. <sup>52</sup> This indicates a potential two-staged WM retention. For deaf and deaf-blind patients, tactile STM has been shown to have enhanced than healthy controls, indicating sensory enhancement for certain sensory systems in the absence of one or more sensory stimuli. <sup>53</sup> But this may only be true in the case of early onset of the disability. <sup>54</sup> Moreover, there is also evidence of crossmodality interaction in WM. Recent studies have suggested the role of olfactory bulb in the modulation of activity in entorhinal cortex, ventral hippocampus and mPFC circuit <sup>55,56</sup>, which is part of the narrative comprising the olfactory spatial hypothesis. <sup>57</sup> The field of working memory is actively growing with more research being directed to relatively less-studied sensory modalities.

# 1.3. Molecular correlates of working memory

Limitations of cognitive theories of WM necessitates a deeper, molecular level understanding for potential pharmacological interventions in cases of WM-related impairments. Attempts at such an understanding of molecular mechanisms that might sustain sensory information is fairly new. Remarkably, ionotrpic glutamate receptors (iGluRs) involved in LTM formation has been shown to have significant role in WM. The key players of neural correlates of WM are two ionotropic receptors that respond to the excitatory neurotransmitter Glutamate, namely α-amino-3-hydroxy-5-methyl-4-isoxzolepropionic acid (AMPA) and N-methyl-D-aspartate (NMDA).<sup>58</sup> These receptors have been shown to play significant roles in long-term potentiation (LTP).<sup>59,60</sup> These receptors are cation channels that primarily open to Na<sup>+</sup> and Ca<sup>2+</sup> ions respectively.<sup>58</sup> AMPA receptors can be formed by a composition of different subunits, GluA1, GluA2, GluA3 and GluA4.<sup>61</sup> Under certain circumstances, AMPA receptors can become permeable to Ca<sup>2+</sup> ions whereas NMDA receptors are chiefly voltage dependent cation channels, primarily Ca<sup>2+</sup>.<sup>58</sup> GluA1 AMPA receptors has been shown to rapidly trafficked, both via membrane diffusion as well as exocytosis, to post-synaptic density upon

glutamate is released from the pre-synaptic neuron. This process is believed to be essential for induction of LTP. So, when researchers looked at the working memory performance of GluA1 knock-out (KO) mice in a radial arm maze, the KO mice showed significant impairment in comparison to controls. Upon a weak Theta-burst stimulation (TBS), slices from control mice showed a short-lasting LTP whereas slices from GluA1 KO mice did not. This research draws a striking link between long-term potentiation (LTP) and working memory (WM), emphasizing that synaptic changes via LTP are critical for maintaining transient memory, especially in the prefrontal cortex (PFC) and hippocampus.

On the other hand, NMDA receptors, composed of NR1 and NR2A subunits, has been shown to play crucial role in working memory tasks. 67 NMDA receptor function has been shown to be crucial for sustained activity in the PFC during WM task. Mice trained for spatial working memory task in a radial maze, NR1KO mice showed significantly higher error rate in retaining memory of baited arms in contrast to controls. 68 Due to the slow-acting nature of the receptors, they have been thought of being useful in sustaining neural representations during the delay period in WM tasks.<sup>69</sup> Non-competitive NMDA antagonist, Dizocilpine, produced marked impairment in rodents performing odor span task, a standard task employed to investigate WM capacity. 70 In humans, administration of NMDA antagonist, Ketamine, resulted in impairments in working and semantic memory in healthy adults.<sup>71</sup> Functional Magnetic Resonance Imaging (fMRI) studies during administration of NMDAR antagonist produced pronounced decline in spatial working memory performance and activity in the Dorsolateral prefrontal cortex (dlPFC). 72 Inhibition via gamma-Aminobutyric acid (GABA)-ergic interneurons have also been shown to play crucial role in delay period activity. Administration of GABA antagonist in the PFC has been shown to impair delayed response task in monkeys.<sup>73</sup> Further, important role of GABAergic interneurons have been shown to be important for spatial tuning of cortical neurons involved in WM in dorsal PFC (dPFC) of monkeys performing an oculomotor task. 74 Recent research has also elucidated potential roles of brain-derived neurotrophic factor (BDNF) and associated TrkB receptor in regulating WM in PFC.75 With the growing body of work, it becomes more and more apparent that a fine balance between the excitatory and inhibitory circuitry is essential for the functioning of WM tasks.

# 1.4. A brief introduction to olfactory working memory

Despite some early work<sup>76</sup>, olfaction has long been ignored as a sensory modality when it comes to memory research. After the distinction between short and long-term memory was laid out in the fall of 1960<sup>29,77</sup>, several studies reported olfactory impairment in patients, particularly Wernicke-Korsakoff patients who showed impaired odor discrimination. 78 During this time, whether olfactory STM was a capacity-limited system, was also being investigated. 79 In a delayed odor recognition task, human subjects performed better in case of one odor over five-odor condition. This work was further reconfirmed with a more number of odor sets and performance of the participants invariably indicated towards a capacity-limited nature of OWM.80 Patients with temporal lobectomy showed significant impairment in odor memory task and cross-modal matching tasks.81 There are several other paradigms that assess different aspects of WM. N-back recall tasks are one of the more commonly used paradigms employed that looked at WM capacity for different sensory modalities. 82 In such task, human participants or trained animals are required to recall from a series of stimuli, e.g., visual, olfactory or auditory, a specific stimuli or recall in reverse order. 16,17,83 In order to study OWM capacity when n-back odor recall task was employed, participants did not show any effect of odor recency on delayed recall.84 Though later studies have shown a some effect of recency on OWM. 85,86 Recent fMRI studies looking at OWM and Visual WM uncovered activation of common brain regions like the precentral gyrus, superior frontal gyrus, inferior parietal gyrus etc., suggesting shared neural substrates across sensory modalities.87 Odors with high verbalizability were seen eliciting stronger activation pattern in language related brain regions implicating a more distributed network involving cross-modal interactions with the language system, reconfirming previous studies suggesting strengthening of working memory representations upon semantic associations.88

Neural correlates of OWM is still largely unknown. Some studies have speculated a role of the phonological loop in assigning semantic tags on familiar odors.<sup>89</sup> Further supporting this claim, one recent study that employed fMRI to look at brain region-specific activity in humans performing a DMNS task, found a double dissociation in

processing familiar and novel odors.<sup>90</sup> They reported increased activity in the prefrontal areas associated to language while spike in activity in the piriform cortex for non-familiar odors. The mist surrounding a detailed mechanistic understanding of OWM stems partially from the uniquely complex architecture of the olfactory systems.<sup>91</sup> Therefore, a comprehensive outline of the olfactory system becomes necessary before approaching the more nuanced subject of the neural basis of OWM.

#### 1.5. A brief introduction to the mammalian olfactory system

Sensory decision-making is crucial for survival for both animals living in the wild and humans. Foraging, habitat selection, protecting territory, social communication etc. require real-time decision-making by the animal. In all these regards, the sense of olfaction is among the most relied upon by a large number of species. Humans were thought to have a poor sense of smell in comparison to many other animals, especially dogs and rodents. But this long-standing view is changing. In humans, the study of olfaction has been largely overshadowed by other sensory systems, especially visual and auditory systems. Excent years have seen an exponential rise in olfactory studies in both humans and rodents. The COVID-19 outbreak and the subsequent loss of sense-of-smell in millions of symptomatic patients as well as asymptomatic carriers excruciatingly highlighted the importance of olfactory based therapeutic interventions. But there are experimental and ethical constraints while working with humans. As rodents rely heavily on olfaction, they provide a suitable system for studying olfaction at molecular and systems neuroscience level.

Binding of odorants to the olfactory sensory neurons (OSNs) in the olfactory epithelium in the nasal cavity marks the initiation of the olfactory transduction pathway in mammalian olfactory system (Figure 1.3). The OSNs express around 350 receptor genes in humans and over 1000 genes in rodents. <sup>100</sup> Though during maturation one OSN can transiently express multiple receptor genes <sup>101</sup>, mature OSNs express only a single olfactory receptor gene. <sup>102</sup> The OSNs extend axons through the cribriform plate to enter the olfactory bulb (OB). OB, a part of the central nervous system, is arranged in multiple concentric layers with each layer housing cell bodies of different cell types. <sup>103</sup>

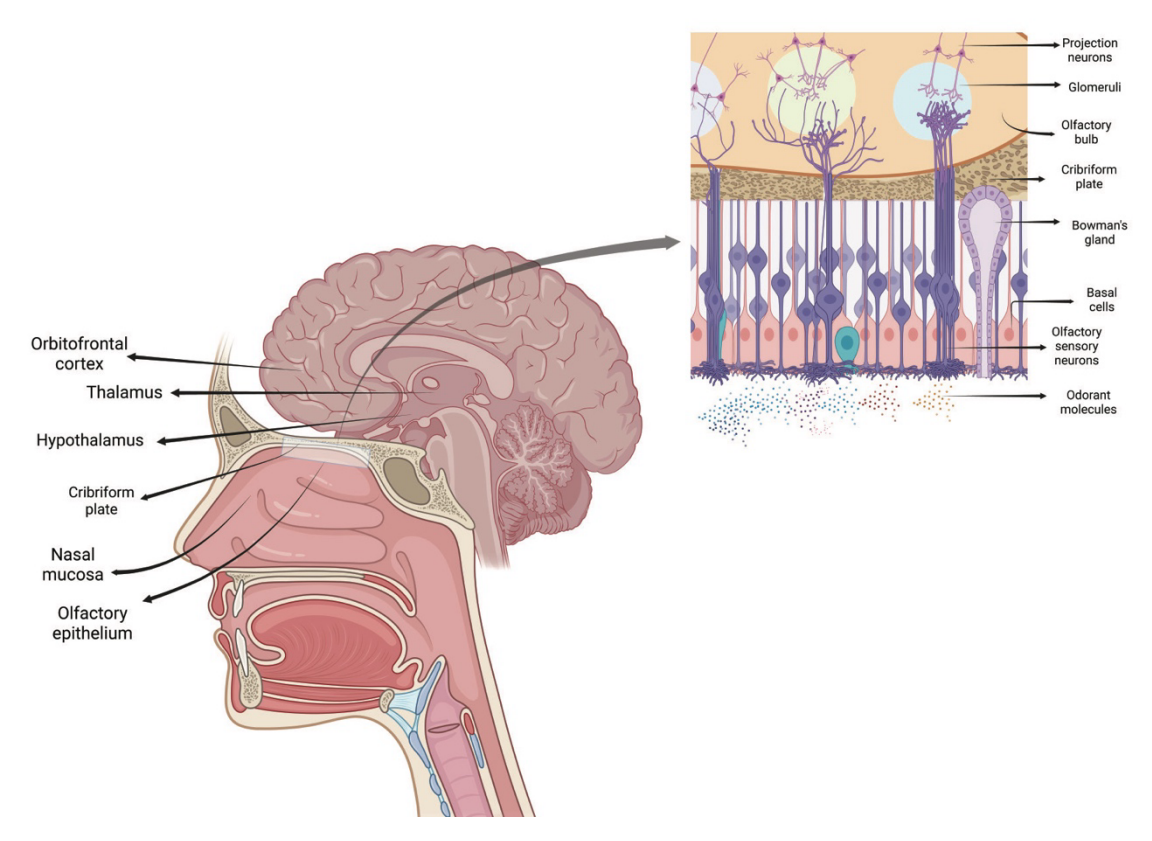


Figure 1.3. Schematic representation of the human olfactory system. (Created using Biorender and Adobe Illustrator)

Multiple OSNs, expressing the same olfactory receptor converge in spherical glomeruli. Rodents have a 1:2 ratio of olfactory receptor genes and the number of glomeruli, i.e., about 2000 glomeruli for each OB. There is striking similarity between the modular design of the olfactory bulb in both humans and rodents (Figure 1.4). But unlike rodents, a staggering 5,500 glomeruli have been reported in each human OB. <sup>104</sup> In the glomeruli, the OSNs further connect to excitatory projection neurons, mitral and tufted (M/T) cells, which transduce the signal to multiple higher brain regions. There is a sophisticated interplay of excitatory and inhibitory neurons at multiple levels in the OB. <sup>105</sup> Glomeruli are innervated by different types of interneurons, like superficial Short Axon (sSA) cells, Periglomerular cells (PGCs) and external Tufted (ET) cells. sSA cells and PGCs mostly act in glomerular inhibition whereas ET cells act as excitatory interneurons. <sup>100</sup> Another important inhibitory cell type that constitutes the innermost layer of the OB, is the granule cells (GCs). <sup>106</sup> An apparent lack of axons had put their identity as neurons into question during the early histological studies on the OB. <sup>107</sup> They are, by far, the most abundant inhibitory interneurons in the OB. The rodent OB

harbours a staggering 0.5-3 million GCs, for an estimated, 20,000-50,000 M/T cells.<sup>108</sup> GCs have been shown to inhibit M/T cells.<sup>107</sup> This excitation-inhibition (E-I) balance has been shown to play crucial role in odor processing and discrimination.<sup>109–111</sup>

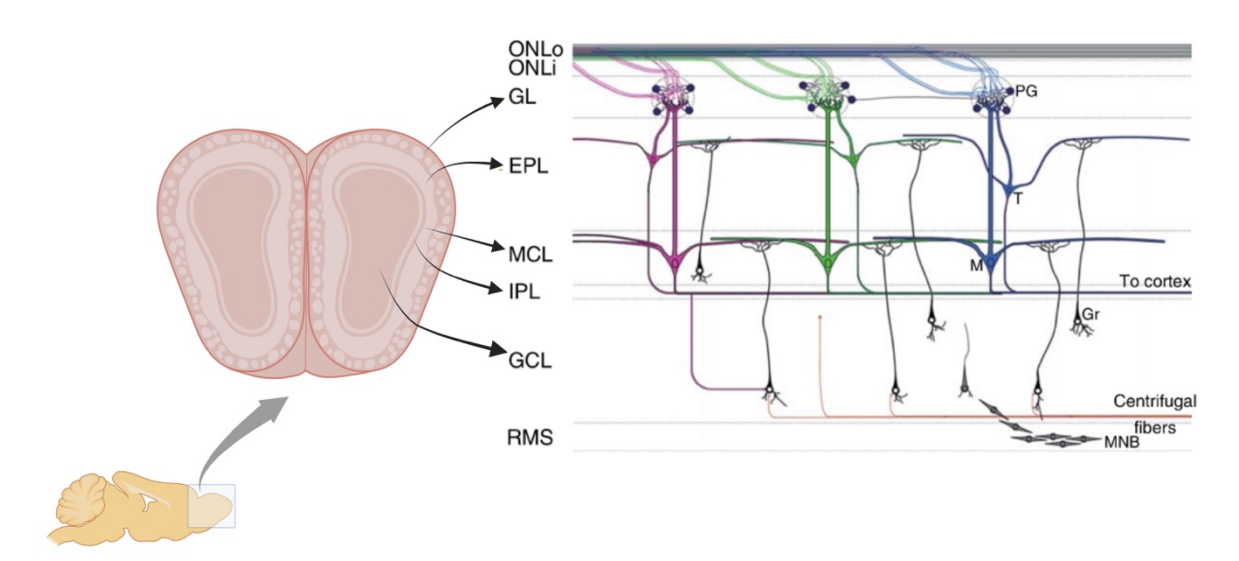


Figure 1.4. Structure of the rodent olfactory bulb. ONLo: Olfactory nerve layer (outside), ONLi: Olfactory nerve layer (inside), GL: Glomerular layer, EPL: External Plexiform Layer, MCL: Mitral Cell Layer, IPL: Internal Plexiform Layer, GCL: Granule Cell Layer, RMS: Rostral Migratory Stream (Adapted and modified from: Greer et. al., 2008<sup>112</sup>)

Projection neurons from the OB, M/T cells, further transmit the odor signal to the olfactory cortex. Any region of the brain that gets direct neural input from OB, collectively, constitute the olfactory cortex. <sup>113</sup> Multiple higher cortical centers like the piriform cortex, anterior olfactory nucleus (AON), olfactory tubercle, lateral entorhinal cortex, prefrontal cortex etc. get direct input from the OB. <sup>114</sup> Among the outputs via the lateral olfactory tract (LOT) from the OB, piriform cortex gets highest number of innervations. It is, therefore, often referred to as the 'Primary Olfactory Cortex'. <sup>115</sup> AON comes next to the piriform cortex in terms inputs received from the OB. Both prefrontal cortex and AON have reciprocal projections with many other higher cortical regions like amygdala, orbitofrontal cortex (OFC), perihippocampal cortex and many others which collectively contribute to higher order olfactory processing. <sup>116,117</sup> Piriform cortex and AON themselves have been reported to play crucial role in olfactory learning and memory. <sup>118,119</sup> Olfactory stimulus thus invoke activity in a wide range of cortical

structures.<sup>120</sup> The role of different cortical regions in olfactory information processing remains an active area of research.

# 1.6. Probing olfaction: Past and Present

We encounter a wide variety of odors everyday which influences our daily activities and decision-making at both conscious and sub-conscious level. The sheer number of the odors we encounter and can distinctively identify, begs the question of the number of odors humans can successfully discriminate amongst. Surprisingly, it turns out, we do not have a precise estimate. Human olfactory repertoire has long been speculated upon, but little empirical investigation has gone into quantifying the human odor discrimination space.

Olfaction has been a fascination to many philosophers and thinkers from antiquity. 122 Carolus Linnaeus was the first to classify odors in a seven-category system<sup>123</sup>. Almost a century after Linnaeus, Dutch physiologist Hendrik Zwaardemaker developed a primitive olfactometer, partly using odourless kaolin to deliver odors directly to inside the nostrils with metal odor vials. He modified Linnaeus's classification and categorized odors into nine groups<sup>124</sup>. During early twentieth century, Hans Henning, famously developed a hypothetical 'smell prism' with each corner representing an odor type. 125 In 1927, Crocker and Henderson classified odors to be of four types, namely, fragrant, acid, burnt and caprylic. 126 These different types of odors can vary across a nine-point scale. This proposition results in a cumulative 9^4 or 6561 probable odors that humans should be able to perceive. 127 They also made a commercially available kit with each vial containing an odor and its rating on the ninepoint scale. This number somehow got rounded up to 10,000.<sup>128</sup> From then onwards, most of the literature on the subject assumes human odor space to be confined to 10,000 odors. The largest study on human olfactory perception has been carried out by the National Geographic Society with an astronomical 1.5 million people participating in it. 129 But human olfactory space remained disputed with a rough estimation of perceivable odors. In a recent paper, based on their limited psychophysical experiment and mathematical extrapolation, researchers speculate the number of discriminable odors to be as high as a trillion. 94 Though this result has been questioned and the

mathematical methods been criticized as flawed<sup>94,121</sup>, the actual human olfactory space remains debated till date.

A multitude of different methods have evolved over time to probe human olfactory range. Some of them try to probe the perceptual odor space in humans by collecting subjective responses through questionnaires, while others provide actual odors to subjects and record their responses. University of Pennsylvania Smell Identification Test (UPSIT)<sup>130</sup> and sniffin' sticks test<sup>131</sup> are probably the most widely used. In UPSIT, the participants are provided with 4 booklets where the microencapsulated odors are to be sampled in a scratch-and-sniff manner. Based on their subjective response, they had to identify from four alternate choices provided. As in case of the sniffin' sticks test, concentration gradients for different odors are given and subjects are scored based on odor detection threshold(T), detection(D) and identification(I)<sup>132</sup>. Evidently, these methods lack both controlled odor delivery and specified response window while relying, chiefly, on the subjective perception of the subject. Many other paradigms like Subjective Importance of the Sense of Smell Questionnaire (SISSQ)<sup>133</sup>, SmellSpace<sup>134</sup> etc. have been developed over the years. But most of them suffer from biases and variability introduced by the participants or experimenter.

Olfactory matching is a delayed match to odor paradigm where the two-odor stimulus separated by a delay are presented. The participant responds by choosing whether the present odor stimuli are same or different. Delayed match to sample (DMS) paradigms are extensively and almost solely used for studying aspects of working memory. First introduced in late 1950s, DMS tasks intended to probe WM related tasks in non-human primates. The forced delay period serves as a crucial parameter to make the paradigm useful for studying WM related tasks. Variations of DMS has been successfully applied to study different aspects of WM across species, including humans, for different sensory modalities.

# 1.7. Neural basis of working memory

Several studies have emphasized the role of persistence of neural representations as a cornerstone of working memory maintenance. Most of these research has probed into the activity dynamics of several brain regions during the delay period, following the first or sample stimulus. Prefrontal cortex (PFC) remains as the primary neural correlate when to comes to delay period activity in WM tasks. One of the first clues of the involvement of the frontal lobes came nearly a century ago, through a series of frontal lobe lesions. Monkeys showed impairment in delayed response task post-PFC-lobotomy. Monkeys showed impairment in delayed response task post-PFC during the delay period in DMS tasks. More recently, functional magnetic resonance imaging (fMRI) studies in humans have shown activity in PFC during spatial and non-spatial WM tasks. Most of these

Despite evidence of activation of PFC in WM tasks, coherent understanding of the correlation between the complex structural organization of PFC and stimulusspecific sustenance of information during WM was lacking. In the fall of the 20th century, Goldman-Rakic suggested that there could be anatomical segregation in the prefrontal cortex in terms of working memory function. 149 Though sensory modalityspecific domains can exist independently, they can interact while processing complex or multi-sensory stimuli. Following this domain-specific WM model, researchers mapped the PFC in macaque monkeys for areal segregation for facial identification and showed localized selectivity in PFC circuitry while processing facial imagery. 150 In a similar fashion, showing functional compartmentalization in the PFC, inferior convexity in the frontal areas were shown to selectively responsible for processing of non-spatial features of visual information, whereas dIPFC serves in spatial aspects of WM function. 150,151 Subsequent research has found contradictory evidence to this model with some studies failing to identify spatial vs non-spatial organization in the PFC. 152 Also, recent work involving single neuron recording from PFC neurons while monkeys performed a recognition task of two visual stimuli followed by a delay (two-object delay period), suggests mixed selectivity and distributed encoding of information. 153

Interestingly, despite its crucial role in WM, the role of PFC as a site for storage of stimulus identity has been questioned. 154 It turns out that the sensory cortical areas are likely candidates for short-term storage of stimulus-specific information during the delay period. 155-157 Delay-period activity in anterior piriform cortex, part of the olfactory cortex, has been shown to maintain odor-specific information during delay period. 158 Outside of the PFC, mediodorsal (MD) thalamus, that shares reciprocal connections with the medial PFC (mPFC)<sup>159</sup>, has been shown to play crucial role in the sustaining the neural representation during the delay period in WM tasks. 160 Classic experiments that induced disruption to mPFC and MD thalamus pathway showed detrimental effect to delayed response tasks in monkeys<sup>161,162</sup>. Lesions in MD thalamus has also been linked to impairment in spatial working memory in rodents. 163 Single neuron spiking activity in MD thalamic nuclei has been shown to display altered activity by inducing PFC-specific cerebral hypothermia during a delayed response task in monkeys. 164 In more recent research, when mice were subjected to a radial maze-based spatial WM task, spatial sampling did not show any interaction between these two regions, while active choice-making did. 160 These researchers also identified a specific neural population that showed delay-specific firing that relied on MD and hippocampal connections.

Another important area that has been implicated in WM is the dorsolateral prefrontal cortex (dlPFC). <sup>165</sup> In non-human primates, layer III neurons maintain information during delays, while layer V neurons handle response-related processing. <sup>166,167</sup> Reversible inactivation of dlPFC disrupts WM, confirming its role in cognitive maintenance. <sup>168</sup> Human fMRI studies show dlPFC involvement in WM tasks, with superficial layers processing information manipulation, and deeper layers handling response execution. <sup>169</sup> WM load increases activity in superficial layers more than deep ones. dlPFC activity changes across different WM phases, with manipulation tasks engaging it strongly. Voxel-based lesion-symptom mapping studies have investigated how white matter fiber tracts connect the dlPFC and parietal cortex, assisting working memory and general intelligence. <sup>170-172</sup> Moreover, damage to orbitofrontal cortex, a neighbouring region of the dlPFC has been shown to affect working memory performance and has implications of higher executive functioning. <sup>173</sup>

A recent study examined working memory (WM) in mice using a delayed non-match to sample (DNMS) task for olfactory and tactospatial modalities, aiming to decipher the role of the claustrum (CLA). The CLA, a thin, irregular structure situated between the insular cortex and the striatum has been implicated in complementing the PFC by providing a transient buffer for sensory-specific information, facilitating short-term decision-making processes. Calcium imaging showed sustained CLA neuron activity during delays, indicating cue identity encoding. More than half of the CLA neurons showed persistent activity during the delay period. Chemogenetic and optogenetic inhibition of CLA neurons caused noticeable WM impairments. CLA activity accurately predicted cues, but this accuracy declined with longer delays.

Recently, the role of persistent activity being central to WM has been questioned. Oculomotor delayed response (ODR) has been one of the foremost experiments used to make the case for persistent activity during delay period. <sup>178,179</sup> In this paradigm, monkeys are trained to focus on a central dot and perform a directed eye movement (saccade), following a brief delay, once a cue appears at another location on the screen. But the persistent activity observed in ODR task has been suspected to be a preparatory firing for known motor movement rather than WM maintenance itself. <sup>179</sup> Further, computational studies that trained recurrent neural networks (RNN<del>CC</del>) to perform several WM-dependent tasks, suggested that short-term synaptic changes can be sufficient to sustain memory representations during delay period without the need for persistent activity, given the delay period is sufficiently short. <sup>180,181</sup>

#### 1.8. Attentional control and working memory

Other than the WM capacity, one of the most important factors that effects WM-related processing, is attentional control. There is consensus over the fact that WM can store multiple pieces of information over a short period of time. But for a concrete decision making, a strong transient selective mechanism must be employed. Despite debates over how attention is defined the prevailing hypothesis seems to be a mechanism in place that allows for selectively and often transiently prioritizing one set of information over others in the WM store. One of the most compelling pieces of evidence regarding advantage of attentional selection and decision making comes from

retro-cue experiments.<sup>186</sup> In this experiment, subjects were presented with a set of visual cues where one of the cues was selectively highlighted indicating a higher likelihood of presentation during the test phase. When people were presented with that highlighted cue, the recall was significantly faster than other items in the list. It, therefore, does not come as a surprise that WM deficits and conditions with attentional deficits like attention deficit hyperactivity disorder (ADD) are highly correlated.<sup>187</sup>

# 1.9. Evolution of working memory: the emergence of cognitive trade-off

Research on the evolution of working memory as a tool for decision making in primates and subsequently, in humans, has a very short history. Contemporary understanding of WM has been greatly decelerated by adamant adherence of the idea that a transient memory system has evolved just to supplement the evolution of language and communication. As humans became bipedal and therefore, more terrestrial, the sub-systems that make up WM-system may have evolutionarily diverged from their primate ancestor who spend most of their times above ground.

Species-specific loss and gain-of-function of WM sub-systems may have resulted in differentially able working memory in primates and humans. This selectivity may become more apparent while comparing cognitive tasks that humans and nonhuman primates can perform. Of the different aspects of the visually driven cognitive tasks that have been explored, speed of motion, spatial frequency and orientation have been shown to be retained for considerably longer than parameters like stimulusdirection, texture etc. 189 This has led researchers to believe a selectivity in cognitive features when WM tasks are being performed. 190,191 An intriguing example of this selectivity and the process of visual WM become apparent when a mask is introduced during the delay period between the sample and test stimulus in ODR task. In such a task, the sample display shows a set of dots moving in variable motion but had a mean directionality of motion. 189 During the delay period, a distractor, the mask, is employed where another set of dots move in random direction. In the test phase, monkeys were displayed a set of dots moving uniformly in a certain direction. The monkeys had to identify whether the sample and the test had the same mean direction of movement. Invariably, there was a decline in performance. But humans have been shown to be

much better their primate relatives in retaining delay period representation of stimuli in the presence of interference. <sup>192,193</sup> This divergence maybe deeply intertwined with the evolution of the neocortex, especially the PFC. <sup>194</sup>

The PFC has greatly increased in size over the course of evolution in primates and hominids. PFC's involvement is crucial but not limited to sustained temporary representations of stimulus. Extensive planning, abstraction, coordination and overall higher cognitive function has been largely attributed to the increased cortical area of PFC. PFC has been speculated to greatly enhance working memory and associated sub-systems, one of which has been instrumental to development of language.

There is little doubt that selectivity depending on the nature of presented stimuli has been crucial to adaptive radiation of primates. One of the forebearer of the Comparative Cognitive Science (CCS) research<sup>197</sup>, Tetsuro Matsuzawa, has been able to train chimpanzees to perform visuo-spatial working task at astonishingly fast pace when compared to humans. Over a set of several experiments where a screen displayed Arabic numerical, from 1-9, three chimpanzees outperformed human subjects at remembering location of each numerical on the display screen. 198 They showed much less latency while performing the task in comparison to human subjects. Though chimpanzees performed poorly in a variety of cognitive tasks requiring abstraction, the results clearly indicated an astronomical difference in performance when it comes to WM capacity. Despite having a seemingly larger PFC, humans fall short of the performance of their primate relatives. In an attempt to explain this discrepancy in performance, he proposed the radical idea of cognitive trade-off.<sup>199</sup>. Though a recent study has shown a superior performance in the task by humans when the numeric span was increased to accommodate numbers from 1-19.200 The cognitive trade-off hypothesis remains a leading attempt in explaining observations related to superior visuo-spatial working memory in chimpanzees.

# 1.10. Working memory impairment and disease: A special look at olfaction

Working memory dysfunctions can range from temporary speech problem to serious cognitive impairment. Impairments can manifest through any of the several components of WM (as laid out previously). Often such deficits are accompanied by clinical findings of existing neurological conditions making them harder to diagnose as an isolated STM deficit.<sup>201</sup> For example, patients who display phonological memory impairments, often have focal lesions in the left temporal regions.<sup>202</sup>A classic case of verbal STM comes from patient J.B. who had extreme difficulty in remembering spoken names or phone number, even when she immediately tried writing them down.<sup>203</sup>

Working memory (WM) impairments are observed in various neurological and psychiatric conditions including mild cognitive impairment (MCI), Alzheimer's disease (AD), multiple sclerosis (MS), Parkinson's disease and several other neurodegenerative conditions.<sup>204-207</sup> One of the most severe form of STM deficit can be seen in case of Alzheimer's patients. A study involving 39 Alzheimer's patients found that two of them had severe visual pattern memory (a visual WM task), while normal memory for retaining sequences of targeted movement (a spatial WM task).<sup>208</sup> A malfunctioning central executive has also been reported in Alzheimer's patients. 209,210 Research suggests WM deficits in MCI and AD follow a gradient, with MCI patients experiencing milder impairments compared to AD patients, who have significant difficulty maintaining and manipulating information.<sup>211</sup> Pathophysiologically, WM impairments in AD involve disruptions in the prefrontal cortex (PFC) and hippocampal networks, affecting attention, inhibitory control, and executive function. 212 Synaptic loss and amyloid-beta accumulation in critical cortical and subcortical regions contribute to declining WM performance in AD<sup>213</sup>, compounded by reduced connectivity between the PFC and medial temporal lobe. 214 Neuroimaging studies show functional changes in the dlPFC impact executive functions such as selective attention and interference control, which are essential for WM.<sup>215</sup> In MS, demyelination and cortical atrophy result in slowed cognitive processing, further impairing WM.<sup>207</sup>

Working memory (WM) impairment in Parkinson's disease (PD) arises from corticostriatal-thalamo-cortical (CSTC) loop dysfunction<sup>216</sup> and dopaminergic depletion<sup>217</sup> while non-dopaminergic pathology has also been investigated.<sup>218</sup> Imaging studies show altered connectivity in the dorsolateral prefrontal cortex (dlPFC) and caudate nucleus, affecting cognitive flexibility and executive function.<sup>219</sup> Spatial WM shows significantly worse impairment than object WM due to greater dopamine loss in the dorsal caudate.<sup>220</sup> Working memory impairments are also prevalent in children with developmental deficits that lead to slowed or stagnant intellectual functioning<sup>221</sup>, e.g., down syndrome<sup>222</sup>, William's Syndrome<sup>223</sup> etc. At a molecular level, several neurocognitive impairments and psychiatric disorders disrupt molecular correlates of WM which often manifests as one or more symptoms. Impaired functioning of NMDA has been implicated in Schizophrenia in both humans<sup>224</sup> and animal models.

Olfactory dysfunction has been shown to be an early indicator for severe neurocognitive impairments like Alzheimer's<sup>225</sup> and Parkinson's disease.<sup>226</sup> Age-related cognitive decline is sometimes accompanied or predated by progressive hyposmia.<sup>227</sup> Olfactory detectability has been shown to be highly effective in sieving out asymptomatic COVID-19 patients during the first wave of the pandemic.<sup>228</sup> Moreover, olfactory DNMS task has been shown to successfully probe neurocognitive deficits in symptomatic COVID-19 patients as well as recovered subjects.<sup>97</sup> This method may still be used to identify and gather a quantitative understanding of cognitive decline in patients with Long COVID.<sup>229</sup> Olfaction therefore remains highly promising as a sensory modality that may be employed for early diagnosis as well as probing existing neurocognitive deficits.

# Chapter 2

## Materials and Methods

## 2.1. Olfactory matching paradigm in humans

# 2.1.1. Study Population

As per guidelines, subjects above 18 years and below 80 years were included in the study. Participants were called between 10 AM to 5 PM time periods on weekdays only. Prior to the experiments subjects had to fill up a detailed questionnaire describing details relevant to their olfactory abilities, food preferences, smoking habits etc. Participants who registered online had to fill up a short format providing basic personal details and weekday availability slots. They were later called based on availability. Only healthy subjects with no known neuropathology were called to participate in this study.

## 2.1.2. Inclusion and exclusion criteria

Participants aged between 18-80 years were included in the study. Subjects with any diagnosed history of neuropathy or neuropsychiatric conditions were excluded.

Participants who had known history of anosmia, hyposmia or parosmia, were excluded.

### 2.1.3. Ethics committee guidelines

The experimental paradigm and associated procedures are approved by the Human Ethics Committee at IISER Pune. According to the guidelines, all experiments were performed between 10 AM to 5 PM and only on weekdays. The timings coincided with the availability of health care services on campus, in case of any emergency. Participants could choose to discontinue at any point during the commencement of the experiment.

# 2.1.4. Study location

All experiments with healthy subjects were carried out on the IISER Pune campus.

# 2.1.5. Olfactory detection task

Before the commencement of each session, each participant was put through a detection task where each odor included in the experiment was individually presented. The participant had to confirm if the odor was detectable. Only successfully detected odors were included in the experiment. In case any odor was reported as aversive or uncomfortable by the participant, it was not included in the olfactory matching (OM). Completion of the detection task then led to the OM paradigm. For both simple and complex odor detection task, we had a mean detection accuracy of over 90%.

# 2.1.6. Olfactory Matching Paradigm

OM paradigm consisted of 20 trials for each session. Each trial was characterized by presentation of two odors, each for 4s, separated by an interval, called the interstimulus interval (ISI). After the offset of the second odor, an additional 5s window was provided to ensure that the participant had ample time to respond. ISIs were varied across subjects but remained constant throughout each session. The odors were generated by a random-pair generator program that created random odor pairs based on the odors detected by the participant in the odor detection task. The two odors delivered in each trial, were either the same or different. The participant needed to choose one of two options. They had the freedom to repeat a trial in case they wanted to. Two trials were separated by 4s of inter-trial interval (ITI). After the participant has given a response for all the 20 trials in a session, the overall accuracy for the session is displayed by the in-built program. Individual trial responses along with reaction time were also recorded in real time. OM has been done with both simple and complex (binary mixtures) odors. The basic sequence of events remained constant throughout all the OM sessions.

# 2.1.7. Simple odor matching task

Simple odor matching tasks followed the sequence of events as described above with monomolecular odors. A pool of 9 odors were used (Table 2.1). Four different ISIs were employed in simple odor matching sessions: 2.5s, 5s, 7.5s and 10s. Comparable numbers of participants were assigned to all four ISI sessions. Once the detection task was complete, a specific ISI was assigned to each participant by the experimenter.

After that, based on the detectability of the participant, random simple odor pairs were generated.

## 2.1.8. Complex Odor matching

Complex odor matching task followed the sequence of events as described above with binary mixtures of monomolecular odors. Two different types of odor mixtures have been employed, 60-40 and 80-20 binary mixtures. Both these mixtures were used for OM in independent sessions. As odors are made in pairs in case of complex odors, pair generation is accordingly calibrated to generate same or different odor pairs from the same group.

## 2.1.8.1. 60-40 binary mixtures

Two monomolecular odors were mixed at 60:40 ratio to make a binary odor mixture. A total of 10 odors were used (Table 2.2). Two different ISIs were employed: 5s and 10s. Comparable numbers of participants were assigned to both the ISI sessions. Once the detection task was complete, a specific ISI was assigned to each participant by the experimenter. After that, based on the detectability of the participant, random 60-40 odor pairs were generated.

# 2.1.8.2. 80-20 binary mixtures

Two monomolecular odors were mixed at 80:20 ratio to make a binary odor mixture. A total of 10 odors were used (Table 2.2). Two different ISIs were employed: 5s and 10s. Comparable numbers of participants were assigned to both the ISI sessions. Once the detection task was complete, a specific ISI was assigned to each participant by the experimenter. After that, based on the detectability of the participant, random 80-20 odor pairs were generated.

## 2.1.9. Apparatus

### 2.1.9.1. Olfactory-action meter

We custom-built an olfactory-action meter (Figure 2.1A) that maintains controlled odor delivery to the nostrils of the participants. Odorized air is delivered using 10 airflow meters via a 12-channel glass funnel. The funnel delivered odor via an extended nozzle

that further connected to a breathing mask. An exhaust connected near the glass nozzle helps in the removal of residual odor in the tube. The sequence of events in an olfactory matching trial is shown in Figure 2.1B. To check if odors are properly delivered to the nostrils of the subjects, we carried out Photoionization detection (PID) detection measurements (Figure 2.1C). We delivered individual odors for a duration of 4 seconds and corresponding voltage traces are recorded using an oscilloscope. Values are averaged across 10 trials.

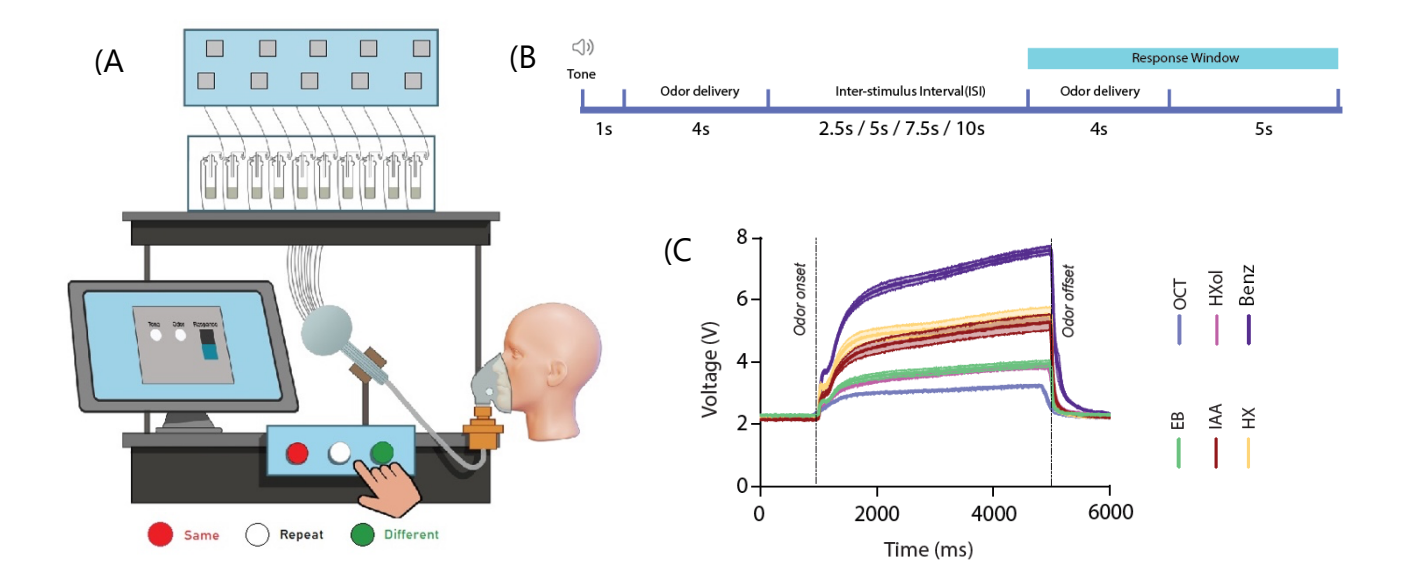


Figure 2.1. Olfactory action meter for quantitative analysis of human olfactory matching ability.

Schematic diagram of the olfactory-action meter. Participants received two odors separated by an inter-stimulus interval (ISI). After sampling the second odor, the participant had to decide if same or different odors were delivered. Based on the decision, SAME or DIFFERENT buttons kept in front must be pressed within the response window. In case of any confusion, the REPEAT button could be pressed to reinitiate the trial. (B) Sequence of events during an olfactory matching trial is depicted. Each trial started with a tone. Once the first odor is delivered for 4s, a pre-decided ISI is applied, which is followed by a 4s delivery of the second odor. An additional response window of 5s was provided. The participant could respond as soon as the second odor delivery started. Two trials are separated by an inter-trial interval (ITI) which is kept constant at 4s. (C) Photoionization detection (PID) measurements of voltage

fluctuations for simple odors are plotted. Odor is delivered for 4s. Values are averaged across 10 sets of measurements.

# 2.2. Odors used in the experiment

All the odorants used in the experiments were at least 99% pure (Sigma-Aldrich). Odor bottles were sealed every time after use and stored in vacuum at room temperature throughout the experimental period. Odors that needed refrigeration were accordingly preserved.

# 2.2.1. Odor Preparation

Simple odor matching task. For simple odor matching tasks, a maximum of 9 monomolecular odors were used corresponding to different chemical classes and vapor pressures (Table 2.1). Highly pure odors were diluted in mineral oil in 1:50 ratio. 80 µl of odor was diluted in 4 ml of mineral oil. Odors were freshly made every week to ensure efficient odor concentration throughout the sessions.

Odor	Chemical class	Vapour pressure	Classificatio
		(VP) <sup>230,231</sup>	n based on
			VP
Geraniol (Ge)	Monoterpenoid	0.03 mm Hg at 25 °C	Lower
Eugenol (Eu)		0.0221 mm Hg at 25	
	Phenylpropanoid	°C	
Octanol (OCTol)	Alcohol	0.0794 mm Hg at 25	
		°C	
Octanal (Oct)	Aldehyde	0.6 mm Hg at 20 °C	Medium
Hexanol (Hxol)	Alcohol	0.928 mm Hg at 25 °C	
Benzaldehyde (Benz)	Aromatic aldehyde	1.27 mm Hg at 25 °C	
Isoamyl Acetate (IAA)	Ester	5.6 mm Hg at 25 °C	High
Hexanal (Hx)	Aldehyde	11.3 mm Hg at 25 °C	
Ethyl Butyrate (EB)	Ester	14.0 mm Hg at 20 °C	

Table 2.1. List of Odors used for Olfactory Matching

Complex odor matching task. For complex odors matching tasks, odor preparations were done by diluting odor in mineral oil in 1:100 ratio.

60-40 binary mixtures: A total volume of 40  $\mu$ l of odors was diluted in 4 ml of mineral oil. A total of 9 different monomolecular odors were used to make 5 pairs of binary mixtures (Table 2.2). Odors were added to 4 ml of mineral oil by volume, 24  $\mu$ l and 16  $\mu$ l, respectively. Odors were freshly made every week to ensure efficient odor concentration throughout the sessions.

80-20 binary mixtures: A total volume of 40  $\mu$ l of odors was diluted in 4 ml of mineral oil. A total of 9 different monomolecular odors were used to make 5 pairs of binary mixtures (Table 2.2). Odors were added to 4 ml of mineral oil by volume, 32  $\mu$ l and 8  $\mu$ l, respectively. Odors were freshly made every week to ensure efficient odor concentration throughout the sessions.

S/N	60-40 binary mixtures	80-20 binary mixtures		
1	60% Ge + 40% Eu	80% + 20% Eu		
2	60% Eu + 40% Ge	80% Eu + 20% Ge		
3	60% IAA + 40% EB	80% IAA + 20% EB		
4	60% EB + 40% IAA	80% EB + 20% IAA		
5	60% Act* + 40% Oct	80% Act + 20% Oct		
6	60% Oct + 40% Act	80% Oct + 20% Act		
7	60% Benz + 40% Hxol	80% Benz + 20% Hx		
8	60% Hxol + 40% Benz	80% Hxol + 20% Benz		
9	60% IAA + 40% Hx	80% IAA + 20% Hx		
10	60% Hx + 40% IAA	80% Hx + 20% IAA		
Table 2.2. List of Complex odor mixtures				

# 2.3. Modified olfactory action meter for probing cognitive health in patients with COVID-19 infection

To meet the safety guideline of the Ministry of Health, Govt. of India, necessary precautionary measures were taken, and the olfactory-action meter was extensively modified to ensure safe and reliable measurements.

## 2.3.1. Apparatus

A custom-built ten-channel olfactory-action meter which delivers odors with high temporal precision is used for the present study. Odorized air (HEPA sterilized) passes through a glass funnel into an odor delivery unit. Further, the air passes through a filter that removes any background odor. The air channels divided using a metallic manifold are further connected to ten mini–Mass Flow Controllers (MFCs) and one Main MFC (Pneucleus Inc.). This allows control on the volume of air passing through each of them. The output from each of the ten mini MFCs are connected to its respective odor reservoirs, each filled with 4mL of diluted monomolecular odorant. The odor volatiles then travel through Tygon tubing and mixes with clean air before entering the nozzle. The volumetric concentration (%v/v) of the odor is thus defined as the ratio of the volume of odor volatiles to the total volume of odorized air. We have selected these concentration levels ranging from 9.1-50% (v/v) for measuring the DIs.

Cross-contamination between subjects was avoided by using separate odor delivery units comprising of a long-tube fitted with four layers of filters (surgical mask grade) and a suction outlet guarded by 0.2-micron PES filter (Whatman Uniflow). The PES filter is attached to a vacuum pump operating at ~ 450 mbar. Two HEPA and one PES filter (each of 0.2-micron size) are fitted in the exhaust line which finally releases into the activated carbon filter. Vacuum is only switched off during the duration of odor delivery to the nozzle. A wall that separates the instrument from the subject was established that prevented contact with the components of the olfactory action-meter and maintained physical distancing from the experimenter.

### 2.3.2. Detection task

During the detection task, each participant undergoes a series of trials, where the detection ability of the participants for different odors are evaluated with stepwise increase in concentration of the odors. Each odor is presented for 4 seconds. The

participant is alerted just prior to the odor delivery and once the odor is delivered, the subject verbally confirms whether the odor is detected or not. After an interval, the next odor is presented and so on. From a pool of 10 odors (see table 2.1), participants are presented with the lowest concentration of stimuli of 9.1% (20 ccm of pure odorized air + 200 ccm of ambient air). After the participant is done with the first set of odors at 9.1% concentration, a higher odor concentration of 16.6% (30 ccm of pure odorized air + 200 ccm of ambient air) in the same sequence as the previous one. Once this set of odors at 16.6% concentration is over, 23.1% (40 ccm of pure odorized air + 200 ccm of ambient air) and 50% (200 ccm of pure odorized air + 200 ccm of ambient air) is presented respectively. Once the detection task comprising of sampling of 40 stimuli is complete, a concentration-wise detection indices (DIs) are calculated.

DI is calculated as a ratio of successful detection of odor and total odors presented at that odor concentration.

# | D| = | Total number of odors detected successfully for a given concentration | | Total number of odors presented at that concentration

As the next paradigm involves odor matching task at 50% odor concentrations, therefore, only the participants with a DI score of >0.5 are allowed to perform the odor matching task (Figure 2.2A). This step is employed to make sure that people who are unable to detect odor for either nasal congestion or hyposmic for some unknown reason, are sieved out.

List of odors used for odor detection task

Odor	Chemical class	Vapour pressure
		(VP) <sup>230,231</sup>
Eugenol (Eu)	Phenylpropanoid	0.0221 mm Hg at 25 °C
Acetophenone (Act)	Ketone	0.397 mm Hg at 25 °C
Octanal (Oct)	Aldehyde	0.6 mm Hg at 20 °C
1,8-Cineole (Ce)	Monoterpenoid	0.9 mm Hg at 25 °C

(+)-Limonene	Cyclic Monoterpene	1.55 mm Hg at 23.5 °C	
(-)-Limonene		1166 11111 118 612 516	
Isoamyl Acetate (IAA)	Ester	5.6 mm Hg at 25 °C	
Hexanal (Hx)	Aldehyde	11.3 mm Hg at 25 °C	
Ethyl Butyrate (EB)	Ester	14.0 mm Hg at 20 °C	
(-)-Carvone (Cv)	Terpenoid	15.5 mm Hg at 25 °C <sup>232</sup>	

Table 2.3. Odors used for experiments involving COVID-19 subjects

# 2.3.3. Odor matching task

In this odor matching paradigm, subjects were presented with two odor stimuli based on the odor pair generated by the program. To ensure no contamination and maximal safety, odors were delivered through a nozzle. The participants were asked to put their nostrils in front of the nozzle and wait for a verbal cue for the initiation of the trial. Each participant is carefully warned, never to touch the nozzle with their nose-tip or grab the nozzle with their hands to avoid any surface-mediated contamination. For each trial, the participants were verbally alerted prior to each onset of odors and their response at the end of the trail is recorded by the experimenter. The entire process is kept in such a way that the participants do not need to touch any surface at any given point of the time. Once the session is complete, the accuracy is for the session is communicated to the participants. In a particular trial, the first stimulus is delivered for 4s, followed by an inter-stimulus interval of 5s, following which the second odor is delivered. Out of the detected odors during the detection task, four odors were chosen for pair generation for the subsequent odor matching task (Figure 2.2B).

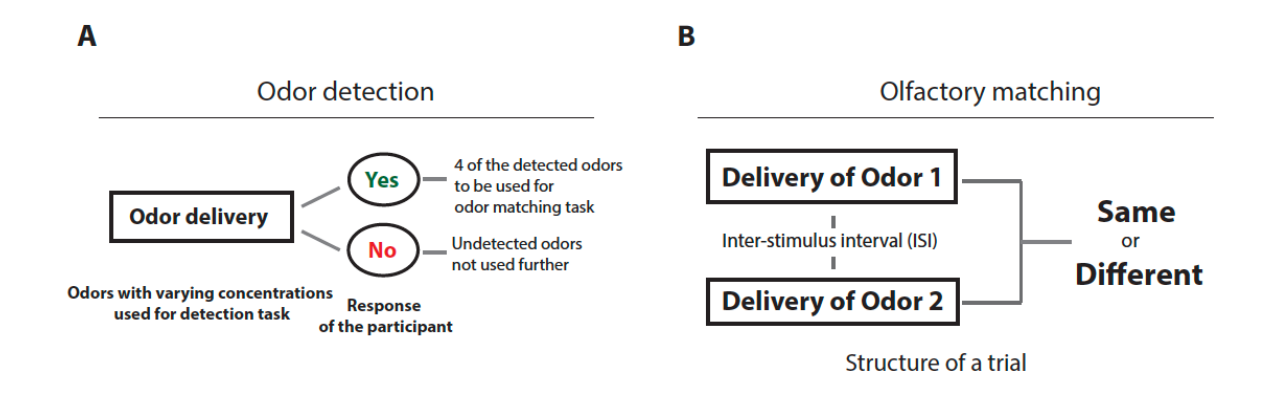


Figure 2.2. (A) Schematic diagram of the odor detection task is shown. 10 monomolecular odors, each at four different odor concentrations, are used for the detection task. Every odor at a given concentration is delivered for 4s using a custombuilt olfactometer. Participants verbally confirm successful detection. Four of the successfully detected odors at 50% concentrations are further used for odor matching experiment. (B) During the odor matching task, participants are presented with two odor stimuli separated by an interval of 5s. Once the second stimulus is presented, the participants can respond on whether the presented odors are same or different. At the end of the session, the percentage of correct responses is calculated.

## 2.3.4. Olfactory learning across sessions

Subjects perform the odor matching task ideally for 5 consecutive days. Two consecutive sessions are kept at least 20 hours apart. A maximum relaxation of two days is accommodated for participants, both patients and healthy, for those who are unable to appear for the experiment on consecutive days. This way, each participant completes the olfactory learning paradigm in a maximum of 7 days. Participants are not informed about their performance score before the end of the final session so as to prevent any confounding effects on experimental outcome.

## 2.4. Olfactory behaviour in mice

# 2.4.1. Olfactory behavioural training using odor matching paradigm

To probe the neural mechanisms of the olfactory matching and investigate the temporal limit of olfactory working memory, a parallel paradigm to human odor matching task is designed for mice. In this paradigm, the two odors to be matched were delivered for duration of 2s while being separated by a delay period. The delay period for the experiments were 2s at the beginning of the training. Once the animals learnt the task for 2s over 6-7 tasks, the interval is then increased depending on the experimental design. The response window is designed to coincide with the delivery of the second odor. The duration of this second odor delivery divided in four 500ms bins. For a successful rewarded trial, the animals are required to lick in at least 3 of the 4 bins and

for a successful non-rewarded trail, the animals should lick in no more than 2 bins. To eliminate any confounding effect of reward criteria, half the animals were trained with same odor matching as rewarded while the other half had different odor matching as rewarded.

# 2.4.2. Behavioural training in freely moving mice

# 2.4.2.1. Apparatus

The apparatus used for behavioural training of mice in the odor matching paradigm is an eight channel olfactometer. <sup>233</sup> A cubic chamber houses the animal during the training. On one side of the chamber a large circular cut-out allows entry of the animal's snout to the sampling and odor delivery port, both in relatively close proximity to each other. <sup>234</sup> The opposite side of the ports houses a concealed opening for an attached exhaust that rids the chamber of any residual odors throughout the duration of the training. Trial is initiated by the animal by breaking an infra-red (IR) beam at the sampling port. A lick port allows for recording the licking of animals during each trial. During each odor delivery odorized from one of 8 channels travel through tygon tubing at a rate of 2 litres per minute. Two valves control the delivery of the odors to the chamber, the odor valve and the final valve. The odor valve opens 500 ms prior to the opening of the final valve. An exhaust is kept on at all times except during the delivery of the odor. For each successful rewarded trail, the animal is rewarded with 3 µl of water.

### 2.4.2.2. Habituation and pre-training

At first a set of 12 C57BL6/J male mice of age no more than 6 weeks were trained for Amyl Acetate and Ethyl Butyrate odor pair for a stimulus delay of 2s. This was carried out as a pilot experiment to ensure optimal functioning of the paradigm. To eliminate any doubt regarding confounding effects of the selected odor pair, a second pair odors, Hexanal and 2-Pentanone are employed.

Animals are habituated with the operant chamber by putting them inside for 5-10 minutes. Unless otherwise required, pretraining phase follows the next day. Animals are water-deprived for no more than 12 hours prior to the experiment each

day. Sincere efforts were taken to ensure that animals were trained at relatively equal intervals every day. At the end of the training, free water is provided for a maximum of 5 minutes.

Pretraining of animal prior to training were carried out as follows:

- Phase 1: Reward for every IR beam break.
- Phase 2: Reward is delayed by 1s after the IR beam is broken
- Phase 3: Reward is delayed by 1s after the IR beam is broken. Additional criteria:
   1 lick, ITI = 5s
- Phase 4:  $BB^{*1} \rightarrow OV^{*2}$  opens for 2s  $\rightarrow$  lick in >1 bin, ITI =5s
- Phase 5: BB → OV & FV\*3 with MO\*4 opens for 2s, lick in >1 bin, ITI=10s\*4
- Phase 6: BB → Odor 1 for 2s → 500ms ISI → Odor 2 for 2s, lick in >1 bin
- Phase 7: BB → Odor 1 for 2s → 500ms ISI → Odor 2 for 2s, lick in >2 bin
- Phase 8: BB → Odor 1 for 2s → 1s ISI → Odor 2 for 2s, lick in >2 bin
- Phase 9: BB → Odor 1 for 2s → 2s ISI → Odor 2 for 2s, lick in >2 bin

\*1BB=Beam Break, \*2OV=odor valve, \*3FV=final valve, \*4MO=mineral oil \*4 ITI is kept 10s from this stage onwards, including training

Animals performed at least 40 trials in each phase. For some animals few additional trials were required if the animals showed sluggish learning of the paradigm or performed in an improper fashion. Usually, a maximum of 60 trials per animal in each phase were enough to complete the pre-training phase.

## 2.4.2.3. Training with olfactory matching paradigm

In order to probe neural mechanisms of odor matching in mice, an equivalent delayed matching paradigm was employed for rodents (Figure 2.4). The rodents were trained in a set of three freely moving olfactometer setups. The sampling port is guarded by an IR beam. As the animals pokes its snout in the sampling port, the IR beam breaks, initiating the trial. The initiation of the trial is marked by the delivery of the first odor for 2 seconds followed by a delay. After the delay, the second odor is delivered for 2s. There

is no separate response window for this paradigm. The response window is superimposed with the delivery of the second odor. The duration of this later odor delivery divided in four 500ms bins. For a rewarded trial, the animal has to lick in at least three of the four bins to get a reward. For a non-rewarded trial to be correct, the animal must not lick in more than two of the four bins. As trained, animals are required to start licking for correct trial as soon as they match the second odor with the first. Animals are trained for 6-7 tasks while initially training for a stimulus delay of 2s, where each task comprises of 300 trials. Once the animals are trained for an ISI of 2s, the delay period is further increased as per the need of the experiment. The entire paradigm is operated by a custom-written program on Igor Pro\*. The number of trials performed by the animals greatly vary depending on the delay period employed and the motivation of the animals. For 2s delay, most animal perform around 50-60 trials each day. But this number goes down significantly for higher ISIs.

## 2.4.3. Measurement of behavioural parameters

Several parameters are characterized while analysing the data, like learning curve, lick pattern, sample pattern and odor matching time (OMT).

# 2.4.3.1. Learning curve

As mentioned before, the animals perform 6-7 tasks where each task consists of 300 trials. The accuracy of odor matching for each animal is calculated for every 100 trails. Consequently, for each task, three data points are achieved that indicate the matching accuracy of each animal for every 100 trails. This way for a 6-task long training, a total of 18 data points is calculated for each animal. As these data points are plotted against the corresponding stage of progression in the training, a learning curve emerges that reliably depicts the learning of the odor matching task.

# 2.4.3.2. Sample pattern

As the animals break the IR beam, it breaks a circuit and the operating program records this with a time stamp. Every time the animal pokes its head inside the sampling port

irrespective of the stage of the trial, a time stamp records this breaking of IR beam. The sensor here samples with microsecond accuracy and each sampling bin averages over a period of 20 ms. This can later be plotted to visualize how often the IR beam was broken. This data serves as an indicator of the animals' performance motivation.

# 2.4.3.3. Lick pattern

As described in the description of the apparatus, the animals perform in a chamber that has a copper plate at the bottom. As soon as an animal starts to lick at the lick port, as trained, a closed electrical circuit, via a wire connected to the outer face of the copper plate, records each lick. The sensor here records with microsecond accuracy and each data point represents an average value of lick over a period of 20 ms. This way, a trial 6 seconds long, comprises of 300 bins. As this data is plotted, the licking behaviour of the animal against the progression of the trial can be visualized.

# 2.4.3.4. Olfactory matching time (OMT)

If the lick patterns are separately plotted for the rewarded and non-rewarded trail, for each animal, performing a t-test for each 20 ms bin correlates to the statistical significance of the divergence of the two curves. Usually, after the delivery of the second odor a well-trained animal tends to vigorously lick for a rewarded trial while retracts its head for a non-rewarded one. This will reflect in the value described previously. As can be seen in Figure 2.3, once the p-value curve is plotted, with rare exceptions, the p-vlue declines below 0.05 and never shoots back up. This indicates a permanent decline or absence of licking in learned animal for non-rewarded trails in comparison to continued licking for rewarded ones. Time taken to reach this statistically significant divergence is characterized as olfactory matching time (OMT). OMT is a correlate of the decision-making time of the animals when rewarded and non-rewarded odor matching trails are taken as a whole.

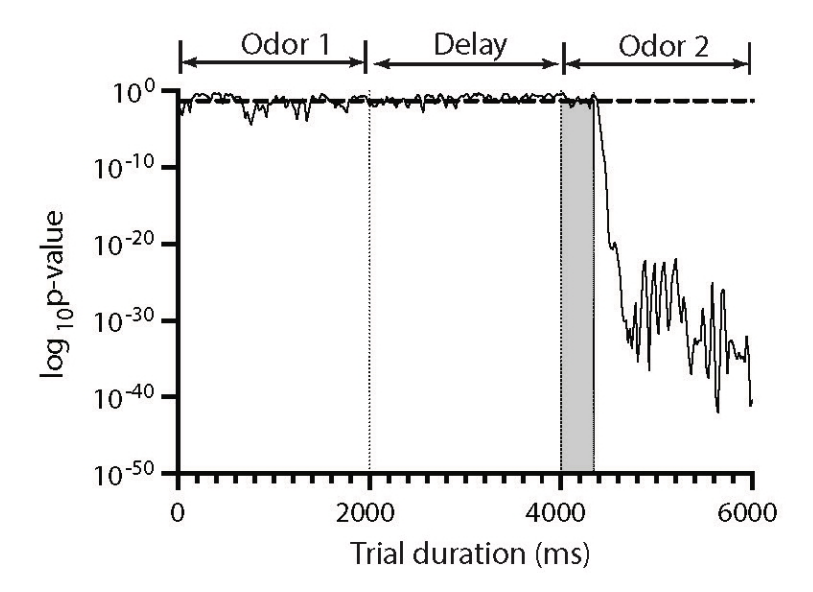


Figure 2.3. Calculation of olfactory matching time (OMT). OMT is calculated as the total time lapsed from the onset of the second odor and the permanent decline of the p-value curve below 0.05. Here the same is depicted with  $\log_{10}$  (p-value) on the y-axis. The shaded region corresponds to the olfactory matching time.

## 2.5. Generation of conditional knockout mice

# 2.5.1. Confirmation of stereotactic coordinates using fluorescent dye

As neurons in the granule cell layer (GCL) of the olfactory bulb (OB) are targeted using Cre-viral particles, an optimization step is undertaken to ensure that the viral particles are delivered to the intended later of the OB. Two C57BL6/J animals are injected with Invitrogen dye (diluted with PBS in 1:1 ratio) (details to be confirmed) at previously optimized coordinates in each of the olfactory bulbs. The animals are then sacrificed, and OB sections are acquired using cryotome. A DAPI staining is carried out to visualize the nuclei in the OB section. The locations of the injected dye were checked using an epifluorescence microscope.

# 2.5.2. Surgical injection of Cre-viral particles

Being a delayed non-match to sample (DNMS) task, olfactory matching (OM) involves components of both sensory and working memory. As the animals are trained for extended periods of time, this is likely to induce long-term potentiation (LTP). AMPA and NMDA receptors are known to play important roles in LTP formation. <sup>235,236</sup> GluA2 and NR1 are sub-units of AMPA and NMDA receptors respectively. GluA2 KO mice will have higher Ca<sup>2+</sup> influx into the cell<sup>237</sup> thereby increasing inhibition on the projection neurons, namely the mitral and tufted (M/T) cells. Whereas NR1 KO would in turn limit cation entry<sup>238</sup> in the Gad2 positive neurons. This would decrease inhibition on the M/T cells. Stereotactic optimization injections were first carried out using a fluorescent dye to check for GCL specificity. Coordinates for stereotactic injections were adopted from Abraham et al., (2010). <sup>109</sup> As first set of experiments with GluA2 conditional KO mice, 12 sham and 12 Cre viral particle injections were carried out for AAV mediated expression of EYFP-Cre. For the second set, we injected Cre viral particles in 12 NR1 lox mice and equal number of sham surgeries. An incubation period of 3 weeks was kept before starting the behavioural experiments.

### 2.5.3. Habituation and pre-training

The task habituation was carried out in an identical fashion as mentioned in the section 2.4.2.

1% odor solutions were used for all experiments and old odor vials were regularly replaced with freshly made odors. Mice received ~3 ul water for each correct response for rewarded trials. For this set of experiments, inter-stimulus interval (ISI) is kept at 2s. For each trial, the 2s lick window started as soon as the second odor is delivered. The animal must lick in more than two 500ms long bins for rewarded trials and two or less 500ms bins for non-rewarded trials in order to be considered as correct trials.

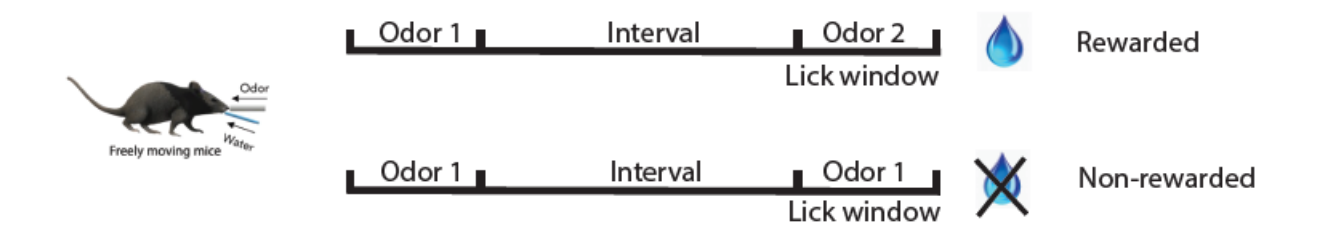


Figure 2.4. Odor matching paradigm for freely moving mice. One group of animals are trained to lick for matching same odor pairs while another group is trained with opposite reward criteria.

## 2.5.4. Measurement of olfactory matching time

Olfactory matching time is calculated using the lick pattern for rewarded and non-rewarded trials in identical fashion as mentioned in section 2.4.2.4.

## 2.5.5. Immunohistochemistry

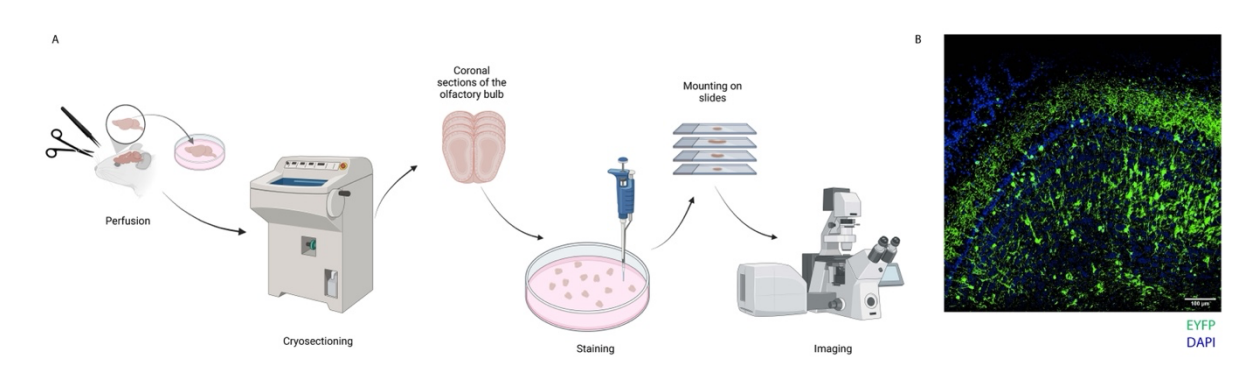


Figure 2.5. (A) A schematic representation of immunohistochemistry of mouse OB. (B) A confocal image of one of the OB sections with EYFP expressed by neurons expressing Cre-carrying viral vectors and nuclei stained with DAPI.

Immunohistochemistry of OB samples (Figure 2.5) were carried out based on previously published work from the lab by Pardasani et al., 2023.  $^{111}$  Once training is complete, animals were perfused with 4% paraformaldehyde (PFA) and the OBs were isolated and kept in 4% PFA overnight at  $^{40}$ C. The next morning, the samples were washed and shifted to 30% sucrose solution for 24-36 hours, till the sample sinks to the bottom of the solution. Once the brain is dehydrated in sucrose solution, 50  $\mu$ m thick

sections were prepared using a cryotome (Leica Biosystems) and the slices are collected in 1X PBS in a 24 well plate. The sections were then washed thrice with 0.1% TritonX PBST solution in order to permeabilize the tissue.

For antibody staining, the permeabilized slices were incubated at 4°C with primary antibody for 12-14 hours and then then secondary antibody is added to the section. This is further incubated for 2-4 hours. Finally, the sections are incubated with DAPI (1µMin PBS) for 15 minutes. For experiments that does not require staining for a specific protein, tissue slices were subjected to DAPI incubation immediately after the permeabilization step. The sections were then mounted on a clean glass slide and fixed with a antifading agent (VECTASHIELD\* Mounting Media) and covered with a thin cover slip. The sections are ready for imaging and are stored at 4 degrees.

#### 2.5.6. Protein estimation

To check whether conditional knockout for intended proteins has been successful, protein estimation is carried out for specific proteins of interest using western blot (Figure 2.6). The protocol was adapted from previously optimized work by Mahajan et al., 2024 (bioRxiv).<sup>234</sup>

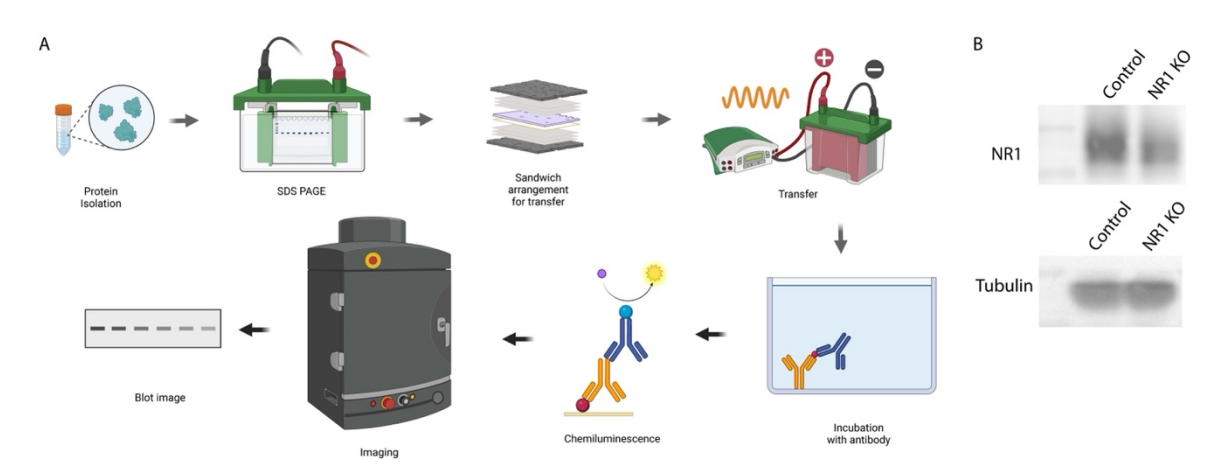


Figure 2.6. (A) A schematic diagram of Western Blot for protein estimation. (B) Blot images comparing NR1 protein levels in mouse OB for controlled and NR1 KO animals while bands corresponding to tubulin acts as control.

Olfactory bulbs for both control and experimental animals are dissected out using 1X PBS and flash frozen using liquid nitrogen (-196 °C). The samples were preserved at -80

°C for processing later. The samples are crushed in 150-200ul RIPA buffer, supplemented with Protease Inhibitor Cocktail; PIC 1:50, using a homogenizer. This mixture is spun at 14000g for 30mins at 4 °C. The supernatant, which contains all the proteins devoid of debris, is taken. Protein concentration is estimated for all samples using BCA Estimation Kit (Thermo Fisher Scientific. #23225). Further, samples for western are prepared by heating the supernatant solutions in 1x Laemmli buffer at 95 °C for 10 minutes. Equal protein amount for both the groups is then loaded on SDS PAGE gel along with a ladder and an electrical potential is applied for a charge-based separation of the protein. Once the gel-run is complete, the separated proteins are transferred to a 0.45 um thick polyvinylidinefluoride (PVDF) membrane (Merck Immobiolon IPVH00010). Following the transfer, the blot was blocked for one hour at room temperature in a solution comprising 5% skimmed milk or 5% BSA dissolved in 1X TRIS-buffered saline (TBS) with 0.1% Tween-20 detergent (Sigma-Aldrich, #P9416). Subsequently, the primary antibody was applied and incubated at 4°C for 12 to 16 hours. The blot was then subjected to three washes, each lasting 15 minutes, using 1X TRIS-buffered saline (TBS) with 0.1% Tween-20. Thereafter, the secondary antibody was added at a dilution of 1:10,000 and left at room temperature for one hour. The blot underwent another series of three washes before being developed using the ECL Western Blotting detection reagent (GE Healthcare Amersham, #RPN2236).

Once image of the blot is acquired, ImageJ was used for quantifying the relative protein levels in the samples. For quantification, an ROI was drawn using box toll in ImageJ around the bands and mean intensity was taken. To make the data more interpretable, the mean intensity values were subtracted from 255. This step is performed because in an 8-bit grayscale image, the pixel intensity ranges from 0 (black) to 255 (white); thus, subtracting the measured mean intensity from 255 provides a measure where higher values correspond to darker bands, indicating higher protein concentration. <sup>239</sup> This approach is useful for visualizing the contrast between the bands more clearly. This was done for both NR1 and Tubulin. A ratio of subtracted intensities of NR1 and Tubulin was taken (NR1/Tubulin) for both control and NR1KO and these normalized values were plotted using GraphPad Prism 10.4.1. Analysis was done using Mann-Whitney Test.

## Chapter 3

# Uncertainty revealed by delayed responses during olfactory matching

#### 3.1. Introduction

Over the past few decades, many psychophysical and psychosocial studies have investigated olfactory capabilities in humans. Interest to probe for different parameters to assess olfactory capabilities in humans grew as a result of the possible correlation of deficits in sense of smell with certain traumas and neurodegenerative diseases.<sup>240,241</sup> Olfactory dysfunction has been indicated as one of the dominant pre-clinical symptoms in Parkinson's and Alzheimer's disease. 242,243 Several other neurocognitive deficits like dementia and neurodegenerative conditions like ALS have been implicated in differential diagnosis long before clinical symptoms become apparent. 244,245 In recent years, COVID-19 associated loss of sense of smell has been a major concern in millions of patients. 96,246-248 While many patients who suffered from SARS CoV-2 infection regained their sense of smell, many did not. This adds to the long list of conditions that share a common pathophysiological threat in the form of olfactory dysfunction. Many tests and assessments indicate decreased odor identification, detection and sensitivity in PD patients. 249,250 Deficits in olfactory capabilities are considered to be the prodromal symptoms for such diseases. Olfactory functions are also negatively affected in patients with certain traumatic brain injuries.<sup>251</sup> Increasing evidence of olfactory impairments in patients suffering from psychosis suggests it to be a non-invasive pre-morbid marker for certain disorders, such as Schizophrenia.<sup>252</sup> There has also been a rise in psychiatric conditions in the advent of the pandemic.<sup>253</sup> Under these circumstances, testing olfactory abilities, therefore, may turn out to be extremely valuable in diagnosing many neurodegenerative and infectious diseases.

Most psychophysical studies in the field and the ones mentioned above utilize semantic or non-semantic, analytical laboratory tests.<sup>254</sup> These include Sniffing stick<sup>255</sup>, University of Pennsylvania Smell Identification test (UPSIT)<sup>256</sup>, Scandinavian odor identification test<sup>257</sup>, two-alternative forced choice odor detection threshold test<sup>258</sup> etc. UPSIT, one of the first odor identification tests to be introduced, is a 'scratch and sniff' test consisting of a booklet of 40 microencapsulated odorants which are released from

the strip upon scratching. 256 In this test, an individual has to choose from one of the four options which closely identifies the odor he/she smelled. Versions of UPSIT are adapted in different countries, particularly due to the varying availability of the odors across these countries. 259 A 12-item Cross-Cultural Smell Identification Test (CC-SIT) was developed<sup>260</sup>, by carefully picking 12 odors from UPSIT to which individuals from different countries, race and age gave similar responses. Sniffing stick test, on the other hand, provided odors as liquid or dissolved in propylene glycol in pen-refills to the patients to carry out detection (based on staircase dilution of the same odorant, nbutanol) discrimination and identification.<sup>261</sup> Discrimination using Sniffing sticks is performed by choosing one differentiating odor out of the three provided at once. 16 such triplets of pen refills are employed for odor discrimination.<sup>262</sup> Odor identification in these tests have semantic grounds which may lead to variation when applied to individuals from different cultural backgrounds. This led to the development of nonsemantic multi-component olfactory tests, for instance, the SMELL-S (sensitivity) and SMELL-R (resolution) tests.<sup>263</sup> These tests involve distinguishing varying pairs of odor mixtures (comprising 30 components) presented in three separate vials for a given trial. This when varied in dilution of mixing, indicated olfactory sensitivity and when varied in the common number of components between the differentiating odors, indicated olfactory resolution.

The presentation of odors in all these tests is either through paper strips, vials or refills, which makes it challenging to control the precise odor delivery and accurately quantify the temporal component of the odor discrimination. Given how the participants can reiteratively smell between the pens or strips containing odors, reliable evaluation of how quickly they can detect and discriminate between odors cannot be done. Although such tests can be used for assessing olfactory capabilities in humans to certain extent, they may not be ideal to probe olfactory decision-making and working memory. Decision-making during discrimination can be influenced by imprecise experimental conditions such as varying the time between the presentation of odors or other complexities like the different chemical classes or the complexity of the odors used. To precisely explore these aspects of human olfactory abilities, we custom-built an 'olfactory-action-meter' which can deliver one odor at a time directly to the nostrils of the individual and allows for a quantitative estimation of accuracy of performance

and the reaction time for discriminating across different classes of odors. To reduce any bias or variability introduced by the experimenter, the entire paradigm from the precise delivery time of the odor to admitting the response of the participant has been fully automated. Olfactory paired association tasks are conducted for which the participant decides whether the two presented odors are same or different. We have carried out such paired association tasks by varying the time duration, i.e, inter-stimulus Interval (ISI) between the odors. Generation of random odor-pairing trials and varying the difference in ISI using the 'olfactory-action meter' allow us to evaluate the effect on the olfactory working memory of humans. We have been able to show that the discrimination performance accuracy decreases with increasing the ISI, suggesting that there is a limit to the duration for which the working olfactory memory can be optimally maintained. We also showed that with increasing the complexity of the odors, accuracy for olfactory discrimination declines while the response time increases significantly. We also report a correlation between longer response time with higher probability of incorrect response and improved olfactory discriminability with repeated sessions. We do not find any effect of age, gender, food preference and smoking habit on participants' olfactory performance although the relative limitation of the number of participants cannot be discounted.

#### 3.2. Materials and methods

### 3.2.1. Chemicals used in the experiment

All odors used in the experiments were ≥99% pure (Sigma-Aldrich). Odor bottles remined sealed after every use and stored in vacuum at normal room temperature throughout the duration of the experiment. Odors that required storage under cold temperatures were refrigerated.

### 3.2.2. Study Population

In accordance with the guidelines, individuals aged between 18 and 80 years were included in the study. Participants were scheduled for appointments between 10 AM and 5 PM on weekdays. Prior to the experiments, subjects completed a comprehensive questionnaire detailing their olfactory abilities, food preferences, smoking habits, and

other relevant information. Participants who registered online provided basic personal details and their availability during weekdays. They were subsequently contacted based on their availability. Only healthy individuals with no known neuropathology were invited to participate in this study.

### 3.2.3. Inclusion and Exclusion Criteria

The study included participants aged between 18 and 80 years. Individuals with any diagnosed history of neuropathy or neuropsychiatric conditions were excluded.

Additionally, participants with a known history of anosmia, hyposmia, or parosmia were not included in the study.

#### 3.2.4. Ethics Committee Guidelines

The experimental procedures and associated protocols were approved by the Human Ethics Committee at IISER Pune. In accordance with the guidelines, all experiments were conducted between 10 AM and 5 PM on weekdays, coinciding with the availability of healthcare services on campus in case of emergency. Participants had the option to discontinue their participation at any point during the experiment.

### 3.2.5. Study Location

All experiments involving healthy subjects were conducted on the IISER Pune campus.

### 3.2.6. Odor Preparation

Simple odor matching. For simple odor matching task, a set of nine monomolecular odors were employed that belong to different chemical classes and exhibit a wide range of vapor pressures (See Table 2.1). Highly purified monomolecular odors were diluted in mineral oil in a 1:50 ratio. 80  $\mu$ l of odor was added in 4 ml of mineral oil in order to make the odor. The concentration for every odor preparation was ~20  $\mu$ l/ml. Odors were prepared afresh every week ensuring optimal and consistent odor concentrations across participants and sessions.

## 3.2.7. Complex odor matching task

For complex odors matching tasks, odors were prepared by diluting odor in mineral oil in a 1:100 ratio. Two different groups of participants had performed the complex odor matching task. For one group, the stimulus odors were 60:40 binary mixtures of monomolecular odors whereas for the other group, 80:20 binary odor mixtures were used. The compositions of different odors are listed in Table 2.2 (Refer to Table 2.1 for odor abbreviations).

## 3.2.7.1.60-40 binary mixtures:

A total volume of 40  $\mu$ l of odors was diluted in 4 ml of mineral oil. A total of 10 monomolecular odors were used to make 5 pairs of binary mixtures for both 60:40 and 80:20 odor mixtures (Table 2.2). Odors were added to 4 ml of mineral oil by volume, i.e., 24  $\mu$ l and 16  $\mu$ l, respectively. All the odor mixtures were freshly prepared every week to ensure optimal and uniform odor concentrations across subjects and sessions.

## 3.2.7.2. 80-20 binary mixtures:

A total volume of 40  $\mu$ l of odors was diluted in 4 ml of mineral oil. A total of 10 monomolecular odors were utilized to prepare 5 pairs of 80:20 binary mixtures (Table 3.2). Odors were added to 4 ml of mineral oil by volume, 32  $\mu$ l and 8  $\mu$ l, respectively. All the odor mixtures were freshly prepared every week to ensure optimal and uniform odor concentrations across subjects and sessions.

# 3.2.8. Olfactory-Action meter

We developed a novel behavioral test that can quantitatively and accurately measure olfactory abilities in healthy human subjects. The behavioral paradigm allowed for evaluation of both odor detection and odor matching abilities of the participants. The paradigm, termed as olfactory matching (OM) consisted of a detection task in order to measure the olfactory sensory abilities. Once the detection task is completed, the OM task was employed to evaluate the sensory-cognitive skills of the subjects. We custombuilt an Olfactory-Action Meter (OAM) for precisely controlled and automated odor

delivery with high temporal precision. A schematic diagram of the instrument can be seen in Figure 3.1A. The odor controlling unit contains 10 mass air flow controllers which can regulate air delivery independent of one another through the existing odor reservoirs. The output from these reservoirs is further diluted with ambient air. The odorair mixture is then directed via 12-channel glass funnel and subsequently through a nozzle attached to a ventilation mask. At the beginning of a session, the subjects are evaluated for their detection abilities. During the detection task, the subjects are presented with each odor individually to evaluate whether they are able to detect the odor or whether they find any odor aversive. If a participant cannot detect or dislikes an odor, it is excluded from the odor matching task. Once the detection task is done, a detection index is calculated for the subject. Only if subjects have a DI index of more than 0.5, OM task is performed. For a trial of an OM task, the participant has to sample and compare the two odors delivered and provide a response of whether the two odor stimuli are 'SAME' or 'DIFFERENT'. The responses are provided using a response console placed in front of the subjects. The response control is a convenient, easy to understand console with three color-coded response option buttons. A display screen placed in front of the participant providing a visual cue to notify the odor delivery onset and a real time response timer to indicate the response window. Along with the visual cue, trial onset is marked by a 200 ms tone.

### 3.2.9. Olfactory detection task

Prior to the commencement of each session, participants were subjected to a detection task wherein each odor included in the experiment was presented individually. Participants were required to confirm the detectability of each odor. Only those odors that were successfully detected were included in the experiment. In instances where an odor was reported as aversive or uncomfortable by a participant, it was excluded from the olfactory matching (OM) task. Upon completion of the detection task, participants proceeded to the OM paradigm. For both simple and complex odor detection tasks, we achieved a mean detection accuracy exceeding 90%.

## 3.2.10. Olfactory Matching Paradigm

The OM paradigm consisted of 20 trials per session. Each trial involved presenting two odors, each for 4 seconds, separated by an interval known as the inter-stimulus interval

(ISI). After the second odor ended, an additional 5-second window was provided to allow the participant sufficient time to respond. ISIs varied across subjects but remained constant throughout each session. The odors were generated by a randompair generator program based on the odors detected by the participant in the odor detection task. The two odors delivered in each trial were either identical or different. The participant selected one of two options and had the option to repeat a trial if desired. Two trials were separated by a 4-second inter-trial interval (ITI). After the participant responded to all 20 trials in a session, the overall accuracy for the session was displayed by the program. Individual trial responses and reaction times were recorded in real time. OM was conducted using both simple and complex (binary mixtures) odors, with the basic sequence of events remaining constant throughout all the OM sessions.

# 3.2.10.1. Simpleodomatching

Simple odor matching tasks followed the sequence of events as described above with monomolecular odors. 9 odors were used (Refer to Table 2.1, Chapter 2). Four different ISIs were employed in simple odor matching sessions: 2.5s, 5s, 7.5s and 10s. Comparable numbers of participants were assigned to all four ISI sessions. Once the detection task was complete, a specific ISI was assigned to each participant by the experimenter. After that, based on the detectability of the participant, random simple odor pairs were generated.

## 3.2.10.2. ComplexOdomatching

Complex odor matching task followed the sequence of events as described above with binary mixtures of monomolecular odors. Two different types of odor mixtures have been employed, 60-40 and 80-20 binary mixtures. Both these mixtures were used for OM in independent sessions (See Chapter 2 for detailed information).

## 3.2.11. Detectability index calculation

Detectability index (DI) for a participant is calculated by the ratio of total number of odors detected and the total number of odor presented.

Detectability index (DI) = 
$$\frac{\text{Number of odors detected}}{\text{Number of odors presented}}$$

### 3.2.12. Calculation of chance level

The chance level can be calculated for each session of OM task. As the number of same and different odor pairs are not fixed for each session, the chance level for each session would vary.

Chance level for any particular session (%) =

$$({}^{n}C_{rs.} (P_s)^{rs} X (Q_s) ({}^{n-rs)} + {}^{n}C_{rd} X (P_d)^{rd} X (Q_d)^{(n-rd)} X (0)$$

where n = total number of trials, rs = number of same trials, rd = number of different trials,

 $P_s$  = Probability of carrying out the same trial correctly,  $P_d$  = Probability of carrying out the different trial correctly,  $Q_s$  = Probability of carrying the same trial incorrectly,  $Q_d$  = Probability of carrying out the different trial incorrectly.

The individual probabilities relating to same and different trials can be added to find the overall chance level of the session. When averaged across all the sessions performed by all the participants, the chance level matching accuracy has been found to be approximately 25%.

## 3.2.13. Data and statistical analysis

All data is plotted using Graphpad Prism® 8. Two-tailed paired and unpaired t-tests, Kolmogorov-Srimov tests, ANOVA with Post-hoc comparisons were carried out.

#### 3.3. Results

# 3.3.1. Development of the Olfactory-action meter for assessing the sensory and cognitive behavioural correlates in humans

Olfactory dysfunction has long been implicated as an early sign of several neurodegenerative diseases. 242,243 Olfactory related cognitive readouts have become more and more relevant in the recent years with the advent of COVID-19 associated loss of sense of smell96 and long-COVID.97 Several paradigms that are either administered by the researchers or the participants themselves can be used to assess olfactory abilities in human subjects. 265 Healthy participants were asked to assess their olfactory ability using common household items available at home. An online questionnaire of the common household items were prepared and participants were asked to perform a detection task at home. Successful detection is marked by a score of 1 while unsuccessful detection drew a score of 0. All 143 participants, each sampled 33 odorous items grouped into different clusters, submitted their response (Figure 3.1A). We see high detectability for most odorous objects across the sampling set except for eggplant and strawberry. This kind of assessment is often crude and has very little or no control over odor delivery. To mitigate such shortcomings and ensure higher control over the odor delivery process, we set out to develop a custom-made olfactometer that can be used to precisely deliver odor plumes to human subjects (Figure 3.1B). We developed a novel behavioral paradigm that can quantitatively measure olfactory abilities in human subjects. The behavioral paradigm consisted of a

detection task to measure the sensory abilities followed by an olfactory matching task to evaluate the sensory-cognitive skills of the subjects. The odor controlling unit (Figure 1B) contains 10 mass air flow controllers which independently regulate air delivery through odor reservoirs. The output from these reservoirs is further diluted with a stream of clean air. The odor-air mixture is then delivered through a 12-channel glass funnel (Figure 3.1A). The output from the funnel is attached to a ventilator mask. At the beginning of a session, the subjects are evaluated for their detection abilities. The odors detected by the subjects during the detection task are then selected for Olfactory Matching (OM) task. For a particular trial of an OM task, the subject has to sample and compare the two odors delivered and provide a response of whether the two odor stimuli are 'SAME' or 'DIFFERENT'. The flow of a single trial is depicted in Figure 3.2A. The responses are provided using a response console placed in front of the subjects. The response control is a convenient, easy to understand console with three colorcoded response option buttons. A display screen placed in front of the participant providing a visual cue to notify the odor delivery onset and a real time response timer to indicate the response window. Along with the visual cue, trial onset is marked by a 200 ms tone.

The odor selected for the experiments belonged to different chemical classes and had varying vapour pressures. This diverse representation on the basis of their physico-chemical properties allowed us to investigate the changes in response patterns across a wide variety of odors. (See Table 3.1). To establish the varying physical properties of the odors and the preciseness of odor delivery, we quantitated the odor delivery pulse using a Photo-Ionisation Detector (PID). The PID measurements proved that the monomolecular odors as well as odor mixtures selected in our experiments had voltage amplitude differences depicting differences in their properties (Figure 3.1C). Irrespective of the intrinsic differences in the odors, the instrument delivered the odor with a sharp pulse which lasted for 4 s. As odors can have varying perceptual intensities across the subjects, it was important to test the detectability for the odors utilized. We measured the Detection Index (DI = number of odors detected/Total number of odors presented) for each participant (Figure 1D). DI values thus represents the subset of odor detected and ranges from 0 (No detection) to 1 (100% detection). Along with monomolecular odors, we were interested in studying

how human subjects fare in odor mixture detection. How humans perceive odor mixtures lacks consensus in the field. 266 While in certain studies, it has been shown that the perception is primarily synthetic wherein human subjects find it difficult to identify the components of odor mixtures. However, when odor concentration is increased or when one component dominates in the mixture, perception can be analytical, wherein subjects can detect the individual components in the mixture. To minimize such confounding effects, we restricted the OM task to binary mixtures (80-20 vs. 20-80 and 60-40 vs. 40-60) with 1% odor concentration. When we measured DI for odor mixtures, we observed that the average DI for binary mixtures were similar to that of the DI observed for monomolecular ones (Two-tailed unpaired t-test, p>0.05), suggesting that subjects could detect simple as well as binary odor mixtures with similar efficiency. The similar average detection values observed for odors belonging to different classes and having differing vapour pressures across the varying complexities further allowed us to use these odors for testing OM task with varying odor delays between the two odor presentations. Thus, the DI served as a sensory index, but to further investigate the sensory-cognitive index, we developed a paradigm of matching of odors when presented in pairs separated only by an interval. We find that the subjects have a minimum mean DI of >0.8, meaning that almost every participants had a success rate of above 80% in identifying the odors presented during the detection task. For few odors, this number often exceeds 0.9 indicating a >90% success rate in detecting these odors upon presentation.

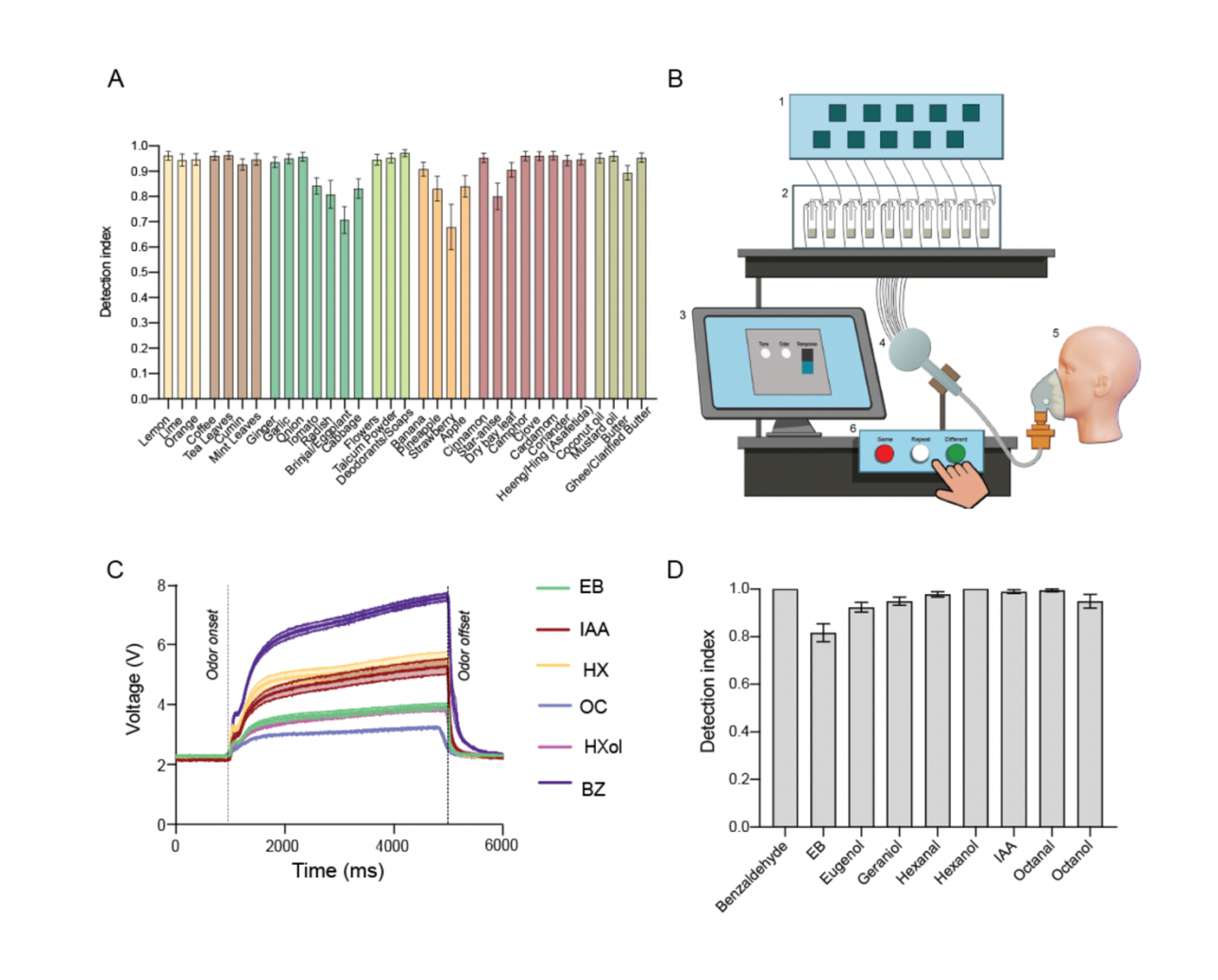


Figure 3.1. Olfactory-action meter for quantitative analysis of human olfactory matching ability. (A) Schematic diagram of the olfactory-action meter. Participants received two odors separated by an inter-stimulus interval (ISI). After sampling the second odor, the participant had to decide if same or different odors were delivered. Based on the decision, SAME or DIFFERENT buttons kept in front must be pressed within the response window. In case of any confusion, the REPEAT button could be pressed to reinitiate the trial. (B) Sequence of events during an olfactory matching trial is depicted. Each trial started with a tone. Once the first odor is delivered for 4s, a predecided ISI is applied, which is followed by a 4s delivery of the second odor. An additional response window of 5s was provided. The participant could respond as soon as the second odor delivery started. Two trials are separated by an inter-trial interval (ITI) which is kept constant at 4s. (C) Photoionization detection (PID) measurements of voltage fluctuations for simple odors are plotted. Odor is delivered for 4s. Values are averaged across 10 sets of measurements. (D) Detection indices of odors delivered via the OAM, averaged across subjects (N = 180 healthy human subjects, average DI values vary from 0.81 to 1 indicating that most participants were able to

successfully detect at least 80% of the presented odors).

[\*Note of acknowledgement: This work has been done with equal contribution from Dr. Meenakshi Pardasani and Dr. Sarang Mahajan]

# 3.3.2. Faster response time correlates to more accurate matching performance

Once we found out that healthy humans can detect monomolecular odors with high accuracy, we set out to look at other more complex olfaction-based neurocognitive readouts. This is worth mentioning here that all these experiments have been carried out during the pre-COVID times. So, any alteration in the sense of smell that may have resulted from SARS CoV-2 infection could be avoided. As described previously, the OM paradigm involves matching two odors that are presented one after the other with a short delay in between. For the purposes of our experiment, we chose four different delay periods, 2.5s, 5s, 7.5s and 10s (Figure 3.2A). A total of 180 subjects ( $N_{2.5s} = 75$ sessions,  $N_{5s}$  = 78,  $N_{7.5s}$  = 53 and  $N_{10s}$  = 63) participated in the OAM-based OM task. Our findings reveal that the employed variation in the delay period durations did not influence the average performance of the participants (Figure 3.2B; p = 0.42, One-Way ANOVA). In the OM task, starting from the onset of the second odor, the participant gets a total of 9s to respond, out of which 4 seconds is the odor delivery period of the second odor and an additional 5 seconds designated solely for the responding. As previously discussed, each OM session involves 20 trails where the subject has to match odor pairs, both same and different odor pairs. We also quantified Olfactory Matching Time (OMT), which is the mean duration taken by the participant to respond in the matching task (averaged over a session of 20 trials). We did not find any significant difference in the OMT values across the ISIs employed (Figure 3.2C;  $N_{2.5s}$  = 75 sessions,  $N_{5s}$  = 78,  $N_{7.5s}$  = 53 and  $N_{10s}$  = 63; p = 0.21, One-Way ANOVA). This implies efficient and robust maintenance of olfactory WM (OWM) across the employed delay periods. As described previously, all sessions comprise the matching of the same and different odor pairs. So, as we compared odor matching accuracy between two types of odor pairs presented during one session, we did not find any significant differences between the groups (Figure 3.2D;  $N_{2.5s}$  = 75 sessions, p = 0.17;  $N_{5s}$  = 78, p = 0.36;  $N_{7.5s}$  = 53, p = 0.24; and  $N_{10s}$  = 63, p = 0.85; Paired t-test). In order to investigate whether there was a perceivable shift in response for individual trials across different delay periods

for the same and different odor pairs for correct and incorrect matching trials, we quantified and compared normalized OMT across groups. Our analysis revealed significantly longer OMT for the incorrect trials across all the ISIs (Figure 3.2E,  $p_{2.5s} < 0.0001$ ,  $p_{5s} = 0.003$ ,  $p_{7.5s} < 0.0001$ , and  $p_{10s} < 0.0001$ , Paired t-test for each ISI plot). This implies a positive correlation between swift decision-making and accurate performance in the odor-matching task. To investigate whether such trend exists for the same and different odor pairs, we further compared OMT values across ISIs. Our analysis shows that subjects took significantly longer while matching the same odor pairs compared to different odor pairs, but only in the case of correct trails (Figure 3.2F;  $p_{2.5s} = 0.0003$ ,  $p_{5s} < 0.0001$ ,  $p_{7.5s} = 0.0003$  and  $p_{10s} = 0.0013$ , Paired t-test for each ISI) and not for incorrect trials (Figure 3.2G;  $p_{2.5s} = 0.34$ ,  $p_{5s} = 0.57$ ,  $p_{7.5s} = 0.58$  and  $p_{10s} = 0.36$ , Paired t-test for each ISI). We further found that for 80% of the correct trials, OMT values lie between 3s to 5.5s (Figure 3.2H).

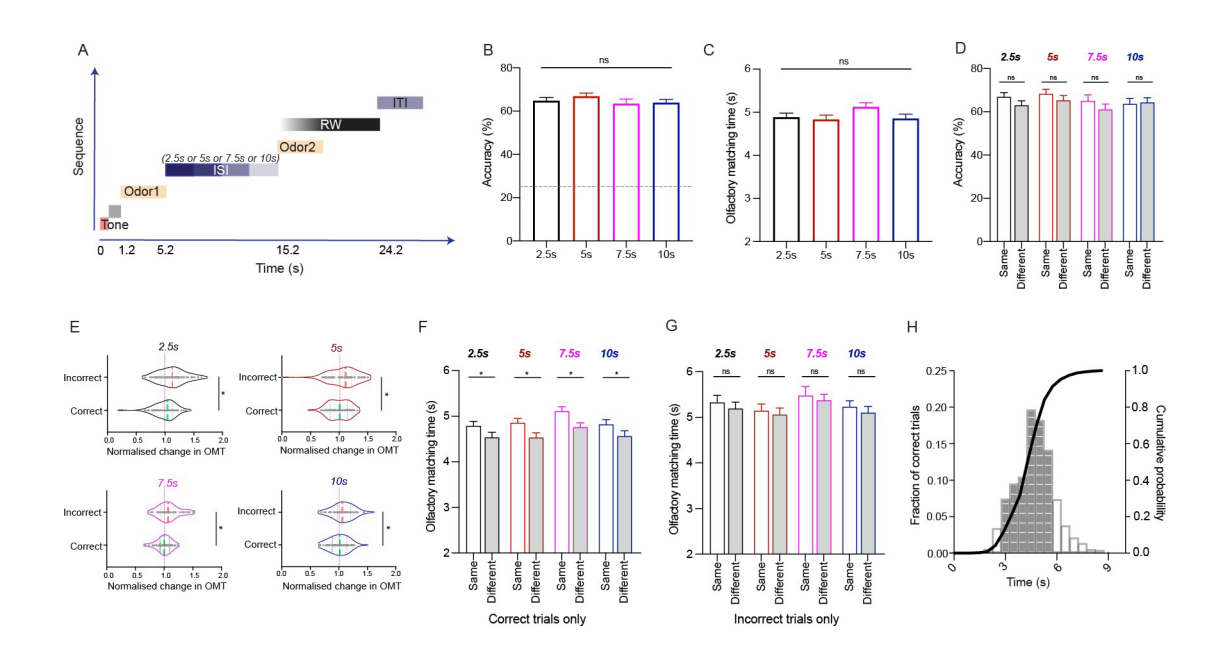


Figure 3.2. Faster response time correlates to more accurate matching performance (A) Schematic depiction of the sequence of stimulus delivery interspaced by delay period and finally being followed by a response window. Each trial starts with a tone that lasts for 200ms. This is then followed by the first odor being delivered for 4s. The delay period follows which may vary across sessions and will be one of the four possible durations, i.e., 2.5s, 5s, 7.5s, and 10s. After the delay, the second odor is presented for 4s, followed by a response window of 5s. The subject is free to respond as soon as the delivery of the 2<sup>nd</sup> odor is

initiated.

- (B) Odor matching accuracy is averaged across all the participants (Each comprises of 20 trials) for varying delay period between stimulus indicated that human OWM is robust enough to maintain an odor memory representation equally well across the different ISIs employed, i.e., 2.5s, 5s, 7.5s and 10s.  $(N_{2.5s} = 75 \text{ sessions (black bar)}, N_{5s} = 78 \text{ (red bar)}, N_{7.5s} = 53 \text{ (green bar)} \text{ and } N_{10s} = 63 \text{ (blue bar)}; p = 0.42, F = 0.93, One-Way ANOVA). The dotted line indicates the chance level of performance which has been separately calculated to be 25.75%.$
- (C) OMT remains comparable across ISIs ( $N_{2.5s}$  = 75,  $N_{5s}$  = 78,  $N_{7.5s}$  = 53 and  $N_{10s}$  = 63; p = 0.21, F = 1.524, Ordinary One-Way ANOVA).
- (D) Accuracies for matching of the same and different odor pairs are compared across the ISIs ( $N_{2.5s}$  = 75, p = 0.17;  $N_{5s}$  = 78, p = 0.36;  $N_{7.5s}$  = 53, p = 0.24; and  $N_{10s}$  = 63, p = 0.85; Paired t-test for comparing same vs different per ISI).
- (E) Normalized changes in OMT values are compared across ISIs for correct and incorrect responses. Green dotted lines indicate the mean normalized OMT for correct trials, whereas the red dotted lines indicate the shift in mean OMT for incorrect trials ( $p_{2.5s} < 0.0001$ ,  $p_{5s} = 0.003$ ,  $p_{7.5s} < 0.0001$  and  $p_{10s} < 0.0001$ , Paired t-test for each ISI plot).
- (F, G) OMT plotted for same and different odor pair matching for correct (p2.5s = 0.0003, p5s < 0.0001, p7.5s = 0.0003 and p10s = 0.0013, Paired t-test for each ISI) and incorrect (p2.5s = 0.34, p5s = 0.57, p7.5s = 0.58, and p10s = 0.36, Paired t-test for each ISI plot) trials respectively.
- (H) Histogram depicting fraction of correct trials distributed across the OMT subdivided into 500 ms bins (y-axis on the left). The shaded area in grey represents ~80% of the correct trials as performed by participants for which OMT lies between 3s to 5.5s. A cumulative probability curve in black is overlaid on the histogram (yaxis on the right).

[\*Note of acknowledgement: This work has been done with equal contribution from Meenakshi Pardasani and Sarang Mahajan]

# 3.3.3. Matching accuracy declines for complex odor matching

To investigate how odor matching performance is affected by increase in the complexity of the stimulus, we decided to use odor matching for binary odor mixtures. We chose two different odor matching groups. In one group, we used 60:40 vs 40:60 odor mixture and in the other, 80:20 vs 20:80. We ensured precise odor onset and offset using the custom-built OAM, which was confirmed by PID measurements (Figure 3.3A). Comparable DI values were observed for all 10 complex odor mixtures for all 107 subjects (Figure 3.3B). We found no statistically significant distance between simple and complex odor DI values (Figure 3.3C, Unpaired t-test). As seen in simple OM, we found no significant difference across ISIs for complex OM accuracy ( $N_{5s}$  = 58 subjects,  $N_{10s}$  = 47) (Figure 3.3D, Unpaired t- test, two-tailed, p=0.48). We further calculated the average chance level for complex odor matching across all the sessions and found it to be 25.04%. When we compared accuracy for same and different odor pair matching, we found no significant difference for either 5s or 10s ISI (Figure 3.3E,  $N_{5s}$  = 58,  $p_{5s}$  = 0.13 and  $N_{10s}$  = 47,  $p_{10s}$  = 0.86, Paired t-test).

As we looked at the OMT values for complex odor matching trials, we did not see any significant difference across ISIs (Figure 3.3F,  $N_{5s}$  = 58,  $N_{10s}$  = 47; p > 0.05, Unpaired t-test), indicating that OWM-based stimulus representation and maintenance does not alter performance for longer delays up to 10s, when compared to stimulus interval of 5s. In order to investigate whether there was a quantifiable shift in response for individual trials across the two delay periods for correct and incorrect matching trials, we quantified and compared normalized OMT across the two ISI groups. Our analysis revealed significantly longer OMT for the incorrect trials for both the ISIs, similar to our previous finding for simple odor matching trials (Figure 3.3G, Paired t-test, p<0.05). The green dotted lines in the violin plots indicate the mean normalized OMT for correct trials while the red dotted lines indicate the shift in mean OMT for incorrect trials.

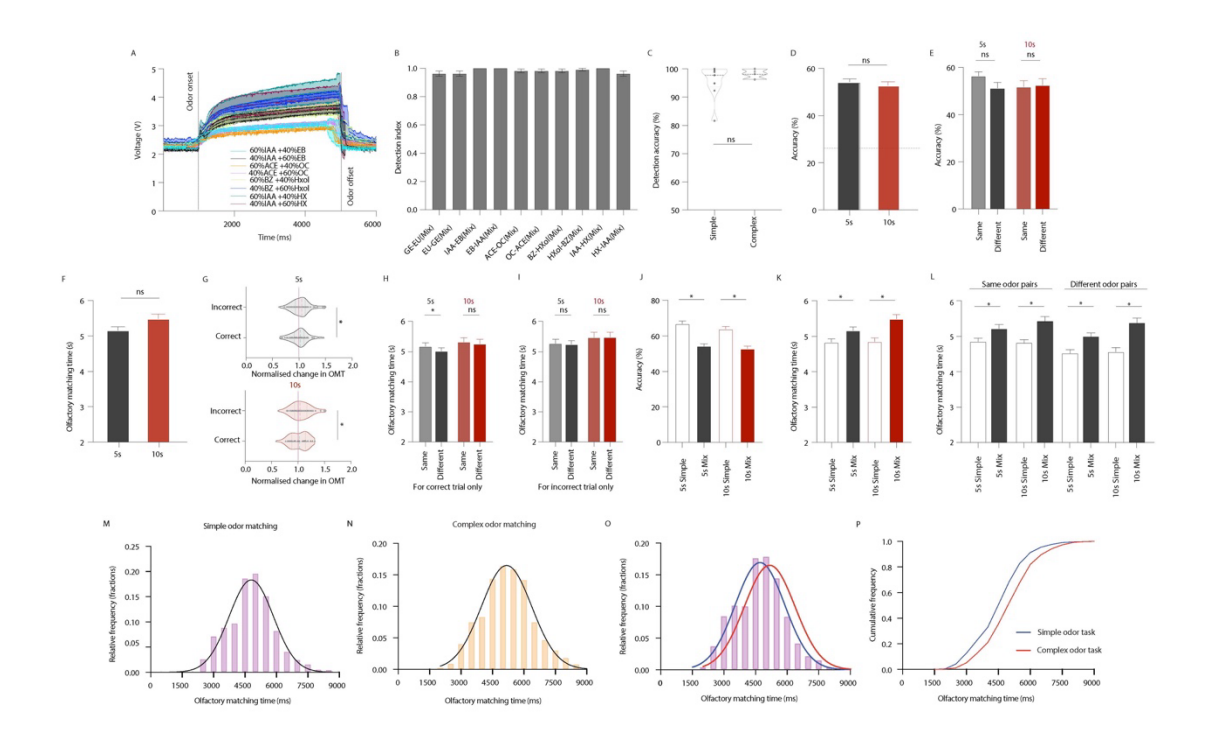


Figure 3. Odor complexity negatively correlates with matching accuracy and positively correlates with odor matching time

- (A) PID measurements for complex odors (60:40 binary odor mixtures) used for odor matching task. (IAA: Isoamyl Acetate, EB: Ethyl Butyrate, ACE: Acetophenone, OC: Octanal, BZ: Benzaldehyde, Hxol: Hexanol, HX: Hexanal).
- (B) Detection indices for binary odor mixtures for odor matching task. All odors show high detectability of >0.9 (N = 107 subjects).
- (C) DI values for simple and complex odor detection tasks are compared ( $N_{\text{simple}}$  odors = 9 odors,  $N_{\text{mix}}$  odors = 10 odors, p = 0.1, Unpaired t-test).
- (D) Accuracy for complex odor matching task is compared for 5s and 10s ISI. Data involving matching of 60:40 and 80:20 odor mixtures are combined. ( $N_{5s}$  = 58 subjects,  $N_{10s}$  = 47; p = 0.48, Unpaired t- test, two-tailed). Chance level performance for a binary mixture OM task was calculated to be at 25.04%).
- (E) Matching accuracy compared for same and different odor pairs for 5s and 10s ISI  $(N_{5s} = 58, p_{5s} = 0.13 \text{ and } N_{10s} = 47, p_{10s} = 0.86, Paired t-test).$
- (F) OMT compared across ISIs in all trials irrespective of trial outcome. ( $N_{5s}$  = 58,  $N_{10s}$  = 47; p > 0.05, Unpaired t-test, two-tailed).
- (G) Normalized changes in OMT values are compared across ISIs for correct and incorrect responses for complex odor matching task. Green dotted lines indicate the mean normalized OMT for correct trials whereas the red dotted lines indicate the

shift in mean OMT for incorrect trials (Paired t-test, p<0.05).

- (H) OMT plotted for correct trials only across 5s and 10s ISI for same and different odor pair matching. Participants took longer for correctly matching same odor pairs in 5s ISI task while no significant difference is observed for 10s ISI. ( $p_{5s}$  = 0.013 and  $p_{10s}$  = 0.6, Paired t-test).
- (I) Accuracy plotted for incorrect trials only across 5s and 10s ISI for same and different odor pair matching. No significant difference is observed for either ISIs. ( $p_{5s}$  = 0.81 and  $p_{10s}$  = 0.91, Paired t-test).
- (J) Comparison of simple and complex odor matching performance for 5s and 10s ISI. Odor matching accuracy declines significantly with increase in complexity (Unpaired t-test, two-tailed, p < 0.0001 for 5s-simple vs. 5s-mixture as well as for 10s-simple vs. 10s-mixture).
- (K) Comparison of OMT for simple and complex odor matching for 5s and 10s ISI. OMT increased significantly with increase in complexity for both the ISIs. (Unpaired t-test, two-tailed, p = 0.028 and 0.0002 respectively).
- (L) OMT compared for correct same and different odor pair matching for 5s and 10s ISI between simple and complex odor matching tasks. ( $p_{5s}$  = 0.0161 and 0.0025 for same and different correct trials between simple vs. mixture tasks respectively when ISI is 5s, p10s = 0.0003 and < 0.0001 for same and different correct trials between simple vs. mixture tasks respectively when ISI is 10s, Unpaired t-test).
- (M) The histogram represents fractions of correct trials for simple odor matching for each 500 ms bins. 77% of these correct trials fall between 4.5s to 6s.
- (N) Histogram shows frequencies of correct trails and their corresponding OMT as segmented in 500ms bins for complex odor matching.
- (O)The histogram represents proportion of correct trials with the OMT segmented into 500 ms bins comparing relative frequencies for simple (in blue) and complex(in red) odor matching trials.
- (P) Comparison of cumulative probability distribution for correct responses for simple and binary mixtures displays significantly longer OMT for complex OM task (p < 0.0001, Kolmogorov-Smirnov test).

[\*Note of acknowledgement: This work has been done with equal contribution from Dr. Meenakshi Pardasani and Dr. Sarang Mahajan]

Further, we compared OMT for correct trials only across 5s and 10s ISI for same and different odor pair matching. Our analysis show that subjects took significantly longer for correctly matching same odor pairs only in the case of 5s ISI task while no such difference was observed for 10s ISI. (Figure 3H, Paired t-test,  $p_{5s}$  = 0.013 and  $p_{10s}$  = 0.6). No difference was found for the same analysis involving incorrect trials (Figure 3I, Paired t-test, p>0.05).

As we looked at the performance in odor matching for complex odors by participants, we found that for both 5s and 10s ISIs, the odor matching accuracy declined significantly in comparison to respective ISIs in OM task with simple odors (Figure 3J, N=Unpaired t-test, p<0.05 for both comparisons). But when we compared OMT values for simple OM trials with complex OM trials, we found that participants performing complex odor matching task took significantly longer for 5s and 10s ISI for correct decision making (Figure 3K, Unpaired t-test, two-tailed, p = 0.028 and 0.0002 respectively). This trend remained consistent when we separately analysed same and different odor pair matching trails across ISIs (Figure 3L, Unpaired t-test, p<0.05). To assess how OMT for correct odor pair matching is distributed, we divided the OMT into 500 ms bins. As we plotted the fraction of correct trial corresponding to that bin, we found that 77% of correct trials, fall into the OMT span of 4 to 6.5s (Figure 3M). Frequency plot for complex odor shows similar distribution (Figure 3N). The rightward shift of the frequency distribution curve becomes apparent when frequency plots for simple and complex odor matching are plotted together (Figure 3O). As expected, due to an overall higher mean OMT for complex odor matching, cumulative probability for complex OM task shows a right shift in comparison to cumulative probability curve for simple odors (Figure 3P, p<0.0001, Kolmogorov-Smirnov test).

#### 3.4. Discussion

A great many systems and procedures have been developed in order to investigate the olfactory space and olfactory deficits in humans. Despite all this progress, including the most widely used ones like UPSIT<sup>130</sup> and Sniffing Stick's Test<sup>131</sup>, to less popular San Diego Odor Identification Test (SDOIT)<sup>267</sup>, California Odor Learning Test<sup>268</sup>, Percepts of Odor Episodic Memory (POEM)<sup>269</sup> etc., a universal scaling system that can be

correlated to disease occurrence and stage of progression with high degree of reliability is yet to be devised. We intend to bridge that gap with our OAM and odor matching task.

In this paper, we introduce a novel method using a custom-built instrument with precise control over odor-delivery which is used to accurately quantify human olfactory discriminability for simple and complex odors. Varying the ISI did not necessarily affect the odor matching accuracy for neither simple nor complex odor matching task. These findings indicate robust OWM related representations of odors, irrespective of monomolecular odors or binary mixtures, that can be maintained efficiently till a duration of 10s. There are not many studies carried out previously that assess the temporal limit of OWM. 270,271 But studies like these often have issues with controlled odor delivery, intuitive user interface and so on. Our custom-built OAM specifically keeps the shortcomings of the previous studies in mind. OAM specifically shows that for monomolecular and binary odor mixtures, the odor matching is unaffected by increase in delay period up to 10s. Further experiments with increasingly higher ISI are required to assess temporal limit of OWM, if at all there exists a such a limit or there is a gradual decline in performance after a certain time delay.

The observation that faster responses lead to higher probability of correct responses may come across as a direct contradiction to the speed-accuracy trade-off. Though several recent works have challenged the universality of speed-accuracy trade off (SAT) and reimagined decision making, it remains one of the towering notions in the field. 273,274 This phenomenon is often explained using drift-diffusion model (DDM) of WM. 275 In this model, noisy sensory data acquisition requires optimal time to gather enough data in order to make correct decisions. Therefore, faster responses lack enough data to make accurate predictions. But for our current observation, a careful analysis of the DDM reveals multiple possibilities allowing for such a finding. One possibility that would allow for a positive correlation between faster response and accuracy is higher drift rate. 276 Higher drift rate in a DDM signifies adequate accumulation of sensory information in shorter period of time. In other words, if there is a high enough flow of incoming information, then fast as well as accurate performance may be achievable. But for our current paradigm the possibility that there was optimal flow of information for such an outcome remains to be tested. Another possibility could

be optimization of decision boundaries.<sup>276</sup> Here, the participant in the WM task may be able to achieve a balance between speed and accuracy, especially when faster decision making is either incentivized or necessary condition of the task. In our case, the fact that a timer sets off right after the second odor presentation may act as a limiting condition in the forced-choice behavioural paradigm and thus pushing the participant to optimize their responses. Given the structure of our current paradigm and response limiting criteria makes up a plausible explanation for our finding. Yet another possibility that would lead to such outcome would be prior knowledge and positive bias on part of the participant<sup>277</sup>, which is clearly not the case and thus can be ruled out.

Despite the apparent contradictions, arguments can be made as to why this is not an ideal paradigm for studying SAT. A crucial feature of behavioural tasks studying SAT is the manipulation of response deadlines or incentivizing for speed versus accuracy.<sup>278</sup> In such paradigms, participants are often explicitly instructed to either focus on maximizing speed<sup>279</sup> or prioritizing accuracy<sup>280</sup>, which allows for the measurement of tradeoffs, if any, between these two factors. However, in this study, participants responded at their own convenience within a fixed response window without any variable urgency. This absence of a speed-pressure condition prevents an accurate analysis of how decision thresholds adjust dynamically. A comprehensive SAT study would maintain consistent stimulus complexity while systematically altering response deadlines.<sup>281</sup> The variations in observed response times within the olfactory paradigm may stem from differences in memory retention and perceptual difficulty, rather than an explicit tradeoff between speed and accuracy.<sup>282</sup>

Many of the neurodegenerative diseases including Parkinson's disease (PD), Alzheimer's disease (AD), Lewy body dementia (LBD), Huntington's disease (HD), have been shown to be associated with olfactory deficit as one of the early symptoms often years ahead of the actual onset of the other more severe, motor and cognitive, symptoms. Olfactory dysfunction is one of the most notable non-motor symptoms in both familial and sporadic PD. Moreover, olfactory deficit precedes diagnosis typically by 4-8 years and in some cases as long as 20 years. In a recent study, patients with idiopathic rapid eye movement (REM), who performed poorly in odor

detection task, were found to be over 700% more likely to develop dementia or PD.<sup>287</sup> In a similar manner, several studies with AD patients show deficit in odor identification<sup>288,289</sup>, higher detection thresholds<sup>290,291</sup> and poor odor memory<sup>269,292</sup>. Impaired odor identification, detection and discrimination has also been reported in patients with HD.<sup>293</sup> Even asymptomatic carriers of HD mutation show selective impairment in odor quality discrimination.<sup>294</sup> The ability to predict the likelihood of many of these diseases or identify diseases in early stages when severe neurocognitive or motor symptoms are hardly manifested may greatly enhance our ability for differential diagnosis and treatment.

In summary, using a novel custom-built OAM we show that the temporal resolution of working memory extends beyond 10s for odor matching tasks in healthy human subjects. Our findings suggest that faster odor matching time correlates to higher accuracy for odor matching task. We also find a decline in odor matching accuracy for complex odors as well as higher matching time with increase in complexity. This finding corroborates with previous studies in animal models. Our system, therefore, holds immense possibility in devising a precise diagnostic tool in PD, AD, dementia and other neurodegenerative diseases with olfactory deficit as early cognitive symptom.<sup>283</sup>

#### Chapter 4

# Persistent neurocognitive deficits during and post-SARS CoV-2 infection

#### 4.1. Introduction

The Coronavirus pandemic has claimed nearly 7 million lives till date<sup>295</sup> imparting a brutal toll on the healthcare system and the economy in most of the affected countries. Despite relatively low death rate in comparison to many other airborne viral infections<sup>296–298</sup>, widespread infection along with emergence of multiple genetic variants of the virus have brought about a pandemic situation. As the virus primarily affects non-neuronal cells in nasal epithelium<sup>299,300</sup>, an early and gradual reduction in the smelling abilities is expected rather than a sudden anosmia. Studies encompassing the binary yes/no questionnaires, which test the ability to smell easily available odorous objects, visual to analog scale ratings that assesses chemosensory abilities and quantitative olfactory detection, and discrimination paradigms have indicated olfactory dysfunctions to be one of the strong predictors of COVID-19<sup>228,301–303</sup>. Indeed, smell and taste changes at the population level gave rise to situations of lockdown across countries, suggesting them as the useful tools to enforce preventive measures to curb the spread<sup>304</sup>.

Along with serving the prominent indicators of disease during the initial months of COVID-19, these olfactory sensory modality and related cognitive functioning can now be functionalized to evaluate neurocognitive changes upon infection. Cognitive decline is, indeed, increasingly being checked for, both through self-assessments and via laboratory-based tests in COVID-19-affected individuals. Even after the recovery from the infection is achieved, cases of neurocognitive frailty are seen<sup>305–307</sup>. These findings display the necessity of using cognitive tests involving our sense of smell for investigating neurological impairments that could evolve as a result of COVID-19 infection.

Viral infections are known to result in neurological impairments. A multitude of case studies have depicted varying central nervous system damages caused due to virus entry and invasion.<sup>308</sup> However, the extent to which a particular viral strain can cause

maladaptive changes to the brain functionality is not yet confirmed. This could be due to several factors, such as, failure in tracking the infected individuals for longer time post the infection, improper identification of the site of infection due to low titer volumes and/or lack of adequate paradigms which can quickly & reliably detect behavioral impairments upon infection.<sup>229</sup>

One of the entry points of the Severe Acute Respiratory Syndrome Coronavirus-2 (SARS CoV-2) is the nasal epithelium, wherein, the Angiotensin converting enzyme 2 (ACE2) receptor and associated transmembrane protease serine 2 (TMPRSS2) are utilized by the virus for initial infection. Immunohistochemical analyses reveal the presence of Spike protein of the virus in neural/neuronal cells expressing the neurofilament and the olfactory marker proteins present in the olfactory mucosa of a small subset of deceased individuals. However, there are more evidence for the viral protein to directly affect ACE2 expressing sustentacular cells which are anatomically as well as functionally connected to the sensory neurons. Cocal inflammatory processes occurring in the naso-mucosal epithelium may also hinder the normal functioning of sensory neurons. Cocurrence of microvascular injuries in postmortem olfactory bulb tissues also hints towards the possible alterations. Such investigations indeed closely associate with the loss or impairment of sense of smell (anosmia, hyposmia or parosmia) being one of the prevalent symptoms of Coronavirus disease 2019 (COVID-19).

Studies encompassing the binary yes/no questionnaires which test the ability to smell easily available odorous objects, visual to analog scale ratings that assesses chemosensory abilities and quantitative olfactory detection, and discrimination paradigms have indicated olfactory dysfunctions to be one of the strong predictors of COVID-19<sup>228,302</sup> This reinforces the importance of systematically investigating the alterations in olfactory sensory perception. Understanding olfactory functioning is a rather expansive discipline that must include testing both sensory as well as the cognitive aspects. Cognitive decline is increasingly being checked for, both through self-assessments and via laboratory-based tests, in COVID-19 affected individuals.<sup>314</sup> Even after the recovery from the infection is achieved, cases of neurocognitive frailty are seen.<sup>315</sup> The source of long-term cognitive dysfunctions could be an amalgamation of vascular,

neural and inflammatory alterations.<sup>316</sup> Olfactory and cognitive functions are known to be processed by overlapping brain regions.<sup>317,318</sup> It is known that the changes in olfactory related functionality can predict cognitive decline in patients suffering from neurodegenerative diseases.<sup>244</sup> Thus, usage of quantitative paradigms to assess olfactory as well as cognitive functioning could be a very necessary tool to investigate the underlying deficits in COVID-19 patients.

OM task involves olfactory working memory among other higher cognitive functions. Retaining and manipulating odor information for short periods of time play important role for decision-making in many animal species, including humans. <sup>319</sup> Working memory for olfactory sensory modality is largely unexplored in comparison to other sensory systems. <sup>11</sup> A recent study from our laboratory has reported significant olfactory deficits in asymptomatic COVID-19 patients. <sup>228</sup> This was inferred after analyzing both olfactory detection and matching skills. While only 15% tested individuals reported problems with their sense of smell on subjective evaluations, more than 80% of them were found to be with olfactory deficits using our method. We further used this optimized paradigm to probe the olfactory learning, a readout that reflects cognitive abilities of symptomatic COVID-19 patients which can track any decline in these abilities over time (see Chapter 2, Section 2.3.4). We acquired 11,683 behavioural readouts from 196 participants (111 males and 85 females) who participated in the assessment of olfactory based neurocognitive fitness paradigm using our custom-built Olfactory-Action Meter (OAM).

# 4.2. Materials and Methods

A custom-built ten-channel olfactory action-meter which delivers odors with high temporal precision is used for the present study. Odorized air (HEPA sterilized) passes through a glass funnel into an odor delivery unit. Further, the air passes through a filter that removes any background odor. The air channels divided using a metallic manifold are further connected to ten mini–Mass Flow Controllers (MFCs) and one Main MFC (Pneucleus Inc.). This allows control on the volume of air passing through each of them. The output from each of the ten mini MFCs are connected to its respective odor reservoirs,

each filled with 4mL of pure monomolecular odorant. The odor volatiles then travel through Tygon tubing and mixes with clean air before entering the nozzle. The volumetric concentration (%v/v) of the odor is thus defined as the ratio of the volume of odor volatiles to the total volume of odorized air. We have selected these concentration levels ranging from 9.1-50% (v/v) for measuring the DIs.

Cross-contamination between participants was avoided by using separate odor delivery units comprising of a long-tube fitted with four layers of filters (surgical mask grade) and a suction outlet guarded by 0.2-micron PES filter (Whatman Uniflow). The PES filter is attached to a vacuum pump operating at ~450 mbar. Two HEPA and one PES filter (each of 0.2-micron size) are fitted in the exhaust line which finally releases into the activated carbon filter. Vacuum is only switched off during the duration of odor delivery to the nozzle. A wall that separates the instrument from the subject was established that prevented contact with the components of the olfactory action-meter and maintained physical distancing from the experimenter.

# 4.2.1. Study population

We analyzed data from five separate groups for our study (Total subject number=196), healthy participants [N=68+20 (participants used for Figure 4.2D)], symptomatic COVID-19 patients (N=49), asymptomatic COVID-19 carriers (N=34) and COVID-19 recovered participants (N=25). Healthy as well as COVID-19 recovered (N=113) participants were from Indian Institute of Science, Education and Research (IISER) Pune campus and were not infected with COVID-19 and/or did not have any influenza-like symptoms at the time of the test. Recovered participants had COVID-19 infection 4-18 months before the data collection (N=20). For olfactory fitness comparison, the data from asymptomatic carriers and the controls (71 participants out of 196), were taken from the previous study by Bhattacharjee et al., 2020.<sup>228</sup>

The measurements from symptomatic patients and asymptomatic carrier groups were carried out at B. J. Government Medical College and Sassoon General Hospitals, Pune, India. Symptomatic COVID-19 patients had symptoms ranging from at least 1 to at most 8

symptoms. Patient-wise details of symptom/s they suffered from at the time of hospitalization are listed in Table 1.

The test sessions for the healthy participants and COVID-19 recovered patients were done at the IISER Pune Biology Department and IISER clinic in locations that matched the ambient environment of the COVID-19 ward at B. J. Government Medical College and Sassoon General Hospitals. As the locations were carefully selected to minimize the variability of odor profiles with varying temperature and humidity, we do not expect any consequences on our readouts.

The data collection was carried out during the following periods:

Asymptomatic carriers: 12<sup>th</sup> May 2020 to 21<sup>st</sup> May 2020

Symptomatic patients: 6<sup>th</sup> October 2020 to 16<sup>th</sup> October 2020

Control participants: 22<sup>nd</sup> April 2020 to 25<sup>th</sup> February 2022

COVID-19 recovered participants: 17<sup>th</sup> September 2021 to 24<sup>th</sup> April 2022

#### 4.2.2. Inclusion/Exclusion criteria:

1. For COVID-19 symptomatic patients, olfactory function test was only performed if they had symptoms at the time of hospitalization (Table 1). None of the asymptomatic carriers and the recovered participants had symptoms at the time of the testing. Details of post-COVID complications for recovered participants are summarized in Table 2.

- 2. COVID-19 infection was confirmed at the designated testing centers in the hospital via Reverse Transcriptase-Polymerase Chain Reaction (RT-PCR) using the nasopharyngeal/oropharyngeal swabs before our test commenced (symptomatic patients and asymptomatic carriers). The protocol for detection of COVID-19 was approved by the Indian Council of Medical Research (ICMR).
- 3. Only the participants who were willing to be a part of the study were included. The consent form was signed by them at the commencement of the test.
- 4. The paradigm was well-explained to all participants. They were allowed to discontinue at any time point during the test.

- 5. None of the participants had any known neurological impairments (other than possible COVID-19 induced) or neurodegenerative disorders that could compromise their olfactory abilities, at the time of testing.
- 6. Only the participants whose detection index value were  $\geq$  0.6 at the tested odor concentrations were allowed to participate in the Olfactory matching test.
- 7. Following are the details of the patients who did not perform the complete battery of olfactory detection and matching tests:

Symptomatic patients BJMC P4, BJMC P7, BJMC P13 and BJMC P25 performed the odor detection test at 50% (v/v) concentration only.

BJMC P13, BJMC P18, BJMC P23, BJMC P24 BJMC P27, BJMC P29, BJMC P46, BJMC P47 and BJMC P48 did not perform olfactory matching test as a result of lower detectability index (DI) (<0.6).

Subsets of participants from the symptomatic (N=18), healthy (N=28) and recovered (N=25) group performed olfactory learning task that involved carrying out a session of olfactory matching task every day. The symptomatic patient group performed for more than one session for a maximum of 5 sessions over a period of 7 days. The control and recovered group performed in the follow up sessions for at least 4 sessions and a maximum of 5 sessions. A separate group of healthy participants (N=20, during pre-COVID-19 period) carried out olfactory learning task for two consecutive sessions on the same day that led to increased performance accuracy in the second session, that served as the rationale for carrying out olfactory learning task in symptomatic patients and recovered participants, as mentioned above. Our previously published work (cf. Figure 3B, Bhattacharjee et el., 2020) shows 17% reduction in olfactory matching accuracy for asymptomatic carriers compared to control participants. We considered this percentage reduction while doing a priori sample size calculation for the experiments reported here. As per the power analysis, we needed a minimum subject number of 11 for the learning experiment we conducted. However, we could acquire the data from 25 recovered participants, 18 symptomatic patients and 28 healthy participants.

# 4.2.3. Sample size calculation

Sample size for the study has been calculated as follows:

$$N = \frac{\sigma^2 (z_{1-\beta} + z_{1-\alpha/2})^2}{(\mu_0 - \mu_1)^2}$$

where, N= Size of the sample

 $\sigma$  = Variation in study population

z = Critical Z value for a given  $\alpha$  or  $\beta$ 

 $\alpha$  = Probability of type I error (usually 0.05)

 $\beta$  = Probability of type II error (usually 0.2)

 $\mu_0$  = Mean value for the control group

 $\mu_1$  = Mean value for the patient group

As per the previously published data from our lab by Bhattacharjee et al., 2020, the difference in mean matching accuracy for control and patient group ( $\mu_0 - \mu_1$ ) has been shown to be 11.4. Hypothesizing that our present study would yield at least this much mean difference, we calculated the sample size using the above-mentioned formula to be  $\sim$  11.

### 4.2.4. Ethics committee approval information

The protocols used in our study was approved by the IISER Ethics Committee for Human Research (IECHR/Admin/2020/001), bio-safety committee at IISER Pune and the Ethics committee at B. J. Government Medical College and Sassoon General Hospitals, Pune, India (BJGMC/IEC/Pharmac/ND-Dept 0420053-053).

#### 4.2.5. Study location

All data points from symptomatic patients and asymptomatic carrier groups were collected at B. J. Government Medical College and Sassoon General Hospitals, Pune,

India. The evaluation sessions for the healthy participants and COVID-19 recovered patients were done at the IISER Pune Biology Department and IISER clinic in locations that matched the ambient environment of the COVID-19 ward at B. J. Government Medical College and Sassoon General Hospitals. As the locations were carefully selected to minimize the variability of odor profiles with varying temperature and humidity, we do not expect any consequences on our readouts.

### 4.2.6. Design of the Olfactory-action meter:

A bespoke ten-channel Odor Administration Module (OAM) with exceptional temporal precision is employed in this study. HEPA-sterilized, odorized air traverses a glass funnel into an advanced odor delivery apparatus. Subsequently, the air undergoes filtration to excise any residual background odors. The air channels are meticulously segregated using a metallic manifold, each connected to one of ten mini Mass Flow Controllers (MFCs) and a primary MFC from Pneucleus Inc., facilitating precise regulation of airflow through each channel. These mini MFCs link directly to individual odor reservoirs, each containing 4mL of pure monomolecular odorant. The volatile compounds then traverse Tygon tubing, amalgamating with purified air before being directed into the nozzle. The volumetric concentration (%v/v) of the odor is quantitatively defined as the ratio of the volume of odor volatiles to the total volume of odorized air. These concentration gradients, spanning from 9.1% to 50% (v/v), are delineated for assessing the Differential Intensities (DIs) as illustrated in Figure 4.1B.9

To mitigate cross-contamination among participants, distinct sterilized odor delivery units were deployed. These units feature elongated tubes equipped with four layers of surgical mask-grade filters and a suction outlet protected by a 0.2-micron polyethersulfone (PES) filter (Whatman Uniflow). This PES filter is affixed to a vacuum pump functioning at -450 mbar. Furthermore, two HEPA filters and a PES filter (0.2 microns each) are incorporated within the exhaust line, which subsequently expels through an activated carbon filter. The vacuum mechanism is deactivated solely during the period of odor delivery to the nozzle. An instrument partition was instituted to preclude any physical interaction with the

olfactory-action meter components and to ensure adherence to social distancing protocols from the experimenter.<sup>228</sup>

#### 4.2.7. Odors

Refer to Chapter 2 for details of odors being used.

#### 4.2.8. Paradigm of Olfactory function test

After acquiring the consent from the participants and explaining the paradigm used for our study, we began the test by first s (one odor at a time) starting from the lowest to the highest concentration levels.

# 4.2.9. Olfactory detectability measurement

Olfactory detectability is defined as the detection abilities of participants for the odors of varying concentrations. Each odor was delivered for 4s with a fixed inter-trial interval of 17.2s, at a particular concentration level. Prior to odor delivery, a set pre-loading time of 3.2s was defined during which the odorized air travelled away from the nozzle and diverted into the suction line of the odor delivery unit. Post the pre-loading period, the odorized air travels to the nozzle for delivery into the nose of the participant. Once the odor is delivered, the participants are expected to inform upon successful detection of the odorant. It was suggested that the participant does not try to identify or provide a valence to the odors. A verbal cue ('odor now') was initiated by the experimenter before each odor was presented. Just after odor is delivered, the participant was expected to say 'YES' if they detected the odor and 'NO' if they were unable to detect it. The answers were duly noted by the experimenter and the detection indices across odors and concentrations

were measured by calculating the number of correct responses. We use the metric, detectability index (DI) to quantify this.

Olfactory detectability index =  $\frac{\text{No. of odors successfully detected by the participant}}{\text{No. of odors presented for a given concentration}}$ 

Measurement of performance in odor matching test:

Participants who performed at ≥ 60% accuracy in the odor detection task were asked to carry out odor matching test for determining the sensory-cognitive abilities and its alterations under SARS CoV-2 infection. A session of this test consists of ten trials. A tone of 200ms followed by a 1s delay, initiates a trial which consists of presentation of two odors. The odors are delivered one at a time. First odor is delivered for 4s, followed by an interstimulus interval of 5s and then, the second odor for 4s. Participant's perception of whether these two odors are 'SAME' or 'DIFFERENT' are then assessed. At the end of each trial, participant is expected to present a verbal response about the same. Experimenter then registers the response on a response console by pressing either on the 'SAME' or the 'DIFFERENT' button and additionally note this information down. A total of 2 pairs of odors (Hexanal vs. Acetophenone and Isoamyl acetate vs. 1,4-Cineole) are used for this test and are presented in a random sequence. If some participant fails to detect any of these four odors during the detection task and have a DI value of more than 0.5, we choose odors from the pool of odors successfully detected by the participants. Accuracy of olfactory matching is measured by calculating the correct responses over a total of ten trials. For participants with whom odor matching was continued over extended days during their hospitalization period (for symptomatic patients), accuracy was plotted for each day to any improvement in olfactory learning over sessions. Matching test for healthy participants (N=20) which was carried out during the pre-COVID19 period was carried out for a total 20 trials, with ≥2 to <5 pairs of odors. Follow up studies were conducted for at least for 4 sessions and a maximum of 5 sessions over a period of a maximum of 7 days. 13 symptomatic patients, 18 control participants and 25 recovered participants (10 of these recovered participants were tested on diluted odors (1-2% v/v in mineral oil) as they showed good detectability indices at the same odor concentration) completed at least 4 sessions.

# 4.2.10. Measurement of Olfactory function score

To have a unified parameter that will reflect measurements from DIs and the odor matching skills, we calculated an Olfactory Function Score (OFS). OFS calculation was done by including the average DI for all four concentrations as well as the normalized olfactory matching accuracy. Equal weightage was given to the individual parameters, and for cases where matching accuracy was not taken, only DI values were averaged. Matching accuracy was normalized against the mean value of performance accuracy of the normal healthy participants.

Differential reduction values calculation: The differential reduction in AUC for a particular odor and mean values for a specific concentration for symptomatic patients and asymptomatic carries are done by calculating the % reduction in AUC (R<sub>%</sub>) for symptomatic and asymptomatic participants in comparison to the control group and then multiplying both values with a common scaling factor derived as follows:

$$R_{\%} = \left(\frac{\text{AUC for control group -AUC for patient group}}{\text{AUC for control group}}\right) * 100$$

scaling factor (s) = 
$$\left(\frac{100}{R\% \text{ for symptomatic +asymptomatic subjects}}\right)$$

Differential reduction value =  $(R_{\%} * s)$ 

#### 4.2.11. Statistical analyses

All statistical analyses were carried out in GraphPad Prism 9.2.0 and MATLAB 2017a and 2020a. Normality was checked using Shapiro-Wilk test. We implemented Analysis of variance (ANOVA) with corresponding post-hoc test (Bonferroni's and Tukey's), unpaired tests (two-tailed), Mann-Whitney test and Receiver Operating Characteristic (ROC) analysis for specificity and sensitivity.

#### 4.3. Results

# 4.3.1. Symptomatic patients of COVID-19 show impaired odor detection

All subjects who participated in the paradigm had to go through a detection task. Participants who had a congested nose, had any trouble breathing or air intake through nostrils were excluded from the study. We presented odors as sets of increasing concentration ranging from 9.1% to 50% (Figure 4.1A). Based on successful detection of odors, detection index for each participant at every concentration tested is calculated. Apart from looking at the detectability of odors at various concentrations across subjects, this task also acted as a screening step for the odor matching paradigm, to be performed next.

A total of 49 symptomatic COVID-19 patients (2818 readouts) (Table 4.1) with one or more symptoms at the time of hospitalization, 25 COVID-19 recovered subjects (2469 readouts) (Table 4.2) and 68 healthy subjects (5522 readouts, 36 of which had been included from a previous study<sup>228</sup> in our lab) participated in the study. As we assessed the participants for their odor detectability across ten odors and four different concentrations, we found that the symptomatic COVID-19 patients had significantly poorer odor detectability when compared to healthy human subjects across all the odors presented (Figure 4.1B1-10). As we looked at the overall detectability across four different concentrations, we found that the symptomatic patients show significantly impaired detectability when compared to healthy subjects (Figure 4.1C). As we plotted receiver operator function (ROC) for the DIs including the four odor concentrations and calculated several parameters like AUC, Sensitivity etc. (Figure 4.1D). AUC of 0.87 implies of exceptional accuracy of the employed paradigm and the olfactometer along with high sensitivity and specificity of >80%.

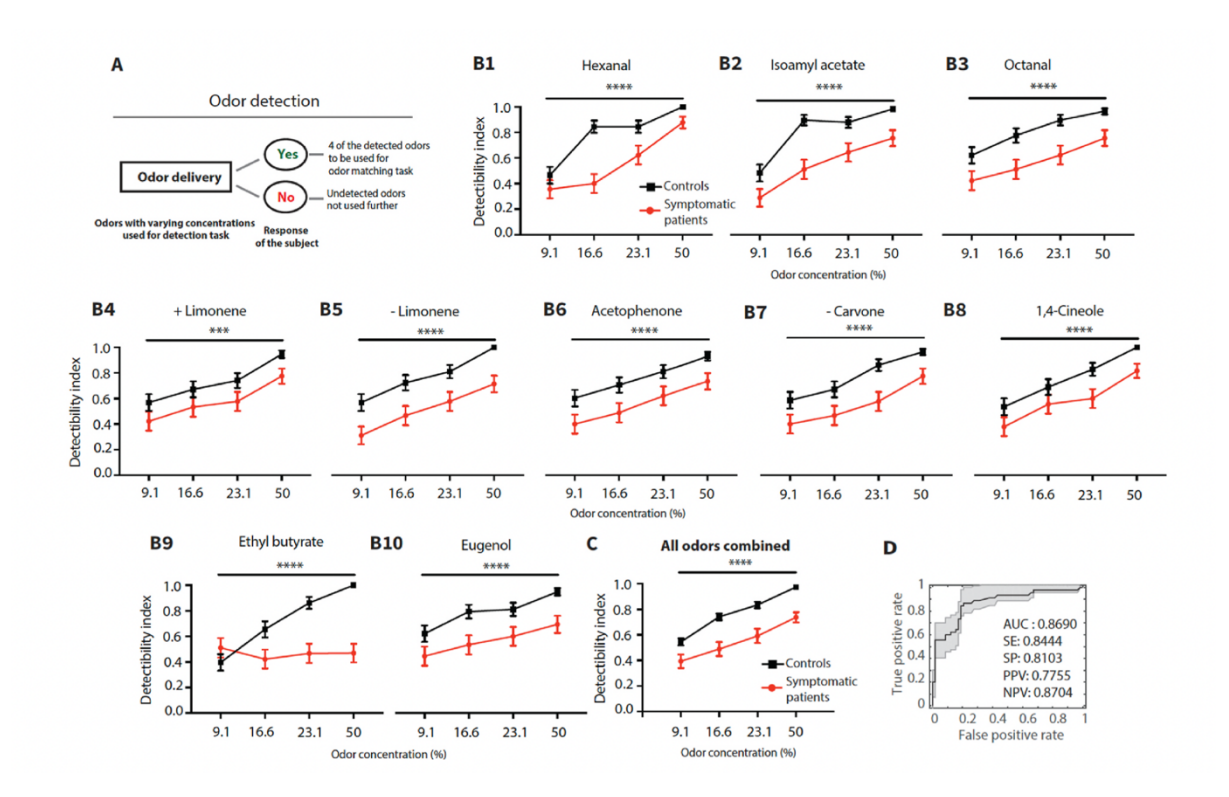


Figure 4.1. Symptomatic COVID-19 patients show compromised odor detectability. (A) A schematic representation of the odor detection task is displayed. 10 monomolecular odors, each at four different odor concentrations, are presented to each participants for the odor detection task. Every odor at the respective concentration is presented for 4s using our custom-built olfactometer. Participants are instructed to verbally confirm to the experimenter upon successful detection. Four of the successfully detected odors at 50% concentrations are further used for the odor matching task. (B) Odor-wise detection indices (DI) of symptomatic COVID-19 patients (N = 49) in comparison to healthy subjects (N = 58), Two-way ANOVA with Bonferroni's multiple comparison test, \*\*\*p < 0.001, \*\*\*\*p < 0.0001. (C) Detectability indices plotted for different odor concentrations for control (N = 58) and symptomatic patient (N = 49) groups (Two-way ANOVA with Bonferroni's multiple comparison, \*\*\*\*p < 0.0001). (D) Receiver operating characteristic (ROC) analysis for predicting olfactory impairment using DI measured for different concentrations of various odors in symptomatic COVID-19 patients. ROC analysis shows an accuracy (AUC) of 0.87, specificity (SP) of 0.81, sensitivity (SE) of 0.84, positive predictive value (PPV) of 0.78, negative predictive value (NPV) of 0.87 for prediction based on DI measured from healthy subjects (N = 58) and symptomatic COVID-19 patients (N = 45). The shaded region in grey indicates 95% confidence interval.

Recovered Subject ID	Age (Years)	Gender	Symptoms at the time of hospitalization	Detectability indices at different odor concentrations (% v/v)  9.1 16.6 23.1 50				Normalized olfactory matching performance index
BJMC-1	59	М	Fever, weakness	0.4	0.4	0.4	0.5	0.92
BJMC-2	53	М	Bone/joint pain	0.5	0.7	0.7	0.7	0.31
BJMC-3	37	М	Sore throat, Mild uneasiness	0	0	0	0.2	NP*
BJMC-4	24	М	Bone/Joint pain	0	0.2	0.7	0.7	0.92
BJMC-5	36	М	Fatigue, shortness of breath, headache, runny nose	1	0.8	0.9	0.9	0.61
BJMC-6	26	М	Fever, sore throat	0.5	0.5	0.6	0.7	0.31
BJMC-7	24	F	Fever, fatigue, shortness of breath, bone/joint	0.9	0.9	1	1	0.92
			pain, headache, runny nose					
BJMC-8	35	М	Fever, fatigue, sore throat, headache	1	0.6	0.8	0.8	0.77
BJMC-9	54	F	Fever, fatigue, shortness of breath	0	0.2	0.6	0.8	0.61
BJMC-10	32	F	Fever	0.6	0.6	8.0	0.9	1.07
BJMC-11	57	F	Fever, headache	0.5	0.1	0.7	0.8	0.61
BJMC-12	30	F	Fever, dry cough, fatigue, bone/joint pain, headache	0	0	0	0.7	0.61
BJMC-13	33	М	Fever, dry cough, shortness of breath, chest pain, hyposmia/anosmia	0.5	0.6	0.8	0.9	0.77
BJMC-14	31	М	Fever, coughing of sputum, shortness of breath, sore throat	0.5	0.6	1	0.9	0.92
BJMC-15	74	М	Fever, headache, runny nose	0.8	1	1	1	0.46
BJMC-16	50	М	Fever, dry cough, fatigue, shortness of breath, bone/joint pain	1	1	1	1	0.46
BJMC-17	43	М	Dry cough, shortness of breath	0.1	0.6	0.4	0.4	NP
BJMC-18	50	М	Fever, dry cough, bone/joint pain	0.7	0.9	1	1	1.07
BJMC-19	22	М	Fever, headache, Sore throat, Hyposmia	0.9	0.3	1	0.9	0.92
BJMC-20	47	F	Fever	1	1	1	1	0.77
BJMC-21	66	F	Fever, bone/joint pain, headache	0	0	0	0	NP
BJMC-22	26	М	Fatigue, sore throat	0	0.3	0.4	0.8	0.92
BJMC-23	55	F	Fever, shortness of breath, loss of sense of taste	0.2	0.2	0.3	0.9	1.07
BJMC-24	68	F	Fever, fatigue, shortness of breath	0	0	0	0	NP
BJMC-25	50	М	Fever, bone/Joint pain, hyposmia, loss of sense of taste	0	0	0.1	0.7	0.92
BJMC-26	32	F	Fever, fatigue, bone/joint pain, runny nose, headache	0.4	0.7	0.8	0.9	0.61
BJMC-27	55	F	Sore throat, headache, Weakness	0.2	1	1	1	0.77
BJMC-28	25	М	Fever, fatigue	0.2	0.6	0.5	0.8	1.23
BJMC-29	29	М	Dry cough, bone/joint pain, sore throat,	0	0	0	0.7	0.92
			headache, runny nose					

BJMC-31	25	F	Shortness of breath, loss of sense of taste	0.5	0.8	0.9	0.9	0.46
BJMC-32	36	F	Fever, dry cough, headache, runny nose	0.1	0.5	0.2	0.5	NP
BJMC-33	55	М	Fever, dry cough, Fatigue, Shortness of breath	0.3	0.4	0.7	0.7	0.77
BJMC-34	32	F	Fever, fatigue, shortness of breath	0.8	0.9	1	1	1.07
BJMC-35	45	М	Fever, dry cough, fatigue, shortness of breath,	0.1	0	0.2	0.8	0.46
			hyposmia, loss of sense of taste					
BJMC-36	32	М	Fever, fatigue, anosmia, loss of sense of taste	0	0	0	0	NP
BJMC-37	67	М	Dry cough, fatigue	0	0	0.1	0.5	
BJMC-38	40	М	Fever, dry cough, fatigue, headache, hyposmia	0	0.1	0.3	0.7	1.23
BJMC-39	46	М	Fever, dry cough, fatigue, headache, runny	0	0	0	0.3	NP
			nose, loss of smell and taste					
BJMC-40	33	М	Dry cough, sore throat, runny nose	0.1	0.6	0.7	0.9	0.31
BJMC-41	58	F	Sore throat	1	1	1	1	1.23
BJMC-42	27	F	Fever, Dry cough, fatigue, sore throat,	1	1	1	1	1.07
			headache					
BJMC-43	51	М	Fever, dry cough, fatigue, headache	0.4	0.7	0.7	0.9	0.77
BJMC-44	61	М	Fatigue, shortness of breath	0.4	0.4	0.3	0.9	0.46
BJMC-45	57	М	Fever, dry cough, fatigue, headache, loss of	0.6	1	1	1	0.31
			sense of taste					
BJMC-46	24	F	Fever				0.7	0.77
BJMC-47**	30	F	Fever				0.3	NP
BJMC-48**	39	F	Fever, dry cough, fatigue, shortness of breath,				0.7	1.07
			joint pain, sore throat, headache, loss of sense					
			of taste					
BJMC-49**	25	F	Fever				0.7	0.31

Table 4.1. Table listing symptomatic patient IDs with their corresponding symptoms at the time of hospitalization, detectability indices and normalized olfactory matching performance indices.

(\*Patients with <0.6 DI at 50% odor concentration did not perform the olfactory matching task. Hence are marked as Not performed (NP)).

(\*\*Patient performed detection task for 50% (v/v) odor concentration only)

Recovered Subject ID  RE-1 RE-2	Age (Years) 22 22	Gender M F	Post-COVID Complications  None  None		differe	ity indice ent odor tions (% 23.1 0.9 0.8		Normalized olfactory matching performance index 0.59
RE-3	44	F	Anosmia for 2.5 months, still hyposmic, irregular menstrual cycle, forgetfulness	0.2	0.8	1	1	0.74
RE-4	43	М	None	0.8	1	1	1	0.44
RE-5	29	М	Tiredness, headache (for 1 week)	1	1	1	1	0.89
RE-6	30	М	None	1	1	1	1	0.59
RE-7	27	F	Loss of sense of smell has not recovered completely	8.0	1	1	1	0.89
RE-8	26	F	Tiredness, decreased sense of smell, irregular menstrual cycle	0.5	0.7	0.9	0.9	0.44
RE-9	44	F	Fatigue, hair loss	0.5	0.7	0.7	0.8	0.89
RE-10	25	F	None	0.7	0.9	1	1	0.74
RE-11	25	F	Fatigue, headache, attention deficit, impaired memory	0.7	0.9	1	1	0.89
RE-12	31	М	None	0.6	0.7	0.8	0.8	0.74
RE-13	25	F	Tiredness, brain fog, irregular menstrual cycle, frequently low bp, reduced stamina	0.4	0.7	0.7	0.9	0.59
RE-14	21	М	None	1	1	1	1	0.74
RE-15	26	F	None	0.8	8.0	8.0	0.9	0.74
RE-16*	25	М	None				1	0.59
RE-17*	28	F	None				1	0.52
RE-18*	27	F	Joint pain				1	1.19
RE-19*	31	F	High pulse rate during daily activities				1	0.97
RE-20*	24	F	None				0.8	1.19
RE-21*	22	М					1	1.04
RE-22*	19	F					0.89	0.97
RE-23*	20	М					0.56	0.74
RE-24*	18	М					0.67	0.74
RE-25*	20	М					0.67	0.82

Table 4.2. Table listing COVID-19 recovered subject IDs with their corresponding post-COVID complications (if any), detectability indices and normalized olfactory matching performance indices (\*: These recovered subjects were tested on diluted odors (2% v/v in mineral oil) as they showed good detectability indices at the same odor concentration).

# 4.3.2. Symptomatic patients and recovered participants of COVID-19 infections how impaired olfactory learning

Once the detection task is complete, the subjects who have a DI score of 0.6 or more, proceed to the next paradigm called olfactory matching. This is a delayed odor matching task where the participant are presented with two odors separated by an interval in a trial (Figure 4.2A). The participant needs to remember the first odor during the delay and match it with the second odor presented post-interval. When we compared the odor DIs across four different concentrations, we found that recovered subjects had virtually indistinguishable odor detectability across odor concentrations (Figure 4.2B, Two-way ANOVA with multiple comparisons, p<0.05). This finding indicates that odor detection ability goes back to normal in COVID-19 patients, post-recovery. This finding is consistent with findings where the loss of olfactory function has been reported to be temporary in significant portion of patients of COVID-19.320 To investigate whether the same holds true for odor matching ability, that involves multidimensional involvement of short term memory, attention, executive functioning etc., we set out to look at the odor matching accuracy in the three different groups. Upon comparing the OM accuracy of the three groups we found that recovered subjects performed at comparable levels of the symptomatic patients which is significantly lower than the control group (Figure 4.2C, One-way ANOVA with multiple comparisons, p<0.05). As the recovered subjects had the infection at least 12 weeks prior to the day of experiment, this finding is indicative of a persistent neurocognitive deficit post-COVID-19 infection. In our prior experiments during the pre-COVID times, we had a cohort of subjects who participated in the odor matching task in two consecutive sessions. For this cohort, we found an improvement in the odor matching accuracy of the subjects (Figure 4.2D, Paired t-test, p = 0.0008). This prompted us to follow subjects of all three groups for a maximum of five consecutive sessions and see whether there was olfactory learning across the sessions (Figure 4.2E, Two-way ANOVA with Bonferroni's Multiple Comparisons, p < 0.0001). This clearly indicates a olfactory learning deficit in COVID-19 subjects during infection that persists long after recovery.

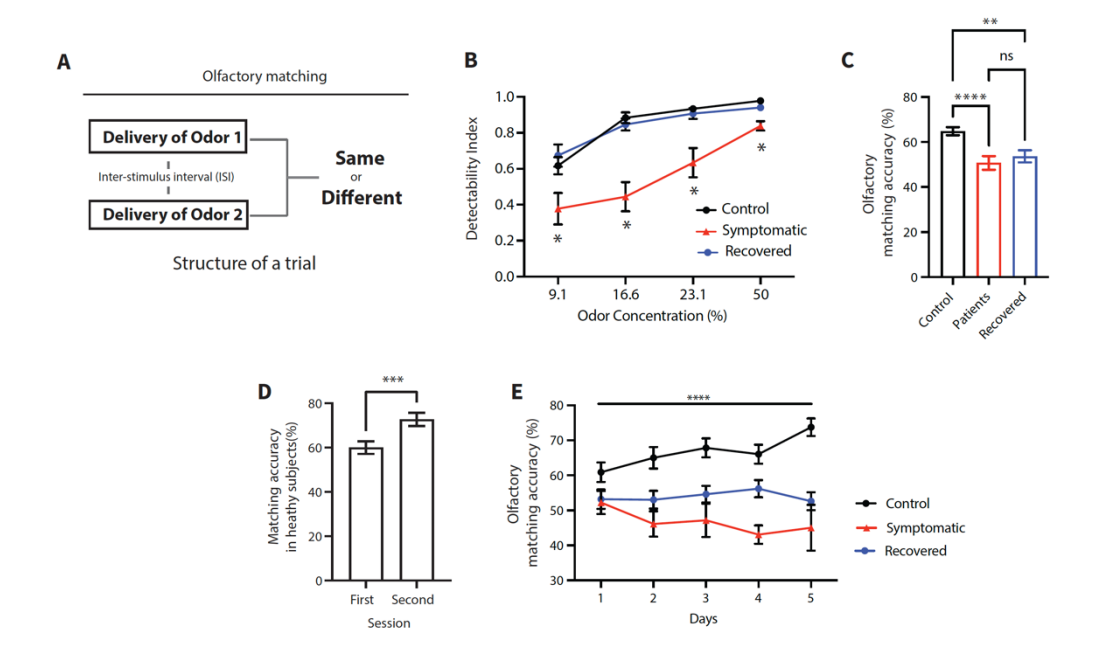


Figure 4.2. Symptomatic COVID-19 patients have lower matching performance and impaired olfactory learning which persists even after recovery (A) Schematic diagram of olfactory matching task is shown. Each trial comprises of two odors being delivered, each for 4s, separated by an inter-stimulus interval (ISI) of 5s. Verbal response of the subject is recorded on whether the two odors are same or different. Odor matching accuracy for each session is calculated based on the number of correct responses at the end of each session. (B) Detectability index plotted for different odor concentration for follow up subjects from control group (N = 18), symptomatic patient group (N = 18) and recovered group (N = 15). (Two-way ANOVA with Bonferroni's multiple comparison, \*\*\*\*p < 0.0001). (C) Odor matching accuracy plotted for symptomatic patients, recovered subjects and control groups. Matching accuracy is calculated based on the number of correct responses after 10-20 trials. Symptomatic patients with low DIs (N = 9) did not perform odor matching task, thus excluded from analysis. (One-way ANOVA with Tukey's multiple comparisons, \*\*p = 0.0085, \*\*\*\*p<0.0001,  $N_{Control}$  = 67,  $N_{Patient}$  = 40,  $N_{Recovered}$  = 25). (D) OM accuracies plotted for healthy subjects (N = 20) for two consecutive sessions. Matching accuracy calculated based on the number of correct responses for 20 trials (Paired twotailed t-test, \*\*\*p = 0.0008). (E) OM accuracies for up to 5 sessions performed by the subjects over a period of maximum 7 days have been plotted for control (N = 28), symptomatic patient (N = 18) and recovered (N = 25) groups. Matching accuracies

calculated based on the number of correct responses for 10–20 trials in each session. (Two-way ANOVA with Bonferroni's multiple comparison, \*\*\*\*p<0.0001).

# 4.3.3. Symptomatic COVID-19 patients show significantly less severe olfactory impairment in comparison to asymptomatic carriers

As we have collected data for symptomatic patients of COVID-19, and previous work from our lab screened asymptomatic patients for their odor detectability and matching accuracy, we planned to compare differential divergence in asymptomatic and symptomatic group. When we compared odor detectability across the ten different odors used for odor detection task, we saw that for all odors, detectability is significantly poorer in asymptomatic patients in comparison to symptomatic ones (Figure 4.3A, Two-way ANOVA with Bonferroni's multiple comparisons, p<0.05). As we looked at odor detectabilities collectively across the four concentrations, the same pattern of reduced detectability is reflected for asymptomatic carriers in comparison to symptomatic patients (Figure 4.3B, Two-way ANOVA with multiple comparisons, p<0.05). We further calculated the reduction in the normalized area under the curve (AUC) values reduction values for a comparative representation that highlights the extent of reduction in detectability for each odor, in comparison to the healthy control group (Figure 4.3C). A similar representation combining all odors across four different odor concentrations is plotted in Figure 4.3D. Olfactory function score, combining odor detection as well as odor matching in a single parameter, is plotted for symptomatic and asymptomatic patients (Figure 4.3E, Mann-Whitney Test, p<0.05).

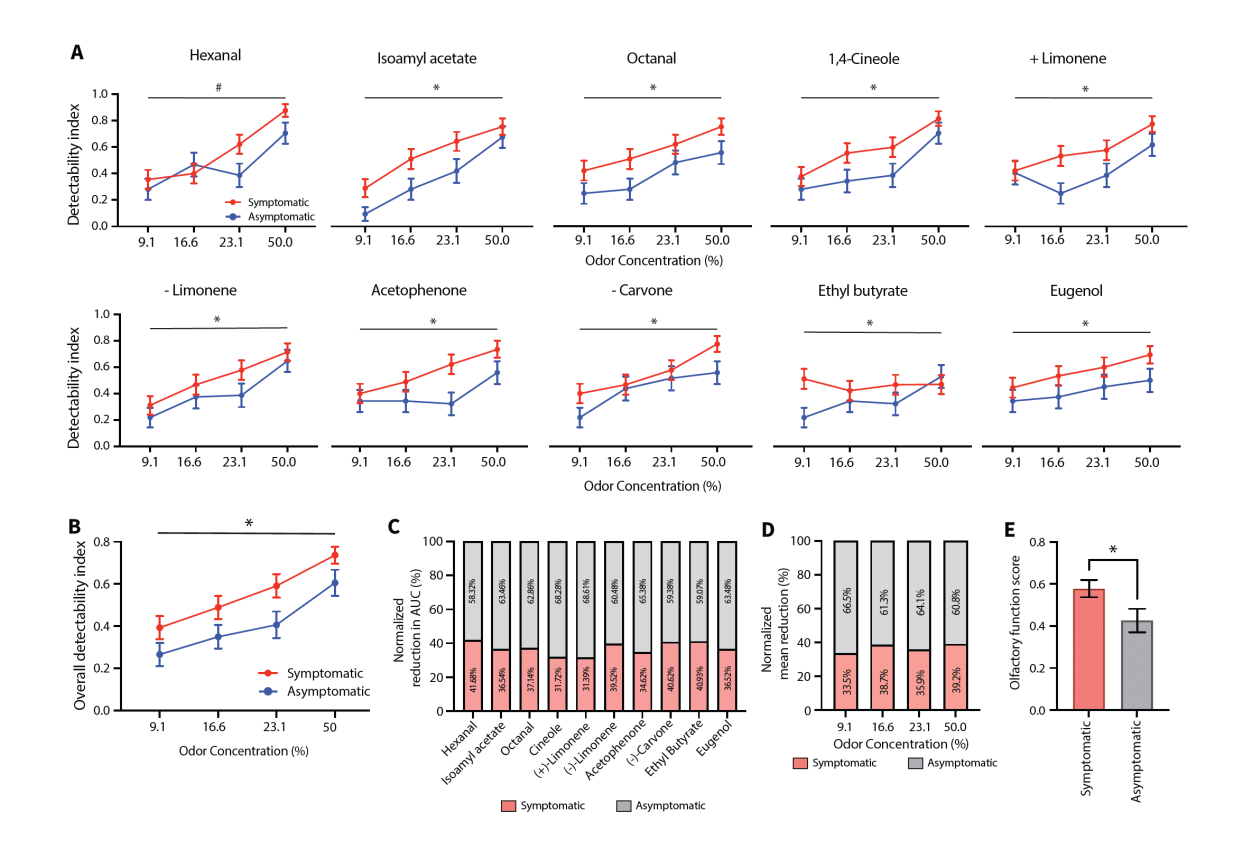


Figure 4.3. Differential impairment visible in olfactory and neurocognitive function in symptomatic patients and asymptomatic carriers. (A) Odor-wise DIs are plotted for symptomatic COVID-19 patients (N = 49) and asymptomatic carriers (N = 34). (p < 0.05 for all odors except Hexanal, #: p = 0.054, Two-way ANOVA). (B) Overall DIs including detectabilities of all odors used for odor detection task, are plotted for the four odor concentrations used for symptomatic COVID-19 patients (N = 49) and asymptomatic carriers (N = 34). (\*p < 0.05, Two-way ANOVA). (C) Odor-wise differential reduction in area under curve (AUC) (R%) values for symptomatic patients (N = 49) and asymptomatic carriers (N = 34) in comparison to the control group (N = 58) are plotted. (D) Differential average reduction (%) in DIs are plotted for four odor concentrations for symptomatic patients (N = 49) and asymptomatic carriers (N = 34) in comparison to the healthy group (N = 58). (E) Olfactory function scores (OFSs) plotted for symptomatic patients (N = 48) and asymptomatic carriers (N = 33) (Mann-Whitney test, \*p = 0.0139).

# 4.3.4. Confounding variables do not affect the experimental parameters

To check whether the behavioural readouts we acquired through the OAM were negligibly affected by the environmental factors, we analysed several of the confounding factors that may have potential impact on the study parameters. We looked at any potential effect of age on the OFS across healthy participants, symptomatic patients and recovered subjects (Figure 4.4A-C). Linear regression score showed no significant correlation between age and OFS. When we looked at only DI values across the same three groups, we saw no correlation (Figure 4.4D-F, Linear regression analysis,  $R^2 << 1$ ). When we analysed whether gender played any role on the olfactory based performance in the three groups, only for healthy subjects we saw females performing significantly better than males when OFS is compared (Figure 4.4G-I). This is consistent with the reports of sexual dimorphism in humans where females have been shown to possess more neurons than males in the OB. $^{321}$  We also did not find any role of gender of odor detectabilities across the three groups (Figure 4.4J-L).

To evaluate the robustness of behavioral readouts we report here, we have analyzed different confounding factors. To avoid any bias on part of the subjects at the time of olfactory function test, we included participants who were willing to be a part of the study. The paradigm was well-explained to all participants, and they were allowed to discontinue at any time point during the test. Further, none of the participants had any known neurological impairments (other than possible COVID-19 induced) or neurodegenerative disorders that could compromise their olfactory abilities, at the time of testing. To probe the effect of confounding variables such as gender and age on the test readouts, we analysed the correlation between these variables and different test readouts, olfactory detection indices and OFSs. Our analyses showed no correlation between these confounding variables and test readouts. Out of 6 comparisons, we observed a difference (p=0.03) only in OFS between males and females of normal healthy subject group, because of the reduced DIs at low concentrations for two male subjects. This is indicative of the robustness of our findings with minimal effects by confounding variables.

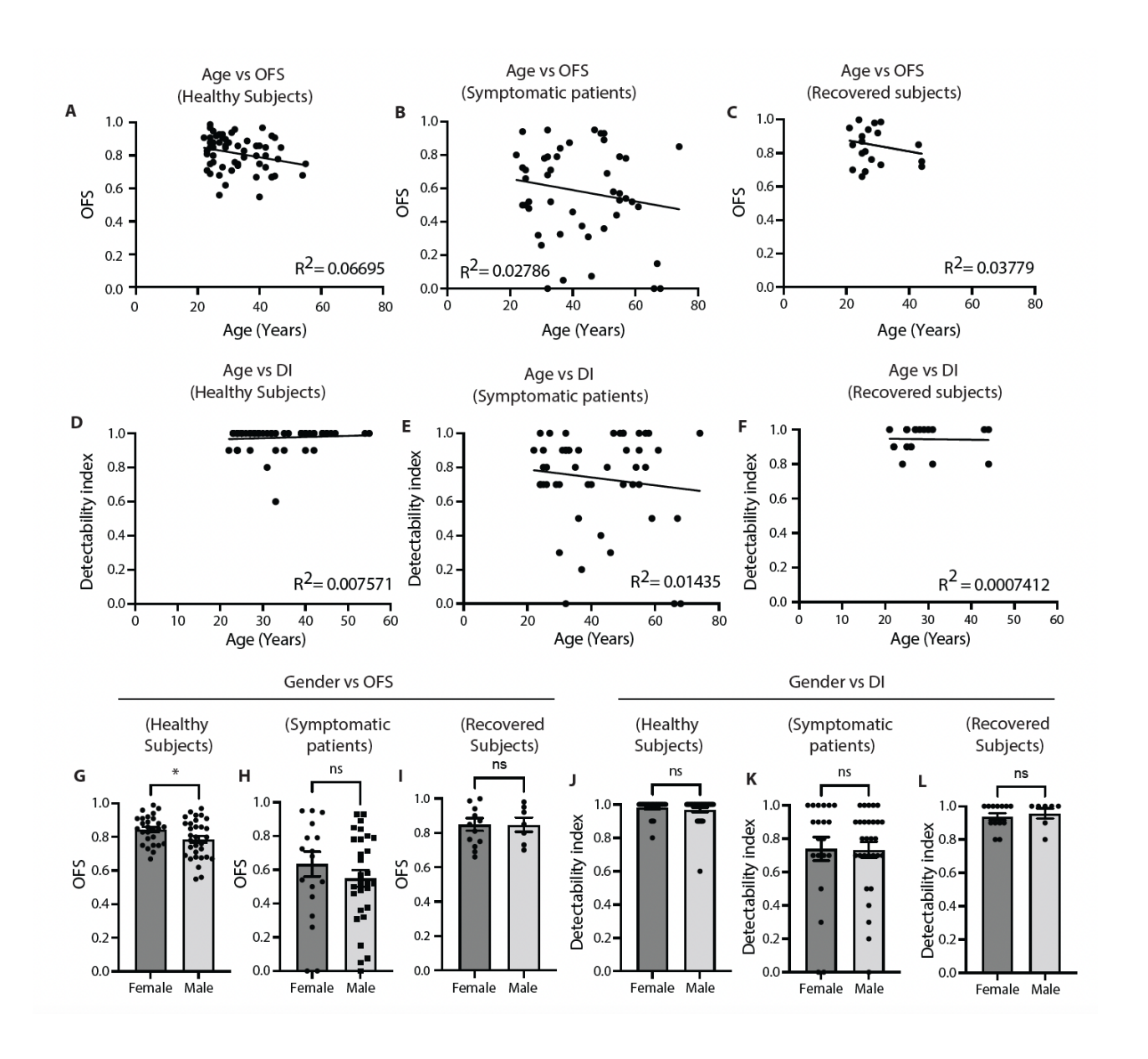


Figure 4. Correlation analysis of confounding variables and olfactory fitness readouts. (A) Olfactory Function Score (OFS) does not vary with the age of healthy subjects (N=58) (Linear Regression Analysis,  $R^2$  = 0.06695). (B) OFS does not vary with the age of symptomatic COVID-19 patients (N=48) (Linear Regression Analysis  $R^2$ = 0.02786). (C) OFS does not vary with the age of recovered subjects (N=20) (Linear Regression Analysis  $R^2$ = 0.03779). (D) Detectability Index (DI) remains unaffected for healthy subjects (N=58) (Linear Regression Analysis  $R^2$ = 0.007571). (E) DI for symptomatic COVID-19 patients (N=48) remains unaffected with the age variable (Linear Regression Analysis,  $R^2$ = 0.01435). (F) DI does not vary with the age of recovered subjects (N=20) (Linear Regression Analysis,  $R^2$ = 0.0007412). (G) OFS values for healthy females (N=27) and

males (N=31) show a marginal difference, primarily, arising as a result of lower DI values at low concentrations for 2 male subjects (Unpaired two-tailed t-test, \*p=0.03). (H) OFS values for symptomatic females (N=19) and males (N=29) patients remains statistically similar (Unpaired two-tailed t-test, p > 0.05). (I) OFS values are comparable for recovered females (N=13) and males (N=7) (Unpaired two-tailed t-test, p > 0.05). (J) DI values for healthy females (N=27) and males (N=31) are comparable (Unpaired two-tailed t-test, p > 0.05). (K) DI values are similar for symptomatic females (N=20) and males (N=29) patients (Unpaired two-tailed t-test, p > 0.05). (L) DI values for recovered females (N=13) and males (N=7) are comparable (Unpaired two-tailed t-test, p > 0.05).

#### 4.4. Discussion

Our work shows a robust new methodology that using custom-built experimental setup to non-invasively quantify neurocognitive deficits in COVID-19 patients. The paradigm is sensitive and reliable enough to identify neurocognitive deficits in recovered subjects while odor detectability returns to normal in human subjects. The results strongly vouch for employing such inexpensive machinery to probe neurocognitive health in patients with potential impairment in cognition on a regular basis. Impaired olfactory detectability observed in symptomatic patients (Figure 4.1B-C) mimics similar findings in that of asymptomatic patients. The phenotype being prevalent across all the odors (Figure 4.1B) points towards an impairment of diffused nature.

Long-term cognitive impairment or 'brain fog' has been one of the major behavioral consequences of the post COVID-19 sequelae of symptoms observed in recovered patients. <sup>322,323</sup> Long covid, as it named in the popular literature, has taken center-stage in the post-COVID chronic morbidity in humans. <sup>229</sup> Prior to assessing cognitive deficits, we opted to look for olfactory detectability. Though previous work that looked at a COVID-19 positive cohort with olfactory dysfunction for 5 weeks, found a 63% recovery <sup>324</sup>, our cohort of recovered subjects, who tested negative for COVID-19 at least 90 days prior to the experiment, had identical olfactory detectability as that of the controls (Figure 4.2B). A recent study has reported ~95%

recovery rate of olfactory dysfunction within 6 months of COVID-19 infection. <sup>325</sup> This indicates towards the reversible nature of the olfactory sensory function in COVID-19. When we assessed neurocognitive functioning olfactory learning task displayed strikingly impaired learning in symptomatic patients as well as recovered subjects while healthy participants showed improved performance over time (Figure 4.2E). Our findings, in accordance with several other studies highlight the severity and extent of long-term impairment in COVID-19. A large-scale study reported impaired cognitive performance in patients with COVID-19 up to three years post hospitalization. <sup>326</sup> In one study, out of a cohort of 96 patients, 27% patients eventually developed long COVID-like symptoms and was related to systemic large-scale inflammation that eventually led to neuronal damage. <sup>327</sup>

The finding of asymptomatic carriers showing more severe deficit (Figure 4.3) may be linked to higher viral load in asymptomatic carriers in comparison to symptomatic patients. 328 Many of the participants reported the odor perception for distinctly different odors to be very similar even after getting better, indicates a rather distorted sense of smell, termed as Parosmia. This distortion in odor perception has been attributed to several factors. 329 Existing studies propose that such phenotype can be manifested due to remaining blockage of the olfactory cleft, residual inflammation in the olfactory epithelium, ACE-2 expressing supporting cells in the olfactory epithelium being invaded by SARS CoV-2. 329-331 Under these circumstances, wider immune profiling including several other inflammatory markers may be necessary to gain a better insight in the prolonged cognitive deficits. Employing recent techniques in brain imaging like PET-MRI<sup>332</sup> and elctrobulbogram (EBG)<sup>333</sup> may offer valuable insight into the underlying phenomena.

Not surprisingly though, COVID-19 induced neuropathology has striking similarities with several neurovegetative conditions.<sup>334</sup> But each olfactory deficit resulting from underlying neurocognitive dysfunction, often comprises of distinct disease-specific neuroanatomical pathology leading to altered functioning of one or multiple subsystems in the CNS.<sup>335</sup> For e.g., pathological investigation with PD patients has revealed the presence of Lewy bodies in OB and olfactory tract (OT)<sup>336</sup>,

misrouted (MR) olfactory projections and ectopic glomerular structures in OB<sup>337</sup>, cell death in AON correlated to disease progression<sup>338</sup> and several other neuroanatomical findings. In AD, tau aggregates or amyloid- $\beta$  plaques have been found in multiple brain regions associated with odor information processing, such as entorhinal and trans-entorhinal cortices, AON, in early stages of the disease.<sup>284</sup> Drastic reduction in the number of mitral cells in OB is also reported which severely disrupts odor processing.<sup>339</sup> A recent study reported presence of mutant Huntington's protein (mHtt) in the OB of HD patients with majority of the aggregates being localized in the anterior olfactory nucleus (AON)<sup>340</sup>, part of the primary olfactory cortex (POC) thought to play important role in episodic odor memory.<sup>341</sup> Damage to the neurotransmitter systems can also alter olfactory function. Acetylcholine (ACh), a crucial neurotransmitter, has been shown to aid in differentiation of oligodendrocytes, the myelin-forming cells in the CNS.<sup>342</sup> As non-myelinated nerve fibers are more susceptible to neurodegeneration, death of cholinergic neurons in the olfactory tubercle in Alzheimer's and Huntington's diseases<sup>343</sup> may help explain olfactory deficit observed in patients. In contrast, the role of dopamine (DA), another important neurotransmitter affected in PD due to loss of dopaminergic neurons, is not clear in the context of the observed smell loss in patients. 344,345 Administering dopamine agonist did not improve odor identification in PD patients<sup>346</sup>. One study found correlation between UPSIT score in PD with hippocampal dopaminergic denervation<sup>250</sup>. Like ACh and DA, the potential role of gamma amino butyric acid (GABA), an inhibitory neurotransmitter synthesized by glutamic acid decarboxylase (GAD), has also been investigated in clinical cases of neurodegeneration. AD patients with severe neuropathology show decreased levels of GABA-A subunits  $\alpha 1$ ,  $\alpha$ 5 and  $\beta$ 3 in the hippocampus<sup>347</sup> while a decline of the  $\alpha$ 1 and  $\alpha$ 2 GABA-A subunits in prefrontal cortex (PFC) is seen in both early and late stages of the disease 348,349. Reduced GAD mRNA in PFC has also been reported in PD patients<sup>350</sup>. Both hippocampus and PFC have direct neural connections with OB349,351 and play important roles in odor information processing<sup>352</sup>. Norepinephrine and serotonin seem to have minimal involvement in neurodegeneration-associated smell loss<sup>283</sup>. Underlying mechanisms of how olfactory abilities decline may vary widely across

neurodegenerative diseases and is not clearly understood. Olfactory deficit has also been one of the hallmarks in a significant proportion of COVID-19 patient<sup>247</sup>. Supporting cells in the olfactory epithelium and not the OSNs, have been shown to express ACE2, receptor for COVID-19 spike protein, thus acting as entry points for the virus to the CNS and subsequently causing smell loss.<sup>353</sup>

Our custom-built OAM has been shown to identify asymptomatic patients with high accuracy<sup>228</sup>. We also reported a learning deficit in olfactory matching in symptomatic patients of COVID-19 as well as recovered COVID-19 participants, followed up for 4 or more days.<sup>97</sup> Careful analysis of performances of patients in odor matching task and modulating experimental parameters in disease-specific fashion may allow us to correlate specific pathology with observed olfactory functioning.

# Chapter 5

# Bidirectional modulation of E/I balance in the olfactory bulb regulates olfactory working memory

#### 5.1. Introduction

Delayed matching paradigms have long been generously employed to study short-term memory-related phenomena. Olfactory matching thus provides a suitable and precise paradigm to study working memory. By the very nature of the paradigm, there are components of detection and discrimination but working memory too plays a crucial role. Though the definition has evolved over the years, broadly, WM is understood as a capacity limited component of memory system utilized to store and manipulated information over short period of time. The fact that many neurocognitive disorders are often accompanied by some olfactory dysfunctions a greater need has emerged to include tests for olfactory impairment into the paradigm of differential diagnosis of neurocognitive deficits. Moreover, recent years have seen overwhelming cases of COVID-19 infections that were accompanied by different degrees of loss of sense of smell. Many of these patients had trouble regaining their neurocognitive abilities even after the other external symptoms have subsided. See-358

Working memory research may be broadly looked at from several different perspectives. For example, one aspect of research may explore whether there is a limiting factor to working memory span and how this short-term memory is achieved by associated neural networks. On the other hand, another aspect may necessitate deciphering how modulations of the neural networks involved alter working memory-based performance. The first, for example, has been a largely debated one. Depending on the sensory modality in question or the experimental design of the paradigm, attempts to answering this question has varied. For STM of words, a popular n-back task the limit has been set at  $7 \pm 2$ . Though other systems have been generously investigated, capacity for olfactory WM (OWM) remains largely misty. Since the introduction of the term working

memory by George Miller,<sup>360</sup> very little attention has been devoted to deciphering the cognitive and neurophysiological intricacies of olfactory working memory (OWM). Meanwhile, visual, auditory and somatosensory systems have received the maximum attention when it comes to WM research possibly because of our inherent psychological predisposition and utmost conscious dependence to these sensory systems.<sup>361</sup> Some scholars have even argued that olfaction lacks distinct, modality-specific neural representations commonly found for other sensory systems, putting the whole of OWM field under question.<sup>362</sup> But continuing research has increasingly consolidated the existence of OWM and its distinct neural correlates.<sup>87,270,363</sup>

Post-stimulus maintenance of stimulus via delay period activity, in a delay stimulus matching task, has long been thought of as an essential element of short-term memory. 364 Work has also highlighted roles of prefrontal cortex 365 and hippocampus 366, among other brain regions in WM. For the olfactory system, in quite a similar fashion, odors have shown to evoke traces that sustain even after the odor stimulus is discontinued. 367 Whether the olfactory bulb plays any role in the transient maintenance and in turn, effects working memory performance, is not very well understood. Though the role of the sensory cortex associated with olfaction has been highlighted with research reporting activity in the piriform cortex during WM tasks in humans. 368 Subsequent work has highlighted the role of anterior piriform cortex (APC) in the sustaining odor information during the delay and thus playing crucial part in DNMS tasks. 158 Transient but not sustained delay activity in the anterior agranular insular cortex (aAIC) has also been reported to be crucial for OWM. 369

A great deal of our current understanding of WM relies heavily on the role of higher cortical regions, like the prefrontal cortex<sup>365</sup>, especially the medial PFC in the context of OWM.<sup>370</sup> Another candidate that has received significant attention over the years in the field of working memory research is the mediodorsal (MD) thalamus.<sup>371</sup> Anatomically, MD thalamus has been shown to form reciprocal connections with PFC as part of a larger corticothalamic circuit.<sup>372</sup> Recent studies suggest that MD thalamus may be involved in sustaining PFC delay period activity<sup>373</sup> and thus may play important role in the maintenance of working memory during the delay. Moreover, persistent activity in category

selective neurons in the hippocampus during delay period in WM-related task has been linked to the degree of confidence in successful recall in long term.<sup>374</sup>

This background necessitates a much more comprehensive understanding of cognitive well-being measured through the sensory modality of olfaction. One of the key elements of working memory is the memory capacity. 11 In the context of olfaction, it may be investigated as a correlate of the maximum number of odors that one can successfully remember for a given duration<sup>375</sup> (an olfactory n-back task) or how long an odor identity be retained in the WM. There has been some work done on the first kind of OWM capacity, while the second kind of correlate is poorly explored. Our pilot study indicates that healthy individuals show no significant performance decline with a delay period extended up to 10 seconds. To investigate the neural correlates, we decided to employ mouse model under a delayed match to sample (DNMS) paradigm. After training the animals for an odor matching task with 2s delay, we incrementally increased the temporal delay between two stimuli to observe how the matching performance changed over increasing delays. To investigate how altering the excitation-inhibition balance in the OB effects the olfactory matching performance in freely moving mice, we generated conditional knockout mice for NR1 subunit of NMDA receptors and GluA2 subunit of AMPA receptors. We trained these two groups with their respective sham groups for a delayed matching task where animals were initially trained for a delay of 2s which is increased to 4s and subsequently 8s. Our findings show that GluA2 KO animals performed significantly better across all ISIs while NR1KO groups showed impaired learning when compared to their respective sham groups.

#### 5.2. Materials and methods

# 5.2.1. Olfactory matching paradigm in freely moving mice

Odor matching is a delayed match to sample task that involves matching two odors separated by an interval. Mice are trained to perform the task for a fixed stimulus delay for a maximum of seven tasks, where each task comprises of 300 trials. For experiments investigating the temporal limit of olfactory WM, mice are first trained for 2s delay and at

the end of 2100 trails, the delay period is set to a higher ISI. Once mice are trained for this second ISI for 300 trials, the stimulus delay is increased again, and the same cycle is repeated. We have trained mice to perform at very high ISIs, up to 52s delay.

For conditional knock out mice, the mice are trained for 2s ISI. Once they complete performing for 1800 trails, the ISI is increased to 4s. The mice are trained with this stimulus delay for 600 trails and then the ISI is increased again to 8s. The training concludes with mice performing odor matching task at 8s ISI for 600 trials. As there is continual regeneration in the mouse OB, there is continual turnover of inhibitory interneurons. Previous works suggest that a significant portion of the granule cell population is replenished with newborn neurons over a period of approximately 3-4 months. <sup>376</sup> However it is worth mentioning here that a subset of the newborn neurons can get integrated in the superficial layer of the GCL and survive for long periods, possibly the entire lifetime of the animal. <sup>377,378</sup> To avoid any confounding effects imparted by this constitutive renewal, all the training experiments for KO and sham groups are completed within 3 months.

# 5.2.2. Apparatus

We use an eight channel olfactometer that has an operant chamber with an odor delivery port and a lick port. A chamber houses the animals during the course of their training. Circular cut-out allows the animal to sniff and sample the delivered odors. Right below the odor delivery port, the lick port is placed. On the other side of the ports a concealed opening allows an exhaust to circulate ambient air into the chamber and thus prevent accumulation of odors inside the chamber. The sampling region is guarded by an IR beam. To start a trial, the mouse inside the chamber must break the beam, ideally with its snout. Trial starts immediately after the mouse has broken the beam.

Delivery of odorized air from one of 8 channels carried out through clean tygon tubings at a rate of 2 litres/minute. A dual valve mechanism controls the odor delivery, namely the odor valve (OV) and the final valve (FV). The OV remains open for 500 ms before the FV is open. An exhaust continuously flushes out any undesired odor from the

tubings at all times except during the delivery of the odors. Mice are rewarded with  $\sim$ 3  $\mu$ l of water for each successful rewarded trial.

#### 5.2.3. Habituation and pre-training

For the pilot experiment, a set of 12 C57BL6/J male mice, aged 6-8 weeks, were trained for an odor pair of Amyl Acetate (AA) and Ethyl Butyrate (EB) for an interstimulus interval of 2s. To get rid of potential confounding effects imparted by the chosen odor pair, another set of animals of similar specifications are trained for a different set of odor pairs, namely Hexanal and 2-Pentanone.

Once availed, animals are habituated in the operant chamber by keeping them there for 5-10 minutes. This is followed by pretraining phase. Mice are deprived of drinking water for a maximum of 12 hours before each day of the experiment.

For more details on the pre-training paradigm, refer to Section 2.4.2.2 in Chapter 2.

Animals were made to perform at least 40 trials in each of the phases. Though some animals required a few more trials than other, the number hardly ever exceeded beyond 60 trials.

#### 5.2.4. Olfactory matching paradigm

As described above, all trials were initiated by the breaking of the IR beam by the animal. Once the beam is broken, odorized air carrying the first odor is delivered for 2s. This is followed by a delay of 2s, at the end of which the second odor is presented for 2s. The lick window coincided with that of the presentation of the second odor. The lick window is divided into four 500 ms bins and the lick criteria was set as follows:

- For rewarded trials, animals must lick for more than 2 bins to get a reward.
- For non-rewarded trials, animals should not lick for more that 2 bins for the trials to be registered as correct.

#### 5.2.5. Measurement of behavioural parameters

Different parameters were used to characterize the behavioural data, e.g., learning curve, lick pattern, sample pattern and odor matching time (OMT).

#### 5.2.5.1. Learning curve

As specified earlier, the animals perform 6-7 tasks, depending on the experimental paradigm, where each task comprised of 300 trials. Matching accuracy for every animal is calculated every 100 trails. For a 7-task long training paradigm, thus a total of 21 values, each depicting the mean accuracy for 100 trials are plotted against the associated trail number. This gives us a learning curve which represents the learning for each animal in the odor matching task.

#### 5.2.5.2. Sample pattern

With each break of the IR beam, the operating program records a time stamp that can later be used to identify sampling behaviour of the animal during the odor presentation or the delay period. The sensor placed here can sample with microsecond precision. Every value presented to the corresponding sampling bin represents an average over 20 ms duration. This can later be plotted to visualize how often the IR beam was broken. This data acts as a correlate of the motivation of the animals performing.

#### 5.2.5.3. Lick pattern

As an animal starts licking at the lick port, a sensor can record with microsecond precision. Every value presented to the corresponding lick bin represents an average over 20 ms duration. As this data is further plotted against duration of the trail averaged over all trials in a task, a representative lick pattern emerges that correlates to relative licking frequency and decision making during the course of the task for each animal (Refer to Section 2.4.3.3 for more details).

#### 5.2.5.4. Calculation of Olfactory matching time (OMT)

A t-test is run comparing the lick values corresponding to each 20 ms bin starting at onset of the second odor between rewarded and non-rewarded trials. The point where the p-value goes below 0.05 and does not come back up beyond 0.05, is considered to the point of significant divergence between the rewarded and non-rewarded trails. This bin value (nth bin x 20ms) acts as a correlate to the delay the animal took to match the first odor with the second during the task. The delay is taken as the olfactory matching time (*Refer to Figure 2.3 in Chapter 2 for a schematic representation*).

#### 5.2.6. Generation of conditional knockout mice

As the animals are trained for extended periods of time, this is likely to induce long-term potentiation (LTP). AMPA and NMDA receptors are known to play important roles in LTP formation. <sup>235,236</sup> GluA2 and NR1 are sub-units of AMPA and NMDA receptors respectively. GluA2 KO mice will have higher Ca<sup>2+</sup> influx into the cell<sup>237,379</sup> thereby increasing inhibition on the projection neurons, namely the mitral and tufted (M/T) cells. Whereas NR1 KO would in turn limit cation entry<sup>238</sup> in the Gad2 positive neurons. This would decrease inhibition on the M/T cells. Stereotactic optimization injections were first carried out using a fluorescent dye to check for GCL specificity. As first set of experiments with GluA2 conditional KO mice, 12 sham and 12 Cre viral particle injections were carried out for AAV mediated expression of EYFP-Cre. For the second set, we injected Cre viral particles in 12 NR1 lox mice and equal number of sham surgeries. An incubation period of 3 weeks was kept before starting the behavioural experiments.

#### 5.2.7. Habituation and pre-training

The task habituation was carried out in a similar fashion as mentioned in the section 5.2.3. *Refer to Section 2.4.2.2 in Chapter 2 for more details*.

#### 5.2.8. Immunohistochemistry

For immunohistochemical studies, previously published procedure from the lab by Pardasani et al., 2023 have been adapted. (For more details refer to 2.5.5 in Chapter 2).

#### 5.2.9. Protein level quantification

For protein estimation, optimized procedure from the lab by Mahajan et al., 2024 (bioRxiv) and Marathe et al., 2024 (bioRxiv) have been adapted (Refer to Section 2.5.6 in Chapter 2 for more details).

#### 5.3. Results

#### 5.3.1. Mice learn to perform odor matching with high delay periods

Freely moving mice were trained to perform a delayed odor matching upon initial pretraining (See section 5.2.3.). Mice were gradually introduced to odor pairs separated by an interval. The training was counterbalanced with same odor pairs rewarded for half of the animals and opposite reward criteria for the other half (Figure 5.1A). For the pilot experiment Amyl acetate and ethyl butyrate odor pairs were used and a delay period of 2s was employed. As they were trained over 2100 trials, mice could learn to perform the task with high accuracy of nearly 90% (Figure 5.1B, N=7). To rule out any bias towards the odor pair used, another group of animals were trained with 1, Hexanal-2, Pentanone odor pair. Mice could successfully learn to match odors with similar accuracy as the first odor pair when trained over 2100 trials (Figure 5.1C, N=11). Once we confirmed that mice could learn odor matching irrespective of the odor pairs chosen, we decided to increase the stimulus delay and see how the matching accuracy is affected. Previous studies have shown that mice are unable to perform well with high delay period matching tasks with abrupt increase in delay period.381 We, in contrast, chose to increase the delay in gradual bouts for the already trained mice with 2s delay. With each new delay period, we trained the mice for 300 trials before changing the delay again. As we trained the mice for increasing delay periods up to 52s, we observed that mice are able to perform the task with high accuracy even for very high delays (Figure 5.1D 1-14, Mice were trained for 4s (N=10), 6s (N=10), 8s (N=10), 10s (N=8), 12s (N=6), 14s (N=5), 16s (N=5), 18s (N=5), 20s (N=5), 24s (N=5), 28s (N=5), 36s (N=5), 44s (N=5) and 52s (N=4)). Though mice have been extensively trained by the end of the entire training period of nearly seven months, observation of this kind where freely moving mice performed with high accuracy for such long delays has been unprecedented. As we compared the learning curve for each delay period, we see a gradual decline in the extent of learn with increasing ISI (Figure 5.1E). As we quantified the area under the curve (AUC) for all the individual learning curves across ISIs, we see that the AUC is negatively correlated with ISI (Figure 5.1F). A linear regression analysis for the odor matching accuracy for the last 100 trails for each ISI,

show that increasing ISI strongly correlated with declining accuracy (Figure 5.1G, Linear regression analysis,  $R^2$ = 0.9213, p<0.0001).

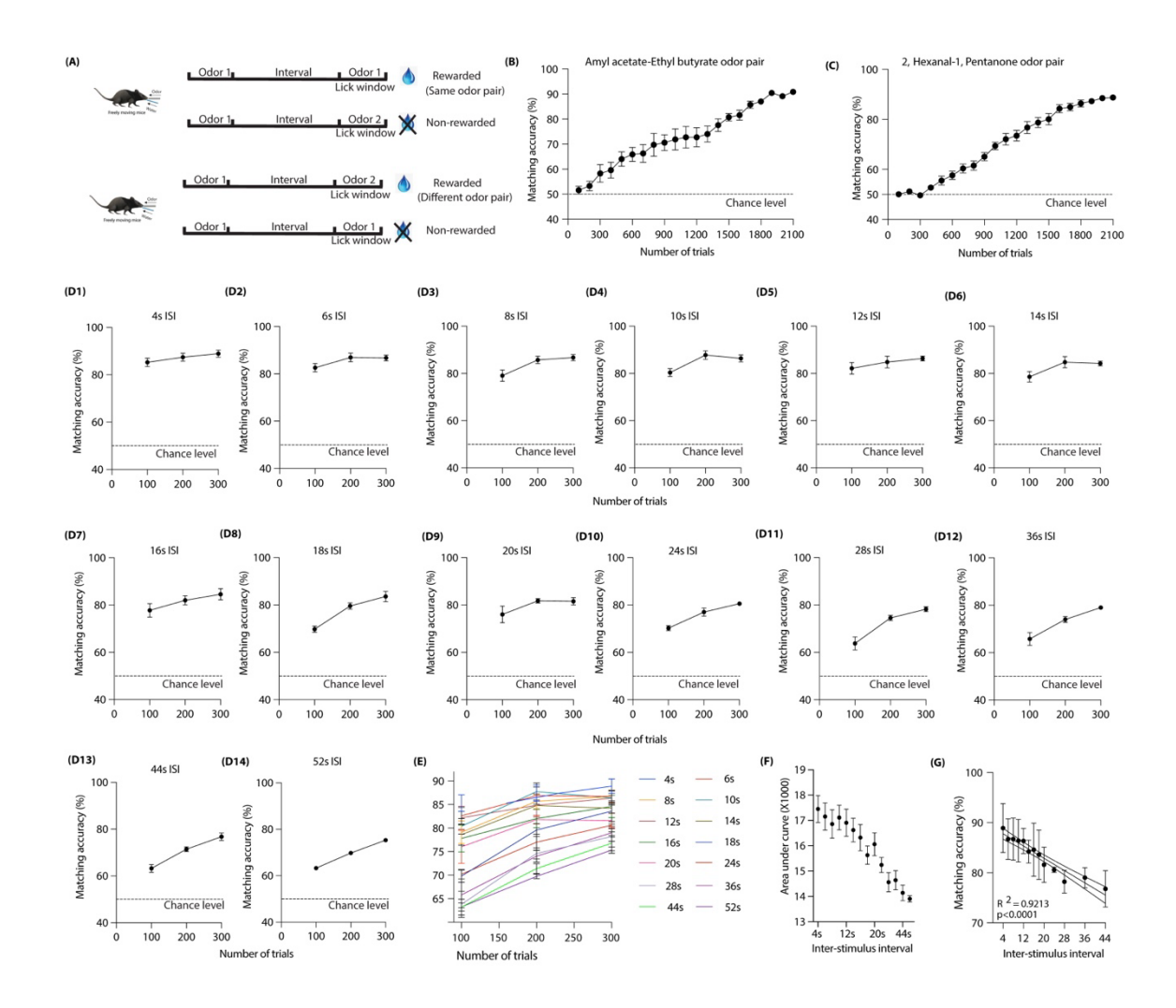


Figure 5.1. Mice can be trained to perform working memory tasks with high delay periods. (A) Mice are trained on a freely moving delayed odor matching task where the reward criteria are counterbalanced. Two odors are delivered in sequence separated by a stimulus interval. Upon the delivery of the second odor, mice are rewarded upon successful licking based on the reward criteria. For half of the animals, same odor pair is

(B) As a pilot study, mice were trained for Amyl-acetate and Ethyl Butyrate odor pair (N=7) for a delay period of 2s. Mice learn to perform the task with high accuracy within 2100 trials.

rewarded while for the other half, different odor pairs are rewarded.

- (C) To establish that the performance is equally reproducible for other odor pairs, 2, Hexanal-1, Pentanone odor pairs are used for another set of animals (N=11). Like the previous odor pairs, mice learn to perform with high accuracy for 2s inter-stimulus interval. (D1-14) Learning curves for different ISIs are plotted. Once the mice performed with high accuracy for 2s ISI, the stimulus interval is increased gradually for the same set of animals. For each new ISI, mice are trained for 300 trails before moving to a higher ISI. Mice are trained for 4s (N=10), 6s (N=10), 8s (N=10), 10s (N=8), 12s (N=6), 14s (N=5), 16s (N=5), 18s (N=5), 20s (N=5), 24s (N=5), 28s (N=5), 36s (N=5), 44s (N=5) and 52s (N=4). For 52s ISI, one animal performed 220 trails instead of 300 trials. Considering the difficulty level of the task and high performance of the animal for 52s delay, data for this animal is included in the analysis. Despite a few dropouts as the paradigm becomes increasingly harder to perform, mice successfully learn to perform odor matching task for up to 52s.
- (E) Learning curves for different ISI are compared where it is evident that odor matching accuracy declines with increasing ISI (Two-way ANOVA with Tukey's multiple comparison, \*\*\*\*p<0.0001)
- (F) Area under curve (AUC) for the learning curves of all the mice are calculated for each ISI. The AUC are shown to decline as the stimulus interval increases.
- (G) Mean odor matching accuracy for the last 100 trails for each animal is plotted across ISIs. Linear regression analysis shows a strong negative correlation between stimulus delay and odor matching accuracy. Data for 52s is excluded as only 3 animals completed the entire 300 trials. The dotted lines show 95% confidence interval (Linear regression analysis,  $R^2$ = 0.9213).

#### 5.3.2. Odor matching activity undergoes refinement with progression of training

There are several parameters that may shed light on the behaviour of the freely moving mice other than the odor matching accuracy. Sampling pattern and lick pattern are among the most recognizable among them. Throughout a trial, mice can be seen sampling and licking at various times. As each trial is initiated by breaking of an IR beam (see Chapter 2 and Materials and methods section of Chapter 5 for details), sampling is registered every time the IR beam is broken throughout the trial. And so is the lick pattern. The lick pattern is registered every time the mice lick at the lick port. Though at the beginning of training,

mice can be observed to be sampling or licking somewhat randomly, these behavioural parameters undergo significant refinement as the animals undergo training. Here we looked at lick pattern for the animals across four representative tasks, starting with Task 1 till Task 7 where the lick probabilities for rewarded and non-rewarded trials can be seen diverging more and more with progression of training (Figure 5.2A). Similar optimization can be seen in the case of sampling pattern with random and scattered sampling behaviour in Task 1 and progressively more refined sampling behaviour as the task progresses (Figure 5.2B). As we looked at the lick pattern for higher ISIs we see similar refined licking behaviour across all ISIs. Here, we present the lick pattern for two representative stimulus delays, one representing one of the lowest delays of 6s and one on the highest end, i.e., 52s (Figure 5.2C). The lick patterns can be characterized by heightened licking starting with the first odor that sees a relatively steep decline right after. This is followed by marginal licking behaviour during the delay period. Moreover, right after the second odor is delivered, a further decline in lick behavior is observed which is followed by a heightened lick for rewarded odor trials and a diminished licking for nonrewarded ones. This pattern of licking gives us a glimpse at how the animal decides to lick during decision-making period while minimizing lick during the delay period. We used the diverging lick patterns for rewarded and non-rewarded odors to calculate the odor matching time (OMT) for each ISI. As we ran a linear regression analysis across all the ISIs, we do not find any correlation between delay interval and OMT (Figure 5.2D, Linear regression analysis,  $R^2$ = 0.05384, p= 0.4053). Though the mice took longer, on average, to match simple odor pairs, when compared to olfactory-based go-no go tasks<sup>379</sup>, there matching times seem to be independent of the stimulus delay.

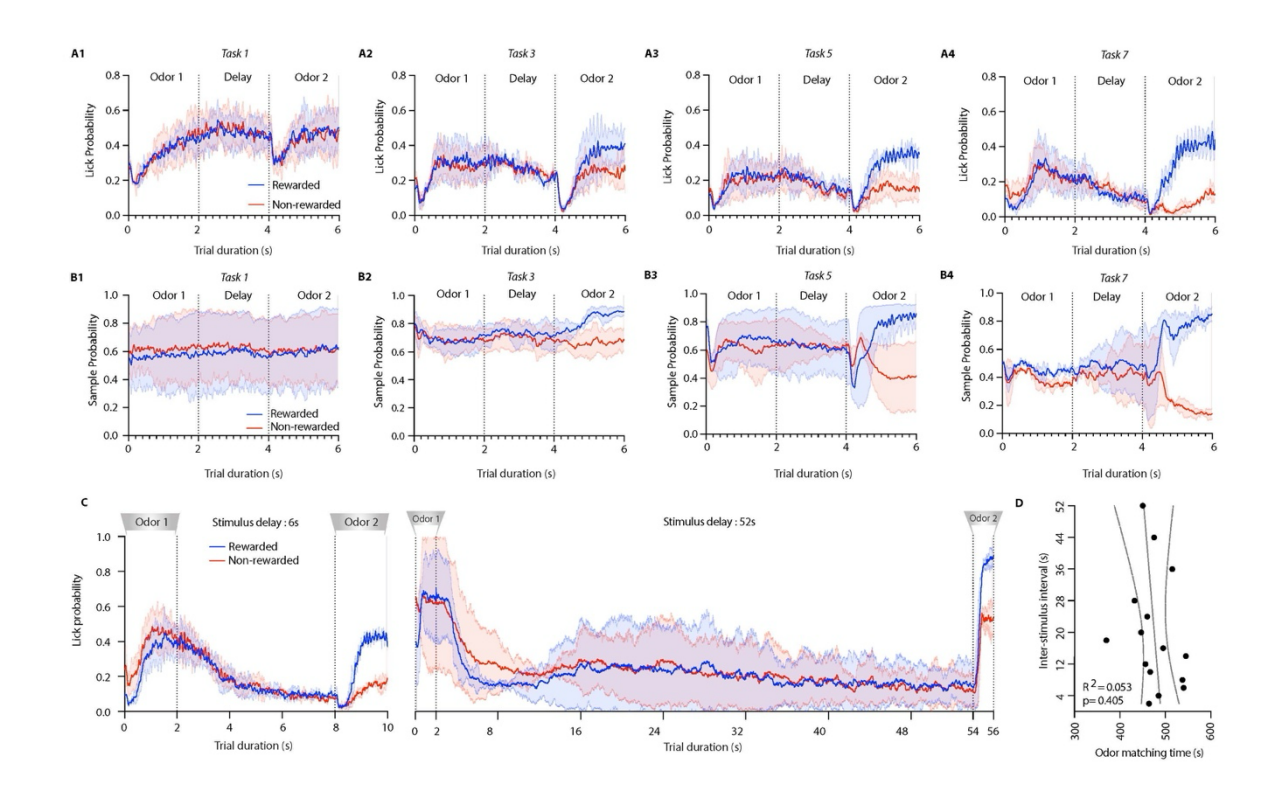


Figure 5.2. Lick and sample pattern undergo refinement with training.

- (A1-4) Representative lick pattern for two mice for rewarded and non-rewarded trials show gradual divergence in licking behaviour in the animals as the training progresses. The delay is 2s and animals are trained for 7 tasks where each task comprises of 300 trails with equal number of rewarded and non-rewarded trials.
- (B1-4) Representative sample pattern for two mice for rewarded and non-rewarded trials show gradual divergence in sampling behaviour in the animals as the training progresses.

  The delay is 2s and animals are trained for 7 tasks where each task comprises of 300 trails with equal number of rewarded and non-rewarded trials.
- (C) Lick pattern for one representative low ISI (6s) and one representative high ISI (52s ISI) are depicted. The lick pattern depicts dramatically decreased licking during the delay. After the presentation of the second odor, following a brief decision-making window, the lick pattern diverges with sharply increased licking for rewarded trials and virtually unchanged for non-rewarded trials.
- (D) Olfactory matching time calculated using the lick pattern for rewarded and non-rewarded trials are plotted for different delay periods. A linear regression analysis shows

no correlation between increasing ISI and odor matching time (Linear regression analysis with 95% confidence interval,  $R^2$ =0.05384, p=0.4053).

# 5.3.3. Increased inhibition on projection neurons in mouse olfactory bulb improves odor matching

Working memory performance depend strongly on excitation-inhibition (E/I) balance.<sup>382</sup> There have been several reports of manipulation at the level of primary olfactory cortex or pre-frontal cortex affecting olfactory working memory. 270,365 But how working memory performance is affected when the E/I balance at the level of OB is altered, remained elusive. Under this pretext we decided to bidirectionally modulate the E/I balance in OB and see how this affects the odor matching performance. One of the convenient ways of manipulating E/I balance is by modulating the activity of granule cells (GCs) in the granule cell layer (GCL) of OB. GCs are GABAergic interneurons that form reciprocal synapses with the projection neurons Mitral and Tufted (M/T) cells in OB. 106 So, stronger depolarization of GCs would inevitably increase inhibition on M/T cells and vice versa. 379 One strategy to achieve this is via knocking out GluA2 sub-units of AMPA receptors. GluA2-containing AMPA receptors, which are usually Ca<sup>2+</sup>-impermeable<sup>383</sup>, can be made permeable to Ca<sup>2+</sup> if the GluA2 subunit is knocked out.<sup>379</sup> Using Cre-lox system<sup>384</sup>, we generated conditional knockout mice for GluA2 (Figure 5.3A) by injecting Cre-containing AAV9 viral vector in the GCL of the OB of GluA2-floxed mice (Figure 5.3B, also see Section 2.5 of Materials and Methods). After an incubation period of minimum 3 weeks, mice could be sacrificed for immunohistochemical (IHC) studies and western blot purposes for confirmation of GCLspecific knockout of GluA2. As we performed IHC, infected neurons expressing EYFP as part of the viral vector could be visualized (Figure 5.3C, confocal microscopy, 20X, scale bar: 50 µm). We see most of the infected cells in the desired GCL of the OB with their projections extending to the mitral cell layer (MCL) and external plexiform layer (EPL). A higher magnification image (60X) of a single infected granule cell shows the cell body localized in the GCL with its apical dendrites projecting to the MCL (Figure 5.3D, confocal microscopy, 60X, scale bar: 50  $\mu$ m). As we trained the animals for three different ISIs, namely 2s, 4s and 8s respectively, under freely moving condition, we found that GluA2 KO mice performed significantly better than the sham group for all three

stimulus delays (Figure 5.3E, Two-way ANOVA with Bonferroni's multiple comparisons, p<0.05). As we further compared the OMT for the two groups across ISIs, we found that the GluA2 KO group were significantly faster than the sham group for 2s and 4s ISIs (Figure 5.3F, Unpaired t-test, p<0.05).

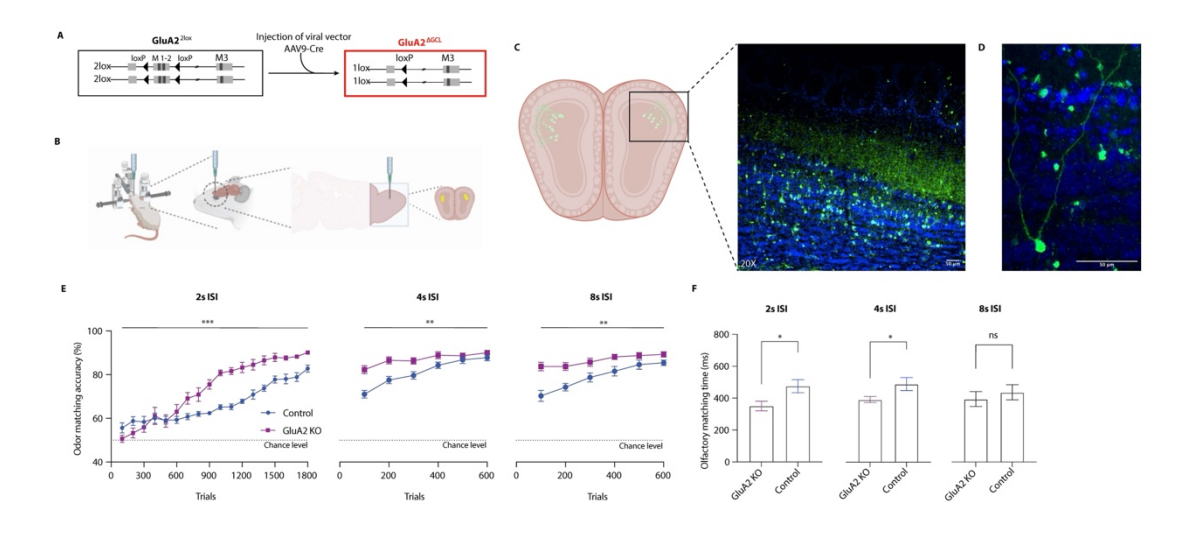


Figure 5.3. GluA2 knockout mice show faster learning in olfactory matching task

- (A) The schematic diagram represents Cre-recombinase mediated ablation of the transmembrane regions 1 and 2 of the GluA2 gene flanked with loxP sites by AAV9-mediated expression of Cre upon GCL-specific stereotactic injection in the OB (GluA2<sup>ΔGCL</sup>).
- (B) Stereotactic surgeries are carried out in GluA2-floxed mice (6-8 weeks old) under anaesthesia where Cre-viral particles are injected in the GCL of OB (See Section 2.5 of Materials and methods for details). An incubation period of 21 days is maintained upon which mice are subjected to behavioural training.
- (C) Schematic representation shows infected cells in the GCL after the incubation period. Next to the schematic diagram, a confocal image of the mouse OB shows infected cells expressing EYFP (in green) in the GCL with projections reaching to the MCL and EPL in mouse OB. DAPI staining of the nuclei is represented in blue (20X, Scale bar: 50 µm).

- (D) A singular granule cells expressing EYFP can be seen with its nucleus in the GCL and projections reaching MCL (63X, Scale bar: 50 um).
- (E) GluA2KO mice trained for three different ISIs, 2s, 4s and 8s, show faster learning in comparison to sham group across all ISIs (Two-way ANOVA with Tukey's multiple comparison, p<0.05).
- (F) When olfactory matching times are compared, GluA2KO mice show faster matching time for 2s and 4s ISI while matching times remained comparable for 8s ISI (Unpaired t-test with Welch's correction; p< 0.05, ns>0.05)

# 5.3.4. Decreased inhibition on projection neurons in mouse olfactory bulb improves odor matching

Once we increased inhibition on the M/T cells via GCL-specific GluA2KO of AMPA receptors, we decided to see whether reducing inhibitory effects on projection neurons negatively affects WM performance. One strategy for such manipulation would be to target the NMDA receptors (NMDAR) of the GCs in the GCL. 109 NR1 is one of the seven subunits present in the mouse genome that code for the hetero tetramer of each NMDAR.<sup>385</sup> NR1 is an essential subunit of NMDAR<sup>386</sup> and knocking out of NR1 subunit (Figure 5.4A) renders the NMDAR non-functional. This would potentially result in reduced cation influx in GCs and in turn reduced inhibition on the M/T cells in the OB. In a similar fashion as seen in the case of generation of GluA2 KO mice, we injected Cre-AAV9 viral particles in the GCL of NR1-floxed mice (Figure 5.4B). After an incubation period of three weeks (see Section 2.5 of Chapter 2, Materials and Methods), mice could be sacrificed and processed for IHC and protein quantification to confirm the desired knockout effect. The viral construct allowed for the expression of EYFP in infected cells (see Materials and methods). As we performed IHC, we observed infected cells mostly in the desired GCL of the OB with projections reaching primarily in the MCL and EPL (Figure 5.4C, confocal microscopy, 20X, scale bar: 100 μm). A further zoomed in view shows a cluster of GCs with the cell bodies located in GCL and apical projections reaching MCL (Figure 5.4D, confocal microscopy, 60X, scale bar: 100 µm). We further carried out quantification of protein levels of NR1 using western blot. Protein quantification yielded expected knockout of the NR1 subunit that resulted in reduced levels of the protein (Figure 5.4E-F, Mann-Whitney test, p = 0.0286). As we looked

at the odor matching performance of the NR1KO group in comparison to the sham group, we found that KO group lagged considerably in terms of learning for 2s and 4s ISI (Figure 5.4G, Two-way ANOVA with Bonferroni's multiple comparisons, p<0.05). Similar impairment is observed for OMT as well with the KO group taking longer for 2s stimulus delay (Figure 5.4H, Unpaired t-test, p<0.05).

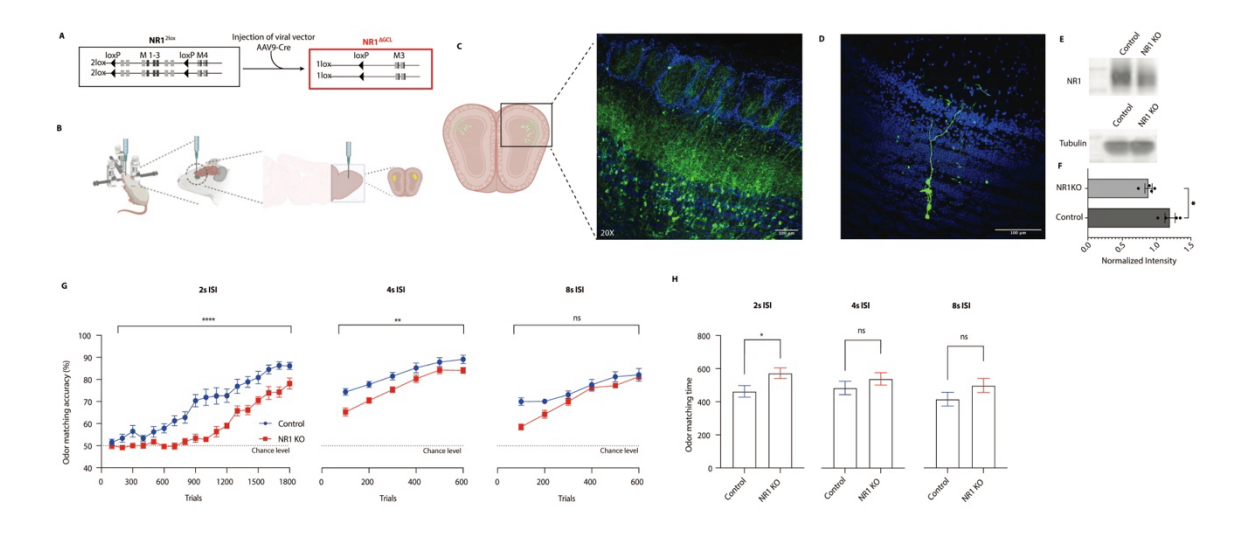


Figure 5.4. NR1 knockout mice show impaired learning in olfactory matching task

- (A) The schematic diagram represents Cre-recombinase mediated ablation of the transmembrane regions 1, 2 and 3 of the NR1 gene flanked with loxP sites by AAV9-mediated expression of Cre upon GCL-specific stereotactic injection in the OB (NR1<sup>ΔGCL</sup>).
- (B) Stereotactic surgeries are carried out in NR1- 2loxP mice (6-8 weeks old) under anaesthesia where Cre-viral particles are injected in the GCL of OB (See Section 2.5 for details). An incubation period of 21 days is maintained upon which mice are subjected to behavioural training.
- (C) Schematic representation shows infected cells in the GCL after the incubation period. Next to the schematic diagram, a confocal image of the mouse OB shows

- infected cells expressing EYFP (in green) in the GCL with projections reaching to the MCL and EPL in mouse OB. DAPI staining of the nuclei is represented in blue (20X, Scale bar:  $100 \, \mu m$ ).
- (D) A singular granule cells expressing EYFP can be seen with its nucleus in the GCL and projections reaching MCL and EPL (60X, Scale bar: 100  $\mu$ m).
- (E) Western blot images for expression of NR1 protein in the olfactory bulb of control and knockout animals. Band corresponding to the expression of tubulin protein expression observed in both the groups.
- (F) Normalized intensity corresponding to NR1 expression. Intensity for NR1 is normalized to that of corresponding tubulin expression. NR1 expression is significantly reduced in the knockout group (Mann-Whitney test, p = 0.0286;  $N_{Control} = 4$ ,  $N_{KO} = 4$ )
- (G) NR1KO mice trained for three different ISIs, 2s, 4s and 8s, show slower learning in comparison to sham group for 2s and 4s ISI (Two-way ANOVA with Tukey's multiple comparison, p<0.05).
- (H) When olfactory matching times are compared, NR1KO mice show slower matching time only for 2s ISI while matching times remained comparable for higher ISIs (Unpaired t-test with Welch's correction; p< 0.05, ns>0.05)

#### 5.4. Discussion

Early research in WM has served as a steppingstone for understanding the nature and neural correlates of OWM as they indicated a capacity-limited nature of olfactory working memory (OWM).<sup>79</sup> Neural correlates of OWM is still largely unknown, but recent studies suggest important roles of the prefrontal cortex<sup>370</sup>, insular cortex<sup>387</sup>, hippocampus<sup>388</sup> and piriform cortex.<sup>270</sup> Odor memory tasks and brain imaging studies have also highlighted the role of orbitofrontal cortex and delay-period activity in the piriform cortex. One of the key aspects of OWM that remains unclear is the temporal limit. Despite being a capacity limited system, whether OWM store has strict temporal boundary conditions is still debated. Several recent studies have probed the problem while coming up with often contradictory results. Using delayed matching paradigms, one recent study found matching performance of head-restrained mice to decline once the stimulus delay is

extended beyond 12s to 20s<sup>389</sup> while another group found that matching accuracy declines rather gradually with increasing delay up to 40s.<sup>158</sup> Our data remains in alignment with the later study, though, in contrast, we employed freely moving mice and the increase in delay was gradual than abrupt (Figure 5.1E). This possibly allowed mice to adapt to changing parameters, in turn, enabling to perform well in high delay period tasks. But this has an obvious caveat of long experimental times and the risk of overtraining of nearly seven months. Though we find peak accuracy to be inversely proportional to delay period, shorter experimental timelines may be necessary for any definitive conclusion about the temporal limit of OWM.

Behavioural refinement is a characteristic feature of learning in animals performing goal-directed tasks. <sup>390</sup> Other than improvement in accuracy for an assigned behavioural task, lick and sample pattern serve as behavioural correlates that can be used to quantify learning. Here we show that lick and sample patterns do get refined over training with drastically reduced licking during the delay periods (Figure 5.2A and 5.2B). This becomes more evident with higher ISIs with animals choosing to minimize licking during the delay period (Figure 5.2C). As we calculated the odor matching time, we find that irrespective of the delay, mean matching time ranged from 400-600 ms. Though this is significantly higher than the discrimination time for odor-based go/no-go tasks<sup>391</sup>, likely due to the greater complexity of the paradigm, the matching time did not show any correlation with the stimulus delay. It is worth mentioning here, though a comparable correlate for decision-making time, discrimination time and odor matching time are two separate variables.

As previously discussed, the role of the pre-cortical circuit, especially the OB, is barely understood in the context of OWM. Bidirectional modulation of the excitation-inhibition balance in the OB allowed us to show that altering OB circuitry can greatly influence OWM performance. The firing of the projection neurons, Mitral and Tufted cells, are modulated primarily by GABAergic granule cells. Stimulated mitral cell lateral dendrites form glutamatergic connections with GCs and GCs in return release inhibitory neurotransmitter, GABA onto the source or nearby M/T cells in the OB. Increased inhibition by GCs may result in more refined temporal patterning at the level of OB and also help in reducing noise. <sup>110</sup> This refinement of stimulus may translate to an improved pattern-separation at

level of the olfactory cortex, especially the piriform cortex. 392 For a multicomponent odor mixture, M/T cells has been shown to be more sensitive to removal of one or more components in contrast to pyramidal cells in anterior piriform cortex (aPCX). 393 When an odor is first encountered, the piriform cortex forms a sparse, distributed representation that can later be reactivated even on partial presentation of the original stimuli.<sup>394</sup> Improved pattern completion at the level of piriform cortex can improve OWM performance by reconstructing whole odor identities from incomplete input or maintained activity, stabilizing odor representations against sniffing variability or environmental changes.<sup>393</sup> This ability of pattern completion at the level of olfactory cortex, thus, can compensate for a decreased mean signal intensity from the projection neurons in the OB. 395 Moreover, a better signal to noise ratio as a result of increased inhibition in OB, may in turn, enhance pattern separation. 110 This series of events may eventually help the animal identify and sustain representations of individual odors better. GluA2KO mice showing faster learning performance in our experimental paradigm (Figure 5.3E) implies strongly towards an improved signal to noise ratio at the level of OB which in turn translates to superior pattern completion at the level of olfactory cortex, and thus, a better overall performance.

One of the logical extrapolations that these set of arguments may lead to is whether increased inhibition at the level of OB may, in turn, be advantageous and thus, be selected for by evolution. Animals live in constantly changing environmental conditions with varying degrees of stimulus intensity being present in the surrounding. Increased inhibition at the level of OB, though may provide selective advantage for a specialized task, may not prove to be a beneficial for the overall survival of the animal or the population, in general. <sup>396,397</sup> As increase in inhibition on the projection neurons leads to a reduced mean signal intensity, this may prove to be detrimental if odor concentration in the surrounding is low to begin with. Optimum E/I balance thus play a crucial role to enable animals to adapt to a wide range of stimulus irrespective of the sensory modality. <sup>398</sup>

#### References

- 1. Shapiro, M. L. Time is just a memory. *Nat Neurosci* **22**, 151–153 (2019).
- 2. Trübutschek, D. *et al.* A theory of working memory without consciousness or sustained activity. *Elife* **6**, (2017).
- 3. Zlotnik, G. & Vansintjan, A. Memory: An Extended Definition. *Front Psychol* **10**, (2019).
- 4. Murray, E. A., Wise, S. P., Baldwin, M. K. L. & Graham, K. S. *The Evolutionary Road to Human Memory*. (Oxford University Press, 2020).
- 5. Bajaffer, A., Mineta, K. & Gojobori, T. Evolution of memory system-related genes. *FEBS Open Bio* **11**, 3201–3210 (2021).
- 6. James, W. *The Principles of Psychology*. (New York: Henry Holt, 1890).
- 7. Cowan, N. Evolving conceptions of memory storage, selective attention, and their mutual constraints within the human information-processing system. *Psychol Bull* **104**, 163–191 (1988).
- 8. Norris, D. Short-term memory and long-term memory are still different. *Psychol Bull* **143**, 992–1009 (2017).
- 9. Dougherty, M. R. P. & Hunter, J. Probability judgment and subadditivity: The role of working memory capacity and constraining retrieval. *Mem Cognit* **31**, 968–982 (2003).
- 10. Li, H.-H., Sprague, T. C., Yoo, A. H., Ma, W. J. & Curtis, C. E. Joint representation of working memory and uncertainty in human cortex. *Neuron* **109**, 3699-3712.e6 (2021).
- 11. Baddeley, A. Working memory: Looking back and looking forward. *Nat Rev Neurosci* **4**, 829–839 (2003).
- 12. Pontecorvo, M. J., Sahgal, A. & Steckler, T. Further developments in the measurement of working memory in rodents. *Cognitive Brain Research* **3**, 205–213 (1996).
- 13. Dudchenko, P. A. An overview of the tasks used to test working memory in rodents. *Neurosci Biobehav Rev* **28**, 699–709 (2004).
- 14. Weinstein, B. Matching-from-sample by rhesus monkeys and by children. *J Comp Psychol* **31**, 195–213 (1941).
- 15. Zentall, T. R. & Smith, A. P. Delayed matching-to-sample: A tool to assess memory and other cognitive processes in pigeons. *Behavioural Processes* **123**, 26–42 (2016).
- 16. Jaeggi, S. M., Buschkuehl, M., Perrig, W. J. & Meier, B. The concurrent validity of the N-back task as a working memory measure. *Memory* **18**, 394–412 (2010).
- 17. Monk, A. F., Jackson, D., Nielsen, D., Jefferies, E. & Olivier, P. N-backer: An auditory n-back task with automatic scoring of spoken responses. *Behav Res Methods* **43**, 888–896 (2011).
- 18. Yaple, Z. & Arsalidou, M. N-back Working Memory Task: Meta-analysis of Normative fMRI Studies With Children. *Child Dev* **89**, 2010–2022 (2018).
- 19. Penley, S. C., Gaudet, C. M. & Threlkeld, S. W. Use of an Eight-arm Radial Water Maze to Assess Working and Reference Memory Following Neonatal Brain Injury. *Journal of Visualized Experiments* (2013) doi:10.3791/50940.
- 20. Kim, H., Park, J. Y. & Kim, K. K. Spatial Learning and Memory Using a Radial Arm Maze with a Head-Mounted Display. *Psychiatry Investig* **15**, 935–944 (2018).
- 21. Cleal, M. et al. The Free-movement pattern Y-maze: A cross-species measure of working memory and executive function. Behav Res Methods **53**, 536–557 (2021).
- 22. Sternberg, S. High-Speed Scanning in Human Memory. *Science (1979)* **153**, 652–654 (1966).

- 23. Vinkhuyzen, A. A. E., van der Sluis, S., Boomsma, D. I., de Geus, E. J. C. & Posthuma, D. Individual Differences in Processing Speed and Working Memory Speed as Assessed with the Sternberg Memory Scanning Task. *Behav Genet* **40**, 315–326 (2010).
- 24. Young, J. W. *et al.* The odour span task: A novel paradigm for assessing working memory in mice. *Neuropharmacology* **52**, 634–645 (2007).
- Anderson Catrona and Colombo, M. Matching-to-Sample: Comparative Overview. in Encyclopedia of Animal Cognition and Behavior (ed. Vonk Jennifer and Shackelford, T. K.) 4097–4102 (Springer International Publishing, Cham, 2022). doi:10.1007/978-3-319-55065-7\_1708.
- 26. Baddeley, A. D. The Psychology of Memory. in *The Handbook of Memory Disorders* 3–16 (John Wiley & Sons, Ltd., 2002).
- 27. Baddeley, A. D. & Hitch, G. Working Memory. in *Psychology of Learning and Motivation* (ed. Bower, G. H.) vol. 8 47–89 (Academic Press, 1974).
- 28. Milner, B. Amnesia following operation on the temporal lobes. in *Amnesia* (eds. Whitty, C. W. M. & Zangwill, O. L.) (London: Butterworth, 1966).
- 29. Shallice, T. & Warrington, E. K. Independent Functioning of Verbal Memory Stores: A Neuropsychological Study. *Quarterly Journal of Experimental Psychology* **22**, 261–273 (1970).
- 30. Allen, R. J. Classic and recent advances in understanding amnesia. *F1000Res* **7**, 331 (2018).
- 31. Atkinson, R. C. & Shiffrin, R. M. Human Memory: A Proposed System and its Control Processes. *Psychology of Learning and Motivation* **2**, 89–195 (1968).
- 32. Craik, F. I. M. & Lockhart, R. S. Levels of processing: A framework for memory research. *J Verbal Learning Verbal Behav* **11**, 671–684 (1972).
- 33. Miller, G. A., Galanter, E. & Pribram, K. *Plans and the Structure of Behaviour*. (Holt, Rinehart and Winston, Inc., 1960).
- 34. Logie, R. H. *Visuo-Spatial Working Memory*. (Hove, East Sussex ; Hillsdale [N.J.] : L. Erlbaum Associates, 1995).
- 35. Baddeley, A. D. & Hitch, G. Working Memory. in 47–89 (1974). doi:10.1016/S0079-7421(08)60452-1.
- 36. Gathercole, S. E., Pickering, S. J., Ambridge, B. & Wearing, H. The Structure of Working Memory From 4 to 15 Years of Age. *Dev Psychol* **40**, 177–190 (2004).
- 37. Baddeley, A. D., Thomson, N. & Buchanan, M. Word length and the structure of short-term memory. *J Verbal Learning Verbal Behav* **14**, 575–589 (1975).
- 38. Vallar, G. & Baddeley, A. D. Fractionation of working memory: Neuropsychological evidence for a phonological short-term store. *J Verbal Learning Verbal Behav* **23**, 151–161 (1984).
- 39. Savin, H. B. & Perchonock, E. Grammatical structure and the immediate recall of english sentences. *J Verbal Learning Verbal Behav* **4**, 348–353 (1965).
- 40. Vallar, G. & Baddeley, A. Phonological short-term store and sentence processing. *Cogn Neuropsychol* **4**, 417–438 (1987).
- 41. Baddeley, A., Papagno, C. & Vallar, G. When long-term learning depends on short-term storage. *J Mem Lang* **27**, 586–595 (1988).
- 42. Baddeley, A., Gathercole, S. & Papagno, C. *The Phonological Loop as a Language Learning Device. Psychological Review* vol. 105 (1998).

- 43. Papagno, C. & Vallar, G. Phonological Short-term Memory and the Learning of Novel Words: The Effect of Phonological Similarity and Item Length. *The Quarterly Journal of Experimental Psychology Section A* **44**, 47–67 (1992).
- 44. Baddeley, A. The episodic buffer: a new component of working memory? *Trends Cogn Sci* **4**, 417–423 (2000).
- 45. Gathercole, S. E. Memory Development During the Childhood Years. in *Handbook of Memory Disorders* (eds. Baddeley, A. D., Kopelman, M. D. & Wilson, B.) 475–500 (John Wiley & Sons, Ltd., 2002).
- Barrouillet, P. & Camos, V. The time-based resource-sharing model of working memory. in *The Cognitive Neuroscience of Working Memory* (eds. Osaka, N., Logie, R. H. & D'Esposito, M.) 59–80 (Oxford University Press, 2007). doi:10.1093/acprof:oso/9780198570394.003.0004.
- 47. Vandierendonck, A. A Working Memory System With Distributed Executive Control. *Perspectives on Psychological Science* **11**, 74–100 (2016).
- 48. Postle, B. R. Working memory as an emergent property of the mind and brain. *Neuroscience* **139**, 23–38 (2006).
- 49. Luck, S. J. & Vogel, E. K. The capacity of visual working memory for features and conjunctions. *Nature* **390**, 279–281 (1997).
- 50. Cowan, N., Rouder, J. N., Blume, C. L. & Saults, J. S. Models of verbal working memory capacity: What does it take to make them work? *Psychol Rev* **119**, 480–499 (2012).
- 51. Gilson, E. Q. & Baddeley, A. D. Tactile Short-Term Memory. *Quarterly Journal of Experimental Psychology* **21**, 180–184 (1969).
- 52. Sinclair, R. J. & Burton, H. Discrimination of vibrotactile frequencies in a delayed pair comparison task. *Percept Psychophys* **58**, 680–692 (1996).
- 53. Papagno, C., Minniti, G., Mattavelli, G. C., Mantovan, L. & Cecchetto, C. Tactile short-term memory in sensory-deprived individuals. *Exp Brain Res* **235**, 471–480 (2017).
- 54. Koehler, H., Croy, I. & Oleszkiewicz, A. Late Blindness and Deafness are Associated with Decreased Tactile Sensitivity, But Early Blindness is Not. *Neuroscience* **526**, 164–174 (2023).
- 55. Salimi, M. *et al.* The olfactory bulb modulates entorhinal cortex oscillations during spatial working memory. *The Journal of Physiological Sciences* **71**, 21 (2021).
- 56. Salimi, M., Tabasi, F., Nazari, M., Ghazvineh, S. & Raoufy, M. R. The olfactory bulb coordinates the ventral hippocampus—medial prefrontal cortex circuit during spatial working memory performance. *The Journal of Physiological Sciences* **72**, 9 (2022).
- 57. Jacobs, L. F. From chemotaxis to the cognitive map: The function of olfaction. *Proceedings of the National Academy of Sciences* **109**, 10693–10700 (2012).
- 58. Sprengel, R. & Eltokhi, A. Ionotropic Glutamate Receptors (and Their Role in Health and Disease). in *Neuroscience in the 21st Century: From Basic to Clinical* (eds. Pfaff, D. W., Volkow, N. D. & Rubenstein, J. L.) 57–86 (Springer International Publishing, Cham, 2022). doi:10.1007/978-3-030-88832-9 4.
- 59. Kessels, H. W. & Malinow, R. Synaptic AMPA Receptor Plasticity and Behavior. *Neuron* **61**, 340–350 (2009).
- 60. Luscher, C. & Malenka, R. C. NMDA Receptor-Dependent Long-Term Potentiation and Long-Term Depression (LTP/LTD). *Cold Spring Harb Perspect Biol* **4**, a005710–a005710 (2012).
- 61. Traynelis, S. F. *et al.* Glutamate Receptor Ion Channels: Structure, Regulation, and Function. *Pharmacol Rev* **62**, 405–496 (2010).

- 62. Xie, X., Liaw, J.-S., Baudry, M. & Berger, T. W. Novel expression mechanism for synaptic potentiation: Alignment of presynaptic release site and postsynaptic receptor. *Proceedings of the National Academy of Sciences* **94**, 6983–6988 (1997).
- 63. Penn, A. C. *et al.* Hippocampal LTP and contextual learning require surface diffusion of AMPA receptors. *Nature* **549**, 384–388 (2017).
- 64. Schmitt, W. B., Deacon, R. M. J., Seeburg, P. H., Rawlins, J. N. P. & Bannerman, D. M. A Within-Subjects, Within-Task Demonstration of Intact Spatial Reference Memory and Impaired Spatial Working Memory in Glutamate Receptor-A-Deficient Mice. *The Journal of Neuroscience* **23**, 3953–3959 (2003).
- 65. Bannerman, D. M. Fractionating spatial memory with glutamate receptor subunit-knockout mice. *Biochem Soc Trans* **37**, 1323–1327 (2009).
- 66. Romberg, C. *et al.* Induction and expression of GluA1 (GluR-A)-independent LTP in the hippocampus. *European Journal of Neuroscience* **29**, 1141–1152 (2009).
- 67. Bannerman, D. M. *et al.* NMDA Receptor Subunit NR2A Is Required for Rapidly Acquired Spatial Working Memory But Not Incremental Spatial Reference Memory. *The Journal of Neuroscience* **28**, 3623–3630 (2008).
- 68. Niewoehner, B. *et al.* Impaired spatial working memory but spared spatial reference memory following functional loss of NMDA receptors in the dentate gyrus. *European Journal of Neuroscience* **25**, 837–846 (2007).
- 69. Wang, X.-J. Synaptic Basis of Cortical Persistent Activity: the Importance of NMDA Receptors to Working Memory. *The Journal of Neuroscience* **19**, 9587–9603 (1999).
- 70. Galizio, M. *et al.* Effects of NMDA antagonist dizocilpine (MK-801) are modulated by the number of distractor stimuli in the rodent odor span task of working memory. *Neurobiol Learn Mem* **161**, 51–56 (2019).
- 71. Adler, CalebM., Goldberg, TerryE., Malhotra, AnilK., Pickar, D. & Breier, A. Effects of Ketamine on Thought Disorder, Working Memory, and Semantic Memory in Healthy Volunteers. *Biol Psychiatry* **43**, 811–816 (1998).
- 72. Driesen, N. R. *et al.* The Impact of NMDA Receptor Blockade on Human Working Memory-Related Prefrontal Function and Connectivity. *Neuropsychopharmacology* **38**, 2613–2622 (2013).
- 73. Sawaguchi, T., Matsumura, M. & Kubota, K. Delayed response deficit in monkeys by locally disturbed prefrontal neuronal activity by bicuculline. *Behavioural Brain Research* **31**, 193–198 (1988).
- 74. Rao, S. G., Williams, G. V. & Goldman-Rakic, P. S. Destruction and Creation of Spatial Tuning by Disinhibition: GABA (A) Blockade of Prefrontal Cortical Neurons Engaged by Working Memory. *The Journal of Neuroscience* **20**, 485–494 (2000).
- 75. Galloway, E. M., Woo, N. H. & Lu, B. Persistent neural activity in the prefrontal cortex: A mechanism by which BDNF regulates working memory? in *Progress in Brain Research* (eds. Sossin, W. S., Lacaille, J. C., Castellucci, V. F. & Belleville, S.) vol. 169 251–266 (2008).
- 76. Heywood, A. & Vortriede, H. A. Some Experiments on the Associative Power of Smells. *American Journal of Psychology* **16**, 537 (1905).
- 77. Milner, B. Amnesia following operation on the temporal lobes. in *Amnesia* (1996). doi:10.1093/neucas/2.4.259-u.
- 78. Mair, R., Capra, C., McEntee, W. J. & Engen, T. Odor discrimination and memory in Korsakoff's psychosis. *J Exp Psychol Hum Percept Perform* **6**, 445–458 (1980).

- 79. Engen, T., Kuisma, J. E. & Eimas, P. D. Short-term memory of odors. *J Exp Psychol* **99**, 222–225 (1973).
- 80. Jones, F. N., Roberts, K. & Holman, E. W. Similarity judgments and recognition memory for some common spices. *Percept Psychophys* **24**, 2–6 (1978).
- 81. Eskenazi, B., Cain, W. S., Novelly, R. A. & Friend, K. B. Olfactory functioning in temporal lobectomy patients. *Neuropsychologia* **21**, 365–374 (1983).
- 82. Wilhelm, O., Hildebrandt, A. & Oberauer, K. What is working memory capacity, and how can we measure it? *Front Psychol* **4**, (2013).
- 83. Young, J. W. *et al.* The odour span task: A novel paradigm for assessing working memory in mice. *Neuropharmacology* **52**, 634–645 (2007).
- 84. Lawless, H. T. & Cain, W. S. Recognition memory for odors. *Chem Senses* **1**, 331–337 (1975).
- 85. Annett, J. M. & Lorimer, A. W. Primacy and Recency in Recognition of Odours and Recall of Odour Names. *Percept Mot Skills* **81**, 787–794 (1995).
- 86. White, T. L. & Treisman, M. A comparison of the encoding of content and order in olfactory memory and in memory for visually presented verbal materials. *British Journal of Psychology* **88**, 459–472 (1997).
- 87. Li, Z. *et al.* Neural correlates of olfactory working memory in the human brain. *Neuroimage* **306**, 121005 (2025).
- 88. Jönsson, F. U., Møller, P. & Olsson, M. J. Olfactory working memory: effects of verbalization on the 2-back task. *Mem Cognit* **39**, 1023–1032 (2011).
- 89. Savic, I. & Berglund, H. Right-nostril Dominance in Discrimination of Unfamiliar, but Not Familiar, Odours. *Chem Senses* **25**, 517–523 (2000).
- 90. Zelano, C., Montag, J., Khan, R. & Sobel, N. A Specialized Odor Memory Buffer in Primary Olfactory Cortex. *PLoS One* **4**, e4965 (2009).
- 91. Mori, K. & Sakano, H. Olfactory Circuitry and Behavioral Decisions. *Annu Rev Physiol* **83**, 231–256 (2021).
- 92. Jacobs, L. F. From chemotaxis to the cognitive map: The function of olfaction. *Proceedings of the National Academy of Sciences* **109**, 10693–10700 (2012).
- 93. McGann, J. P. Poor human olfaction is a 19th-century myth. *Science (1979)* **356**, eaam7263 (2017).
- 94. Bushdid, C., Magnasco, M. O., Vosshall, L. B. & Keller, A. Humans can discriminate more than 1 trillion olfactory stimuli. *Science* (1979) **343**, 1370–1372 (2014).
- 95. Thomas-Danguin, T. *et al.* The perception of odor objects in everyday life: a review on the processing of odor mixtures. *Front Psychol* **5**, (2014).
- 96. Bhattacharjee, A. S., Joshi, S. V., Naik, S., Sangle, S. & Abraham, N. M. Quantitative assessment of olfactory dysfunction accurately detects asymptomatic COVID-19 carriers. *EClinicalMedicine* **28**, (2020).
- 97. Bhowmik, R. *et al.* Persistent olfactory learning deficits during and post-COVID-19 infection. *Current Research in Neurobiology* **4**, 100081 (2023).
- 98. Pandey, S., Bapat, V., Abraham, J. N. & Abraham, N. M. Long COVID: From olfactory dysfunctions to viral Parkinsonism. *World J Otorhinolaryngol Head Neck Surg* **10**, 137–147 (2024).
- 99. Ache, B. W. & Young, J. M. Olfaction: Diverse Species, Conserved Principles. *Neuron* **48**, 417–430 (2005).
- 100. Nagayama, S., Homma, R. & Imamura, F. Neuronal organization of olfactory bulb circuits. *Front Neural Circuits* **8**, (2014).

- 101. Tan, L., Li, Q. & Xie, X. S. Olfactory sensory neurons transiently express multiple olfactory receptors during development. *Mol Syst Biol* **11**, 844 (2015).
- 102. Serizawa, S., Miyamichi, K. & Sakano, H. One neuron—one receptor rule in the mouse olfactory system. *Trends in Genetics* **20**, 648—653 (2004).
- 103. Maresh, A., Rodriguez Gil, D., Whitman, M. C. & Greer, C. A. Principles of glomerular organization in the human olfactory bulb Implications for odor processing. *PLoS One* **3**, (2008).
- 104. Shepherd, G. M., Chen, W. R., Willhite, D., Migliore, M. & Greer, C. A. The olfactory granule cell: From classical enigma to central role in olfactory processing. *Brain Res Rev* 55, 373–382 (2007).
- 105. Imai, T. Construction of functional neuronal circuitry in the olfactory bulb. *Semin Cell Dev Biol* **35**, 180–188 (2014).
- 106. Price, J. L. & Powell, T. P. S. The morphology of the granule cells of the olfactory bulb. *J Cell Sci* **7**, 91–122 (1970).
- 107. Shepherd, G. M., Chen, W. R., Willhite, D., Migliore, M. & Greer, C. A. The olfactory granule cell: From classical enigma to central role in olfactory processing. *Brain Res Rev* **55**, 373–382 (2007).
- 108. Takahashi, H., Yoshihara, S. & Tsuboi, A. The Functional Role of Olfactory Bulb Granule Cell Subtypes Derived From Embryonic and Postnatal Neurogenesis. *Front Mol Neurosci* **11**, (2018).
- 109. Abraham, N. M. *et al.* Synaptic Inhibition in the Olfactory Bulb Accelerates Odor Discrimination in Mice. *Neuron* **65**, 399–411 (2010).
- 110. Gschwend, O. *et al.* Neuronal pattern separation in the olfactory bulb improves odor discrimination learning. *Nat Neurosci* **18**, 1474–1482 (2015).
- 111. Pardasani, M. *et al.* Perceptual learning deficits mediated by somatostatin releasing inhibitory interneurons of olfactory bulb in an early life stress mouse model. *Mol Psychiatry* **28**, 4693–4706 (2023).
- 112. Neville, K. R. & Haberly, L. B. Olfactory Cortex. in *The Synaptic Organization of the Brain* (ed. Shepherd, G.) 415–454 (Oxford University Press, 2004). doi:10.1093/acprof:oso/9780195159561.003.0010.
- 113. Martínez-García, F., Novejarque, A., Gutiérrez-Castellanos, N. & Lanuza, E. Piriform Cortex and Amygdala. in *The Mouse Nervous System* 140–172 (Elsevier, 2012). doi:10.1016/B978-0-12-369497-3.10006-8.
- 114. Illig, K. R. & Wilson, D. A. Olfactory Cortex: Comparative Anatomy. in *Encyclopedia of Neuroscience* 101–106 (Elsevier, 2009). doi:10.1016/B978-008045046-9.00971-2.
- 115. Meissner-Bernard, C., Dembitskaya, Y., Venance, L. & Fleischmann, A. Encoding of Odor Fear Memories in the Mouse Olfactory Cortex. *Current Biology* **29**, 367-380.e4 (2019).
- 116. Aqrabawi, A. J. & Kim, J. C. Olfactory memory representations are stored in the anterior olfactory nucleus. *Nat Commun* **11**, (2020).
- 117. Aqrabawi, A. J. & Kim, J. C. Olfactory memory representations are stored in the anterior olfactory nucleus. *Nat Commun* **11**, 1246 (2020).
- 118. Blazing, R. M. & Franks, K. M. Odor coding in piriform cortex: mechanistic insights into distributed coding. *Curr Opin Neurobiol* **64**, 96–102 (2020).
- 119. Wilson, D. A. *et al.* Cortical Odor Processing in Health and Disease. in 275–305 (2014). doi:10.1016/B978-0-444-63350-7.00011-5.
- 120. Meister, M. On the dimensionality of odor space. *Elife* **4**, (2015).

- 121. Weinstock, J. Contemporary Perspectives on Linnaeus. University Press Of America (1985).
- 122. Zwaardemaker, B. H. *MEASUREMENT OF THE SENSE OF SMELL IN CLINICAL EXAMINATION. LECTURER ON CLINICAL MEDICINE IN THE MILITARY HOSPITAL. Lancet* (1889).
- 123. Philpott, C. M., Bennett, A. & Murty, G. E. A brief history of olfaction and olfactometry. *Journal of Laryngology and Otology* vol. 122 657–662 Preprint at https://doi.org/10.1017/S0022215107001314 (2008).
- 124. Henning, H. Der Geruch. (Verlag von Johann Ambrosius Barth, Leipzig, 1916).
- 125. E.C. Crocker, L. F. H. Analysis and Classification of Odors. *Am. Perfum. Essent. Oil Rev.* (1927).
- 126. Press release: The 2004 Nobel Prize in Physiology or Medicine to Richard Axel and Linda B. Buck NobelPrize.org. https://www.nobelprize.org/prizes/medicine/2004/press-release/.
- 127. Gilbert, A. What the Nose Knows: The Science of Scent in Everyday Life. (CreateSpace Independent Publishing Platform, 2015).
- 128. Wysocki, C. J. & Gilbert, A. N. National Geographic Smell Survey: Effects of Age Are Heterogenous. *Ann N Y Acad Sci* **561**, 12–28 (1989).
- 129. Doty, R. L. et al. Development of the University of Pennsylvania Smell Identification Test: A Standardized Microencapsulated Test of Olfactory Function. Physiology & Behavior vol. 32 (1984).
- 130. Hummel, T., Sekinger, B., Wolf, S. R., Pauli, E. & Kobal, G. 'Sniffin' Sticks': Olfactory Performance Assessed by the Combined Testing of Odor Identification, Odor Discrimination and Olfactory Threshold. Chem Senses vol. 22 https://academic.oup.com/chemse/article-abstract/22/1/39/383479 (1997).
- 131. Croy, I., Buschhüter, D., Seo, H. S., Negoias, S. & Hummel, T. Individual significance of olfaction: Development of a questionnaire. *European Archives of Oto-Rhino-Laryngology* **267**, 67–71 (2010).
- 132. Croy, I., Buschhüter, D., Seo, H.-S., Negoias, S. & Hummel, T. Individual significance of olfaction: development of a questionnaire. *European Archives of Oto-Rhino-Laryngology* **267**, 67–71 (2010).
- 133. Snitz, K. *et al.* SmellSpace: An Odor-Based Social Network as a Platform for Collecting Olfactory Perceptual Data. *Chem Senses* **44**, 267–278 (2019).
- 134. Anderson, C. & Colombo, M. Matching-to-Sample: Comparative Overview. in Encyclopedia of Animal Cognition and Behavior (eds. Vonk, J. & Shackelford, T.) 1–7 (Springer International Publishing, Cham, 2019). doi:10.1007/978-3-319-47829-6 1708-1.
- 135. Konorski, J. A New Method of Physiological Investigation of Recent Memory in Animals. in (Serie des sciences biologiques, 1959).
- 136. Kangas, B. D., Berry, M. S. & Branch, M. N. On the Development and Mechanics of Delayed Matching-to-Sample Performance. *J Exp Anal Behav* **95**, 221–236 (2011).
- 137. Blough, D. S. Delayed matching in the pigeon. J Exp Anal Behav 2, 151–160 (1959).
- 138. Elrod, K., Buccafusco, J. J. & Jackson, W. J. Nicotine enhances delayed matching-to-sample performance by primates. *Life Sci* **43**, 277–287 (1988).
- 139. Critchfield, ThomasS. & Perone, M. Verbal Self-reports of Delayed Matching to Sample by Humans. *J Exp Anal Behav* **53**, 321–344 (1990).

- 140. Jacobson, C. F. Recent Experiments on the Functions of the Frontal Lobes. *Psychol. Bull., Vol. XXV* **25**, 1–11 (1928).
- 141. Finan, J. L. Effects Of Frontal Lobe Lesions On Temporally Organized Behavior In Monkeys. *J Neurophysiol* **2**, 208–226 (1939).
- 142. Finan, J. L. Delayed Response with Pre-Delay Reenforcement in Monkeys after the Removal of the Frontal Lobes. *Am J Psychol* **55**, 202 (1942).
- 143. Miles, J. E. & Rosvold, H. E. The effect of prefrontal lobotomy in rhesus monkeys on delayed-response performance motivated by painshock. *J Comp Physiol Psychol* **49**, 286–292 (1956).
- 144. Fuster, J. M. & Alexander, G. E. Neuron Activity Related to Short-Term Memory. *Science* (1979) **173**, 652–654 (1971).
- 145. Fuster, J. M. Unit activity in prefrontal cortex during delayed-response performance: neuronal correlates of transient memory. *J Neurophysiol* **36**, 61–78 (1973).
- 146. McCarthy, G. *et al.* Functional magnetic resonance imaging of human prefrontal cortex activation during a spatial working memory task. *Proceedings of the National Academy of Sciences* **91**, 8690–8694 (1994).
- McCarthy, G. et al. Activation of Human Prefrontal Cortex during Spatial and Nonspatial Working Memory Tasks Measured by Functional MRI. Cerebral Cortex 6, 600–611 (1996).
- 148. Goldman-Rakic, P. S. Architecture of the Prefrontal Cortex and the Central Executive. *Ann N Y Acad Sci* **769**, 71–84 (1995).
- 149. Ó Scalaidhe, S. P., Wilson, F. A. W. & Goldman-Rakic, P. S. Areal Segregation of Face-Processing Neurons in Prefrontal Cortex. *Science* (1979) **278**, 1135–1138 (1997).
- 150. Levy, R. & Goldman-Rakic, P. S. Association of Storage and Processing Functions in the Dorsolateral Prefrontal Cortex of the Nonhuman Primate. *The Journal of Neuroscience* 19, 5149–5158 (1999).
- 151. Rainer, G., Asaad, W. F. & Miller, E. K. Memory fields of neurons in the primate prefrontal cortex. *Proceedings of the National Academy of Sciences* **95**, 15008–15013 (1998).
- 152. Rigotti, M. *et al.* The importance of mixed selectivity in complex cognitive tasks. *Nature* **497**, 585–590 (2013).
- 153. Riggall, A. C. & Postle, B. R. The Relationship between Working Memory Storage and Elevated Activity as Measured with Functional Magnetic Resonance Imaging. *The Journal of Neuroscience* **32**, 12990–12998 (2012).
- 154. Harrison, S. A. & Tong, F. Decoding reveals the contents of visual working memory in early visual areas. *Nature* **458**, 632–635 (2009).
- 155. Emrich, S. M., Riggall, A. C., LaRocque, J. J. & Postle, B. R. Distributed Patterns of Activity in Sensory Cortex Reflect the Precision of Multiple Items Maintained in Visual Short-Term Memory. *The Journal of Neuroscience* **33**, 6516–6523 (2013).
- 156. Yu, L. *et al.* The causal role of auditory cortex in auditory working memory. *Elife* **10**, (2021).
- 157. Zhang, X. *et al.* Active information maintenance in working memory by a sensory cortex. *Elife* **8**, (2019).
- 158. Walker, A. E. The medial thalamic nucleus. A comparative anatomical, physiological and clinical study of the nucleus medialis dorsalis thalami. *Journal of Comparative Neurology* **73**, 87–115 (1940).

- 159. Bolkan, S. S. *et al.* Thalamic projections sustain prefrontal activity during working memory maintenance. *Nat Neurosci* **20**, 987–996 (2017).
- 160. Olds, M. E. Effects of electrical stimulation and electrocoagulation in cortex and thalamus on delayed response in monkeys. *Exp Neurol* **15**, 37–53 (1966).
- 161. Stamm, J. S. Electrical stimulation of monkeys' prefrontal cortex during delayed-response performance. *J Comp Physiol Psychol* **67**, 535–546 (1969).
- 162. Bailey, K. R. & Mair, R. G. Lesions of Specific and Nonspecific Thalamic Nuclei Affect Prefrontal Cortex-Dependent Aspects of Spatial Working Memory. *Behavioral Neuroscience* **119**, 410–419 (2005).
- 163. Alexander, G. E. & Fuster, J. M. Effects of cooling prefrontal cortex on cell firing in the nucleus medialis dorsalis. *Brain Res* **61**, 93–105 (1973).
- 164. Mars, R. B. & Grol, M. J. Dorsolateral Prefrontal Cortex, Working Memory, and Prospective Coding for Action. *The Journal of Neuroscience* **27**, 1801–1802 (2007).
- 165. Song, D. *et al.* Functional connectivity between Layer 2/3 and Layer 5 neurons in prefrontal cortex of nonhuman primates during a delayed match-to-sample task. in *2012 Annual International Conference of the IEEE Engineering in Medicine and Biology Society* 2555–2558 (IEEE, 2012). doi:10.1109/EMBC.2012.6346485.
- 166. Wang, M. *et al.* NMDA Receptors Subserve Persistent Neuronal Firing during Working Memory in Dorsolateral Prefrontal Cortex. *Neuron* **77**, 736–749 (2013).
- 167. Nigel, R., Zafiris, D. & Paul, F. The relationship between dorsolateral prefrontal cortical inhibition and working memory performance: a combined TMS-EEG study. *Front Hum Neurosci* **9**, (2015).
- 168. Finn, E. S., Huber, L., Jangraw, D. C., Molfese, P. J. & Bandettini, P. A. Layer-dependent activity in human prefrontal cortex during working memory. *Nat Neurosci* **22**, 1687–1695 (2019).
- 169. Gläscher, J. *et al.* Lesion Mapping of Cognitive Abilities Linked to Intelligence. *Neuron* **61**, 681–691 (2009).
- 170. Barbey, A. K. *et al.* An integrative architecture for general intelligence and executive function revealed by lesion mapping. *Brain* **135**, 1154–1164 (2012).
- 171. Barbey, A. K., Koenigs, M. & Grafman, J. Dorsolateral prefrontal contributions to human working memory. *Cortex* **49**, 1195–1205 (2013).
- 172. Barbey, A. K., Koenigs, M. & Grafman, J. Orbitofrontal Contributions to Human Working Memory. *Cerebral Cortex* **21**, 789–795 (2011).
- 173. Bhattacharjee, A. S. *et al.* The claustrum is critical for maintaining working memory information. *bioRxiv* (2024) doi:10.1101/2024.10.28.620649.
- 174. Crick, F. C. & Koch, C. What is the function of the claustrum? *Philosophical Transactions of the Royal Society B: Biological Sciences* **360**, 1271–1279 (2005).
- 175. Liu, J. *et al.* The Claustrum-Prefrontal Cortex Pathway Regulates Impulsive-Like Behavior. *The Journal of Neuroscience* **39**, 10071–10080 (2019).
- 176. Do, A. D., Portet, C., Goutagny, R. & Jackson, J. The claustrum and synchronized brain states. *Trends Neurosci* **47**, 1028–1040 (2024).
- 177. Funahashi, S., Bruce, C. J. & Goldman-Rakic, P. S. Visuospatial coding in primate prefrontal neurons revealed by oculomotor paradigms. *J Neurophysiol* **63**, 814–831 (1990).
- 178. Lundqvist, M., Herman, P. & Miller, E. K. Working memory: Delay activity, yes! persistent activity? maybe not. *Journal of Neuroscience* **38**, 7013–7019 (2018).

- 179. Masse, N. Y., Yang, G. R., Song, H. F., Wang, X.-J. & Freedman, D. J. Circuit mechanisms for the maintenance and manipulation of information in working memory. *Nat Neurosci* **22**, 1159–1167 (2019).
- 180. Masse, N. Y., Rosen, M. C. & Freedman, D. J. Reevaluating the Role of Persistent Neural Activity in Short-Term Memory. *Trends Cogn Sci* **24**, 242–258 (2020).
- 181. Wickens, C. D. The Structure of Attentional Resources. in (1980).
- 182. McElree, B. & Dosher, B. A. Serial retrieval processes in the recovery of order information. *J Exp Psychol Gen* **122**, 291–315 (1993).
- 183. Oberauer, K. Towards a Theory of Working Memory. in *Working Memory* 116–149 (Oxford University Press, 2021). doi:10.1093/oso/9780198842286.003.0005.
- 184. Oberauer, K. Working Memory and Attention A Conceptual Analysis and Review. *J Cogn* **2**, (2019).
- 185. Griffin, I. C. & Nobre, A. C. Orienting Attention to Locations in Internal Representations. *J Cogn Neurosci* **15**, 1176–1194 (2003).
- 186. Kofler, M. J. *et al.* Working memory and short-term memory deficits in ADHD: A bifactor modeling approach. *Neuropsychology* **34**, 686–698 (2020).
- 187. Sala, S. & Logie, R. Neuropsychological impairments of visual and spatial working memory. *Handbook of Memory Disorders* **2**, 271–292 (2002).
- 188. Pasternak, T. & Greenlee, M. W. Working memory in primate sensory systems. *Nature Reviews Neuroscience* vol. 6 97–107 Preprint at https://doi.org/10.1038/nrn1603 (2005).
- 189. Magnussen, S., Greenlee, M. W., Asplund, R. & Dyrnes, S. Stimulus-specific mechanisms of visual short-term memory. *Vision Res* **31**, 1213–1219 (1991).
- 190. Sneve, M. H., Sreenivasan, K. K., Alnæs, D., Endestad, T. & Magnussen, S. Short-term retention of visual information: Evidence in support of feature-based attention as an underlying mechanism. *Neuropsychologia* **66**, 1–9 (2015).
- 191. Carruthers, P. Evolution of working memory. *Proc Natl Acad Sci U S A* **110**, 10371–10378 (2013).
- 192. Parthasarathy, A. *et al.* Mixed selectivity morphs population codes in prefrontal cortex. *Nat Neurosci* **20**, 1770–1779 (2017).
- 193. Bouret, S. *et al.* Linking the evolution of two prefrontal brain regions to social and foraging challenges in primates. *Elife* **12**, (2024).
- 194. Smaers, J. B., Gómez-Robles, A., Parks, A. N. & Sherwood, C. C. Exceptional Evolutionary Expansion of Prefrontal Cortex in Great Apes and Humans. *Current Biology* **27**, 714–720 (2017).
- 195. Friedman, N. P. & Robbins, T. W. The role of prefrontal cortex in cognitive control and executive function. *Neuropsychopharmacology* **47**, 72–89 (2022).
- 196. Matsuzawa, T. Use of numbers by a chimpanzee. *Nature* **315**, 57–59 (1985).
- 197. Matsuzawa, T. Symbolic representation of number in chimpanzees. *Curr Opin Neurobiol* **19**, 92–98 (2009).
- 198. Matsuzawa, T. The chimpanzee mind: in search of the evolutionary roots of the human mind. *Anim Cogn* **12**, 1–9 (2009).
- 199. Muramatsu, A. & Matsuzawa, T. Sequence Order in the Range 1 to 19 by Chimpanzees on a Touchscreen Task: Processing Two-Digit Arabic Numerals. *Animals* **13**, 774 (2023).
- 200. Snowden, J. S. Disorders of semantic memory. in *The Handbook of Memory Disorders* 293–314 (2002).

- 201. Vallar, G. & Papagno, C. Neuropsychological impairments of verbal short-term memory. *The Handbook of Memory Disorders* 249–270 (2002).
- 202. Warrington, E. K., Logue, V. & Pratt, R. T. C. The anatomical localisation of selective impairment of auditory verbal short-term memory. *Neuropsychologia* **9**, 377–387 (1971).
- 203. Kirova, A.-M., Bays, R. B. & Lagalwar, S. Working Memory and Executive Function Decline across Normal Aging, Mild Cognitive Impairment, and Alzheimer's Disease. *Biomed Res Int* **2015**, 1–9 (2015).
- 204. Zokaei, N. & Husain, M. Working Memory in Alzheimer's Disease and Parkinson's Disease. in 325–344 (2019). doi:10.1007/7854\_2019\_103.
- 205. Salmi, J. *et al.* Disentangling the Role of Working Memory in Parkinson's Disease. *Front Aging Neurosci* **12**, (2020).
- 206. Gich, J. *et al.* The nature of memory impairment in multiple sclerosis: understanding different patterns over the course of the disease. *Front Psychol* **14**, (2024).
- 207. Grossi, D., Becker, J. T., Smith, C. & Trojano, L. Memory for visuospatial patterns in Alzheimer's disease. *Psychol Med* **23**, 65–70 (1993).
- 208. Baddeley, A., Logie, R., Bressi, S., Sala, S. Della & Spinnler, H. Dementia and Working Memory. *Q J Exp Psychol* **38**, 603–618 (1986).
- 209. Stopford, C. L., Thompson, J. C., Neary, D., Richardson, A. M. T. & Snowden, J. S. Working memory, attention, and executive function in Alzheimer's disease and frontotemporal dementia. *Cortex* **48**, 429–446 (2012).
- 210. Gagnon, L. G. & Belleville, S. Working memory in mild cognitive impairment and Alzheimer's disease: Contribution of forgetting and predictive value of complex span tasks. *Neuropsychology* **25**, 226–236 (2011).
- 211. Cummings, J. L. *et al.* An overview of the pathophysiology of agitation in Alzheimer's dementia with a focus on neurotransmitters and circuits. *CNS Spectr* **29**, 316–325 (2024).
- 212. Mormino, E. C. & Papp, K. V. Amyloid Accumulation and Cognitive Decline in Clinically Normal Older Individuals: Implications for Aging and Early Alzheimer's Disease. *Journal of Alzheimer's Disease* **64**, S633–S646 (2018).
- 213. Hrybouski, S. *et al.* Aging and Alzheimer's disease have dissociable effects on local and regional medial temporal lobe connectivity. *Brain Commun* **5**, (2023).
- 214. Joseph, S. *et al.* Dorsolateral prefrontal cortex excitability abnormalities in Alzheimer's Dementia: Findings from transcranial magnetic stimulation and electroencephalography study. *International Journal of Psychophysiology* **169**, 55–62 (2021).
- 215. Paulo, D. L. *et al.* Corticostriatal beta oscillation changes associated with cognitive function in Parkinson's disease. *Brain* **146**, 3662–3675 (2023).
- 216. Sawamoto, N. *et al.* Cognitive deficits and striato-frontal dopamine release in Parkinson's disease. *Brain* **131**, 1294–1302 (2008).
- 217. Fallon, S. J., Mattiesing, R. M., Muhammed, K., Manohar, S. & Husain, M. Fractionating the Neurocognitive Mechanisms Underlying Working Memory: Independent Effects of Dopamine and Parkinson's Disease. *Cerebral Cortex* **27**, 5727–5738 (2017).
- 218. Dagher, A. & Nagano-Saito, A. Functional and Anatomical Magnetic Resonance Imaging in Parkinson's Disease. *Mol Imaging Biol* **9**, 234–242 (2007).

- 219. Possin, K. L., Filoteo, J. V., Song, D. D. & Salmon, D. P. Spatial and object working memory deficits in Parkinson's disease are due to impairment in different underlying processes. *Neuropsychology* **22**, 585–595 (2008).
- 220. Vicari, S. & Carlesimo, G. A. Children with intellectual disabilities. in *The Handbook of Memory Disorders* 501–518 (2002).
- 221. Lanfranchi, S., Cornoldi, C. & Vianello, R. Verbal and visuospatial working memory deficits in children with Down syndrome. *Am J Ment Retard* **109 6**, 456–66 (2004).
- 222. O'Hearn, K., Courtney, S., Street, W. & Landau, B. Working memory impairment in people with Williams syndrome: Effects of delay, task and stimuli. *Brain Cogn* **69**, 495–503 (2009).
- 223. Driesen, N. R. *et al.* The Impact of NMDA Receptor Blockade on Human Working Memory-Related Prefrontal Function and Connectivity. *Neuropsychopharmacology* **38**, 2613–2622 (2013).
- 224. Lafaille-Magnan, M.-E. *et al.* Odor identification as a biomarker of preclinical AD in older adults at risk. *Neurology* **89**, 327–335 (2017).
- 225. Haehner, A., Hummel, T. & Reichmann, H. Olfactory dysfunction as a diagnostic marker for Parkinson's disease. *Expert Rev Neurother* **9**, 1773–1779 (2009).
- 226. Kondo, K., Kikuta, S., Ueha, R., Suzukawa, K. & Yamasoba, T. Age-Related Olfactory Dysfunction: Epidemiology, Pathophysiology, and Clinical Management. *Front Aging Neurosci* **12**, (2020).
- 227. Bhattacharjee, A. S., Joshi, S. V., Naik, S., Sangle, S. & Abraham, N. M. Quantitative assessment of olfactory dysfunction accurately detects asymptomatic COVID-19 carriers. *EClinicalMedicine* **28**, 100575 (2020).
- 228. Pandey, S., Bapat, V., Abraham, J. N. & Abraham, N. M. Long COVID: From olfactory dysfunctions to viral Parkinsonism. *World J Otorhinolaryngol Head Neck Surg* (2024) doi:10.1002/wjo2.175.
- 229. European Chemicals Agency (ECHA) Chemicals Database (https://echa.europa.eu). (2024).
- 230. Boublik, T., Fried, V. & Hála, E. The vapour pressures of pure substances. *Berichte der Bunsengesellschaft für physikalische Chemie* **89**, 352–352 (1985).
- 231. National Toxicology Program, Institute of Environmental Health Sciences, National Institutes of Health (NTP). Preprint at (1992).
- 232. Abraham, N. M. *et al.* Maintaining accuracy at the expense of speed: Stimulus similarity defines odor discrimination time in mice. *Neuron* **44**, 865–876 (2004).
- 233. Mahajan, S. *et al.* Mouse olfactory system acts as anemo-detector and -discriminator. Preprint at https://doi.org/10.1101/2024.08.28.610087 (2024).
- 234. van Vugt, B., van Kerkoerle, T., Vartak, D. & Roelfsema, P. R. The contribution of AMPA and NMDA receptors to persistent firing in the dorsolateral prefrontal cortex in working memory. *Journal of Neuroscience* **40**, 2458–2470 (2020).
- 235. Sanderson, D. J., Sprengel, R., Seeburg, P. H. & Bannerman, D. M. Deletion of the GluA1 AMPA receptor subunit alters the expression of short-term memory. *Learning and Memory* **18**, 128–131 (2011).
- 236. Cull-Candy, S., Kelly, L. & Farrant, M. Regulation of Ca2+-permeable AMPA receptors: synaptic plasticity and beyond. *Current Opinion in Neurobiology* vol. 16 288–297 Preprint at https://doi.org/10.1016/j.conb.2006.05.012 (2006).
- 237. Cui, Z. *et al.* Inducible and Reversible NR1 Knockout Reveals Crucial Role of the NMDA Receptor in Preserving Remote Memories in the Brain. *Neuron* **41**, 781–793 (2004).

- 238. Davarinejad, H. Quantifications of Western Blots with ImageJ. https://www.yorku.ca/yisheng/Internal/Protocols/ImageJ.pdf.
- 239. Richard Doty. Smell Identification Ability: Changes with Age. *Science* (1979) **226**, 1441–1442 (1984).
- 240. Doty, R. L. Olfactory dysfunction in neurodegenerative diseases: is there a common pathological substrate? *Lancet Neurol* **16**, 478–488 (2017).
- 241. Doty, R. L. Olfactory dysfunction in Parkinson disease. *Nat Rev Neurol* **8**, 329–339 (2012).
- 242. Zou, Y. M., Lu, D., Liu, L. P., Zhang, H. H. & Zhou, Y. Y. Olfactory dysfunction in Alzheimer's disease. *Neuropsychiatric Disease and Treatment* vol. 12 869–875 Preprint at https://doi.org/10.2147/NDT.S104886 (2016).
- 243. Devanand, D. P. Olfactory Identification Deficits, Cognitive Decline, and Dementia in Older Adults. *American Journal of Geriatric Psychiatry* **24**, 1151–1157 (2016).
- 244. Viguera, C., Wang, J., Mosmiller, E., Cerezo, A. & Maragakis, N. J. Olfactory dysfunction in amyotrophic lateral sclerosis. *Ann Clin Transl Neurol* **5**, 976–981 (2018).
- 245. Li, J., Wang, X., Zhu, C., Lin, Z. & Xiong, N. Affected olfaction in COVID-19: Re-defining "asymptomatic". *EClinicalMedicine* **29–30**, 100628 (2020).
- 246. Rebholz, H. *et al.* Loss of Olfactory Function—Early Indicator for Covid-19, Other Viral Infections and Neurodegenerative Disorders. *Frontiers in Neurology* vol. 11 Preprint at https://doi.org/10.3389/fneur.2020.569333 (2020).
- 247. Moein, S. T. *et al.* Smell dysfunction: a biomarker for COVID-19. *Int Forum Allergy Rhinol* **10**, (2020).
- 248. Ponsen, M. M. *et al.* Idiopathic hyposmia as a preclinical sign of Parkinson's disease. *Ann Neurol* **56**, 173–181 (2004).
- 249. Bohnen, N. I., Gedela, S., Herath, P., Constantine, G. M. & Moore, R. Y. Selective hyposmia in Parkinson disease: Association with hippocampal dopamine activity. *Neurosci Lett* **447**, 12–16 (2008).
- 250. Roberts, R. J., Sheehan, W., Thurber, S. & Roberts, M. A. Functional Neuro-Imaging and Post-Traumatic Olfactory Impairment. https://doi.org/10.4103/0253-7176.78504 32, 93–98 (2010).
- 251. Good, K. P. & Sullivan, R. L. Olfactory function in psychotic disorders: Insights from neuroimaging studies. *World J Psychiatry* **5**, 210 (2015).
- 252. COVID-19 pandemic triggers 25% increase in prevalence of anxiety and depression worldwide. *World Health Organization* (2022).
- 253. Su, B., Bleier, B., Wei, Y. & Wu, D. Clinical Implications of Psychophysical Olfactory Testing: Assessment, Diagnosis, and Treatment Outcome. *Front Neurosci* **15**, (2021).
- 254. Rumeau, C., Nguyen, D. T. & Jankowski, R. How to assess olfactory performance with the Sniffin' Sticks test®. *Eur Ann Otorhinolaryngol Head Neck Dis* **133**, 203–206 (2016).
- 255. Doty, R. L., Shaman, P. & Dann, M. Development of the university of pennsylvania smell identification test: A standardized microencapsulated test of olfactory function. *Physiol Behav* **32**, 489–502 (1984).
- 256. Nordin, S., Bramerson, A. & Liden, E. The Scandinavian Odor-Identification Test: Development, Reliability, Validity and Normative Data. *Acta Otolaryngol* **118**, 226–234 (1998).
- 257. Schubert, C. R. *et al.* Odor detection thresholds in a population of older adults. *Laryngoscope* **127**, 1257–1262 (2017).

- 258. Jiang, R.-S., Kuo, L.-T., Wu, S.-H., Su, M.-C. & Liang, K.-L. Validation of the Applicability of the Traditional Chinese Version of the University of Pennsylvania Smell Identification Test in Patients with Chronic Rhinosinusitis. *Allergy & Rhinology* **5**, ar.2014.5.0084 (2014).
- 259. Doty, R. L., Marcus, A. & William Lee, W. Development of the 12-Item Cross-Cultural Smell Identification Test(CC-SIT). *Laryngoscope* **106**, 353–356 (1996).
- 260. Oleszkiewicz, A., Schriever, V. A., Croy, I., Hähner, A. & Hummel, T. Updated Sniffin' Sticks normative data based on an extended sample of 9139 subjects. *European Archives of Oto-Rhino-Laryngology* **276**, 719–728 (2019).
- 261. Hummel, T., Sekinger, B., Wolf, S. R., Pauli, E. & Kobal, G. 'Sniffin' Sticks': Olfactory Performance Assessed by the Combined Testing of Odor Identification, Odor Discrimination and Olfactory Threshold. *Chem Senses* 22, 39–52 (1997).
- 262. Hsieh, J. W., Keller, A., Wong, M., Jiang, R. S. & Vosshall, L. B. SMELL-S and SMELL-R: Olfactory tests not influenced by odor-specific insensitivity or prior olfactory experience. *Proc Natl Acad Sci U S A* **114**, 11275–11284 (2017).
- 263. DRAVNIEKS, A. Correlation of Odor Intensities and Vapor Pressures with Structural Properties of Odorants. in 11–28 (1977). doi:10.1021/bk-1977-0051.ch002.
- 264. Croy, I., Nordin, S. & Hummel, T. Olfactory Disorders and Quality of Life—An Updated Review. *Chem Senses* **39**, 185–194 (2014).
- 265. Kowalewski, J. & Ray, A. Predicting Human Olfactory Perception from Activities of Odorant Receptors. *iScience* **23**, 101361 (2020).
- 266. Murphy, C. *et al.* Prevalence of Olfactory Impairment in Older Adults. *JAMA* **288**, 2307–2312 (2002).
- 267. Murphy, C., Nordin, S. & Acosta, L. Odor learning, recall, and recognition memory in young and elderly adults. *Neuropsychology* **11**, (1997).
- 268. Dhilla Albers, A. *et al.* Episodic memory of odors stratifies Alzheimer biomarkers in normal elderly. *Ann Neurol* **80**, 846–857 (2016).
- 269. Yang, A. I. *et al.* The what and when of olfactory working memory in humans. *Current Biology* **31**, 4499-4511.e8 (2021).
- 270. Parma, V. & Boesveldt, S. Measurement of Olfaction: Screening and Assessment. in *Sensory Science and Chronic Diseases: Clinical Implications and Disease Management* (eds. Joseph, P. V. & Duffy, V. B.) 45–63 (Springer International Publishing, Cham, 2021). doi:10.1007/978-3-030-86282-4\_3.
- 271. Bhowmik, R. *et al.* Uncertainty revealed by delayed responses during olfactory matching. (2018) doi:10.1101/2022.09.11.507462.
- 272. Shepherd, N. G., Mooi, E. A., Elbanna, S. & Rudd, J. M. Deciding Fast: Examining the Relationship between Strategic Decision Speed and Decision Quality across Multiple Environmental Contexts. *European Management Review* **18**, 119–140 (2021).
- 273. Shepherd, N., Mooi, E., Elbanna, S. & Lou, B. Fast and high-quality decision-making: The role of behavioral integration. *European Management Review* **20**, 679–697 (2023).
- 274. Gupta, A. *et al.* Neural Substrates of the Drift-Diffusion Model in Brain Disorders. *Front Comput Neurosci* **15**, (2022).
- 275. Ratcliff, R. & McKoon, G. The Diffusion Decision Model: Theory and Data for Two-Choice Decision Tasks. *Neural Comput* **20**, 873–922 (2008).

- 276. Mulder, M. J., Wagenmakers, E.-J., Ratcliff, R., Boekel, W. & Forstmann, B. U. Bias in the Brain: A Diffusion Model Analysis of Prior Probability and Potential Payoff. *The Journal of Neuroscience* **32**, 2335–2343 (2012).
- 277. Bogacz, R., Wagenmakers, E.-J., Forstmann, B. U. & Nieuwenhuis, S. The neural basis of the speed–accuracy tradeoff. *Trends Neurosci* **33**, 10–16 (2010).
- 278. Yellott, J. I. Correction for fast guessing and the speed-accuracy tradeoff in choice reaction time. *J Math Psychol* **8**, 159–199 (1971).
- 279. Ruthruff, E. A test of the deadline model for speed-accuracy tradeoffs. *Percept Psychophys* **58**, 56–64 (1996).
- 280. Palmer, J., Huk, A. C. & Shadlen, M. N. The effect of stimulus strength on the speed and accuracy of a perceptual decision. *J Vis* **5**, 1 (2005).
- 281. Ratcliff, R. & Rouder, J. N. Modeling Response Times for Two-Choice Decisions. *Psychol Sci* **9**, 347–356 (1998).
- 282. Doty, R. L. Olfactory dysfunction in neurodegenerative diseases: is there a common pathological substrate? *The Lancet Neurology* vol. 16 478–488 Preprint at https://doi.org/10.1016/S1474-4422(17)30123-0 (2017).
- 283. Murphy, C. Olfactory and other sensory impairments in Alzheimer disease. *Nature Reviews Neurology* vol. 15 11–24 Preprint at https://doi.org/10.1038/s41582-018-0097-5 (2019).
- 284. Marin, C. et al. Olfactory Dysfunction in Neurodegenerative Diseases. Current Allergy and Asthma Reports vol. 18 Preprint at https://doi.org/10.1007/s11882-018-0796-4 (2018).
- 285. Ross, G. W. *et al.* Association of olfactory dysfunction with risk for future Parkinson's disease. *Ann Neurol* **63**, 167–173 (2008).
- 286. Mahlknecht, P. et al. Olfactory dysfunction predicts early transition to a Lewy body disease in idiopathic RBD. *Neurology* **84**, 654–658 (2015).
- 287. Woodward, M. R. *et al.* Validation of olfactory deficit as a biomarker of Alzheimer disease. *Neurol Clin Pract* **6**, 1–10 (2016).
- 288. Bahar-Fuchs, A., Moss, S., Rowe, C. & Savage, G. Olfactory performance in AD, aMCI, and healthy ageing: A unirhinal approach. *Chem Senses* **35**, 855–862 (2010).
- 289. Murphy, C. *et al.* Olfactory Thresholds Are Associated With Degree of Dementia in Alzheimer's Disease. *Neurobiol Aging* **11**, 465–469 (1990).
- 290. Djordjevic, J., Jones-Gotman, M., De Sousa, K. & Chertkow, H. Olfaction in patients with mild cognitive impairment and Alzheimer's disease. *Neurobiol Aging* **29**, 693–706 (2008).
- 291. Gilbert, P. E., Joyce Barr, P. & Murphy, C. Differences in olfactory and visual memory in patients with pathologically confirmed Alzheimer's disease and the Lewy body variant of Alzheimer's disease. *Journal of the International Neuropsychological Society* **10**, 835–842 (2004).
- 292. Nordin, S., Paulsen, J. S. & Murphy, C. Sensory- and Memory-Mediated Olfactory Dysfunction in Huntington's Disease. Journal of the International Neuropsychological Society vol. 1 (1995).
- 293. Larsson, M., Lundin, A. & Wahlin, T. B. R. Olfactory functions in asymptomatic carriers of the Huntington disease mutation. *J Clin Exp Neuropsychol* **28**, 1373–1380 (2006).
- 294. WHO. Weekly Epidemiological Update Coronavirus disease (COVID-19); 7th April, 2025.

- 295. Wilder-Smith, A. COVID-19 in comparison with other emerging viral diseases: risk of geographic spread via travel. *Trop Dis Travel Med Vaccines* **7**, (2021).
- 296. Gold, M. S. *et al.* COVID-19 and comorbidities: a systematic review and meta-analysis. *Postgrad Med* **132**, (2020).
- 297. WHO Scientific Brief: Estimating mortality from COVID-19. (2020).
- 298. Fodoulian, L. *et al.* SARS-CoV-2 Receptors and Entry Genes Are Expressed in the Human Olfactory Neuroepithelium and Brain. *iScience* **23**, (2020).
- 299. Bilinska, K., Jakubowska, P., von Bartheld, C. S. & Butowt, R. Expression of the SARS-CoV-2 Entry Proteins, ACE2 and TMPRSS2, in Cells of the Olfactory Epithelium: Identification of Cell Types and Trends with Age. *ACS Chem Neurosci* 11, (2020).
- 300. Snitz, K. *et al.* A Novel Olfactory Self-Test Effectively Screens for COVID-19. *Medrxiv* (2021) doi:10.1101/2021.02.18.21251422.
- 301. Gerkin, R. C. *et al.* Recent smell loss is the best predictor of COVID-19 among individuals with recent respiratory symptoms. *Chem Senses* (2020) doi:10.1093/chemse/bjaa081/6048917.
- 302. Li, J., Wang, X., Zhu, C., Lin, Z. & Xiong, N. Affected olfaction in COVID-19: Re-defining "asymptomatic". *Eclinical Medicine* **29–30**, (2020).
- 303. Pierron, D. *et al.* Smell and taste changes are early indicators of the COVID-19 pandemic and political decision effectiveness. *Nat Commun* **11**, (2020).
- 304. Woo, M. S. *et al.* Frequent neurocognitive deficits after recovery from mild COVID-19. *Brain Commun* **2**, (2020).
- 305. Burdick, K. E. & Millett, C. E. The impact of COVID-19 on cognition in severe cases highlights the need for comprehensive neuropsychological evaluations in all survivors. *Neuropsychopharmacology* (2021) doi:10.1038/s41386-021-00995-7.
- 306. Jaywant, A. *et al.* Frequency and profile of objective cognitive deficits in hospitalized patients recovering from COVID-19. *Neuropsychopharmacology* (2021) doi:10.1038/s41386-021-00978-8.
- 307. Pardasani, M. & M. Abraham, N. Neurotropic SARS-CoV-2: Causalities and Realities. in *COVID-19 Pandemic, Mental Health and Neuroscience New Scenarios for Understanding and Treatment* (IntechOpen, 2023). doi:10.5772/intechopen.108573.
- 308. Hoffmann, M. *et al.* SARS-CoV-2 Cell Entry Depends on ACE2 and TMPRSS2 and Is Blocked by a Clinically Proven Protease Inhibitor. *Cell* (2020) doi:10.1016/j.cell.2020.02.052.
- 309. Meinhardt, J. *et al.* Olfactory transmucosal SARS-CoV-2 invasion as a port of central nervous system entry in individuals with COVID-19. *Nat Neurosci* (2020) doi:10.1038/s41593-020-00758-5.
- 310. Brann, D. H. et al. Non-Neuronal Expression of SARS-CoV-2 Entry Genes in the Olfactory System Suggests Mechanisms Underlying COVID-19-Associated Anosmia. Sci. Adv vol. 6 http://advances.sciencemag.org/ (2020).
- 311. Solomon, T. Neurological infection with SARS-CoV-2 the story so far. *Nat Rev Neurol* **17**, (2021).
- 312. Lee, S. *et al.* Clinical Course and Molecular Viral Shedding among Asymptomatic and Symptomatic Patients with SARS-CoV-2 Infection in a Community Treatment Center in the Republic of Korea. *JAMA Intern Med* **180**, 1447–1452 (2020).
- 313. Woo, M. S. *et al.* Frequent neurocognitive deficits after recovery from mild COVID-19. *Brain Commun* **2**, (2020).

- 314. Zhou, H. *et al.* The landscape of cognitive function in recovered COVID-19 patients. *J Psychiatr Res* (2020).
- 315. Baker, H. A., Safavynia, S. A. & Evered, L. A. The 'third wave': impending cognitive and functional decline in COVID-19 survivors. *Br J Anaesth* **126**, (2021).
- 316. Yahiaoui-Doktor, M. *et al.* Olfactory function is associated with cognitive performance: results from the population-based LIFE-Adult-Study. *Alzheimers Res Ther* **11**, (2019).
- 317. Stevenson, R. J., Attuquayefio, T., Mroczko-Wasowicz, A. & Hoover, K. C. Human olfactory consciousness and cognition: its unusual features may not result from unusual functions but from limited neocortical processing resources. (2013) doi:10.3389/fpsyg.2013.00819.
- 318. Chai, W. J., Abd Hamid, A. I. & Abdullah, J. M. Working memory from the psychological and neurosciences perspectives: A review. *Frontiers in Psychology* vol. 9 Preprint at https://doi.org/10.3389/fpsyg.2018.00401 (2018).
- 319. Moein, S. T., Hashemian, S. M., Tabarsi, P. & Doty, R. L. Prevalence and reversibility of smell dysfunction measured psychophysically in a cohort of COVID-19 patients. *Int Forum Allergy Rhinol* **10**, 1127–1135 (2020).
- 320. Oliveira-Pinto, A. V. *et al.* Sexual Dimorphism in the Human Olfactory Bulb: Females Have More Neurons and Glial Cells than Males. *PLoS One* **9**, e111733 (2014).
- 321. Ocon, A. J. Caught in the thickness of brain fog: exploring the cognitive symptoms of Chronic Fatigue Syndrome. *Front Physiol* **4**, (2013).
- 322. Theoharides, T. C., Cholevas, C., Polyzoidis, K. & Politis, A. Long-COVID syndrome-associated brain fog and chemofog: Luteolin to the rescue. *BioFactors* **47**, 232–241 (2021).
- 323. Le Bon, S.-D. *et al.* Psychophysical evaluation of chemosensory functions 5 weeks after olfactory loss due to COVID-19: a prospective cohort study on 72 patients. *European Archives of Oto-Rhino-Laryngology* **278**, 101–108 (2021).
- 324. Dias, M., Shaida, Z., Haloob, N. & Hopkins, C. Recovery rates and long-term olfactory dysfunction following COVID-19 infection. *World J Otorhinolaryngol Head Neck Surg* **10**, 121–128 (2024).
- 325. Taquet, M. *et al.* Cognitive and psychiatric symptom trajectories 2–3 years after hospital admission for COVID-19: a longitudinal, prospective cohort study in the UK. *Lancet Psychiatry* **11**, 696–708 (2024).
- 326. Duindam, H. B. *et al.* Systemic inflammation relates to neuroaxonal damage associated with long-term cognitive dysfunction in COVID-19 patients. *Brain Behav Immun* **117**, 510–520 (2024).
- 327. Hasanoglu, I. *et al.* Higher viral loads in asymptomatic COVID-19 patients might be the invisible part of the iceberg. *Infection* **49**, (2021).
- 328. Wu, Y. *et al.* Nervous system involvement after infection with COVID-19 and other coronaviruses. *Brain Behav Immun* **87**, (2020).
- 329. Baig, A. M., Khaleeq, A., Ali, U. & Syeda, H. Evidence of the COVID-19 Virus Targeting the CNS: Tissue Distribution, Host-Virus Interaction, and Proposed Neurotropic Mechanisms. *ACS Chemical Neuroscience* vol. 11 995–998 Preprint at https://doi.org/10.1021/acschemneuro.0c00122 (2020).
- 330. Chen, M. *et al.* Elevated ACE-2 expression in the olfactory neuroepithelium: implications for anosmia and upper respiratory SARS-CoV-2 entry and replication. *European Respiratory Journal* **56**, (2020).

- 331. Najt, P., Richards, H. L. & Fortune, D. G. Brain imaging in patients with COVID-19: A systematic review. *Brain Behav Immun Health* **16**, 100290 (2021).
- 332. Iravani, B., Arshamian, A., Ohla, K., Wilson, D. A. & Lundström, J. N. Non-invasive recording from the human olfactory bulb. *Nat Commun* **11**, (2020).
- 333. Bedran, D., Bedran, G. & Kote, S. A Comprehensive Review of Neurodegenerative Manifestations of SARS-CoV-2. *Vaccines (Basel)* **12**, 222 (2024).
- 334. Fatuzzo, I. *et al.* Neurons, Nose, and Neurodegenerative Diseases: Olfactory Function and Cognitive Impairment. *Int J Mol Sci* **24**, 2117 (2023).
- 335. Daniel, S. E. & Hawkes, C. H. Preliminary diagnosis of Parkinson's disease by olfactory bulb pathology. *The Lancet* **340**, 186–186 (1992).
- 336. Hoogland, P. V, Van Den Berg, R. & Huisman, E. Misrouted olfactory fibres and ectopic olfactory glomeruli in normal humans and in Parkinson and Alzheimer patients. *Neuropathol Appl Neurobiol* **29**, 303–311 (2003).
- 337. Pearce, R. K. B., Hawkes, C. H. & Daniel, S. E. *The Anterior Olfactory Nucleus in Parkinson's Disease. Movement Disorders* vol. 10 (1995).
- 338. Struble, R. G., BRENT CLARKt, H. & CLARK Olfactory, H. B. Olfactory Bulb Lesions in Alzheimer's Disease. *Neurobiol Aging* **13**, 469–473 (1992).
- 339. Highet, B., Dieriks, B. V., Murray, H. C., Faull, R. L. M. & Curtis, M. A. Huntingtin Aggregates in the Olfactory Bulb in Huntington's Disease. *Front Aging Neurosci* **12**, (2020).
- 340. Aqrabawi, A. J. & Kim, J. C. Olfactory memory representations are stored in the anterior olfactory nucleus. *Nat Commun* **11**, 1246 (2020).
- 341. Osamu Imamura *et al.* Nicotinic acetylcholine receptors mediate donepezil-induced oligodendrocyte differentiation. *J Neurochem* **135**, (2015).
- 342. Simpson, J., Yates, C. M., Gordon, A. & Clair, D. M. S. Olfactory tubercle choline acetyltransferase activity in Alzheimer-type dementia, Down's syndrome and Huntington's disease. *Journal of Neurology, Neurosurgery and Psychiatry* vol. 47 1138–1139 Preprint at https://doi.org/10.1136/jnnp.47.10.1138-a (1984).
- 343. Niu, H. *et al.* Alpha-synuclein overexpression in the olfactory bulb initiates prodromal symptoms and pathology of Parkinson's disease. *Transl Neurodegener* **7**, (2018).
- 344. Cersosimo, M. G. Propagation of alpha-synuclein pathology from the olfactory bulb: Possible role in the pathogenesis of dementia with lewy bodies. *Cell Tissue Res* **373**, 233–243 (2018).
- 345. Doty, R. L., Stern, M. B., Pfeiffer, C., Gollomp, S. M. & Hurtig, H. I. Bilateral olfactory dysfunction in early stage treated and untreated idiopathic Parkinson's disease. *J Neurol Neurosurg Psychiatry* **55**, 138–142 (1992).
- 346. Rissman, R. A., De Blas, A. L. & Armstrong, D. M. GABAA receptors in aging and Alzheimer's disease. *Journal of Neurochemistry* vol. 103 1285–1292 Preprint at https://doi.org/10.1111/j.1471-4159.2007.04832.x (2007).
- 347. Luchetti, S. *et al.* Neurosteroid biosynthetic pathways changes in prefrontal cortex in Alzheimer's disease. *Neurobiol Aging* 1964–1976 (2009) doi:10.1016/j.neurobiolaging.2009.12.014.
- 348. Moberly, A. H. *et al.* Olfactory inputs modulate respiration-related rhythmic activity in the prefrontal cortex and freezing behavior. *Nat Commun* **9**, (2018).
- 349. Lanoue, A. C., Dumitriu, A., Myers, R. H. & Soghomonian, J. J. Decreased glutamic acid decarboxylase mRNA expression in prefrontal cortex in Parkinson's disease. *Exp Neurol* **226**, 207–217 (2010).

- 350. Padmanabhan, K. *et al.* Centrifugal inputs to the main olfactory bulb revealed through whole brain circuit-mapping. *Front Neuroanat* **12**, (2019).
- 351. Merrick, C., Godwin, C. A., Geisler, M. W. & Morsella, E. The olfactory system as the gateway to the neural correlates of consciousness. *Frontiers in Psychology* vol. 4 Preprint at https://doi.org/10.3389/fpsyg.2013.01011 (2014).
- 352. Meinhardt, J. *et al.* Olfactory transmucosal SARS-CoV-2 invasion as a port of central nervous system entry in individuals with COVID-19. *Nat Neurosci* (2020) doi:10.1038/s41593-020-00758-5.
- 353. Kim, G. -u. *et al.* Clinical characteristics of asymptomatic and symptomatic patients with mild COVID-19. *Clinical Microbiology and Infection* **26**, (2020).
- 354. Pollock, A. M. & Lancaster, J. Asymptomatic transmission of covid-19. *BMJ* (2020) doi:10.1136/bmj.m4851.
- 355. Mazza, M. G. *et al.* Persistent psychopathology and neurocognitive impairment in COVID-19 survivors: Effect of inflammatory biomarkers at three-month follow-up. *Brain Behav Immun* **94**, (2021).
- 356. Hellmuth, J. *et al.* Persistent COVID-19-associated neurocognitive symptoms in non-hospitalized patients. *J Neurovirol* **27**, 191–195 (2021).
- 357. Bhowmik, R. *et al.* Persistent olfactory learning deficits during and post-COVID-19 infection. *Current Research in Neurobiology* **4**, 100081 (2023).
- 358. Miller, G. A., Baddeley, A., Shiffrin, R. M. & Nosofsky, R. M. *The Magical Number Seven, Plus or Minus Two: Some Limits on Our Capacity for Processing Information. Psychological Review* vol. 101 (1994).
- 359. Miller, G. A., Galanter, E. & Pribram, K. H. *Plans and the Structure of Behavior.* (Henry Holt and Co, New York, 1960). doi:10.1037/10039-000.
- 360. Axel, R. (Nobel Lecture)Scents and Sensibility: A Molecular Logic of Olfactory Perception. (2004).
- 361. Doop, M., Mohr, C., Folley, B., Brewer, W. & Park, S. Olfaction and Memory. in *Olfaction and the Brain* 65–82 (Cambridge University Press, 2006). doi:10.1017/CBO9780511543623.006.
- 362. Dade, L. A., Zatorre, R. J., Evans, A. C. & Jones-Gotman, M. Working memory in another dimension: Functional imaging of human olfactory working memory. *Neuroimage* **14**, 650–660 (2001).
- 363. Fuster, J. M. & Alexander, G. E. Neuron Activity Related to Short-Term Memory. *Science* (1979) **173**, 652–654 (1971).
- 364. Curtis, C. E. & D'Esposito, M. Persistent activity in the prefrontal cortex during working memory. *Trends in Cognitive Sciences* vol. 7 415–423 Preprint at https://doi.org/10.1016/S1364-6613(03)00197-9 (2003).
- 365. Wally, M. E., Nomoto, M., Abdou, K., Murayama, E. & Inokuchi, K. A short-term memory trace persists for days in the mouse hippocampus. *Commun Biol* **5**, (2022).
- 366. Patterson, M. A., Lagier, S. & Carleton, A. Odor representations in the olfactory bulb evolve after the first breath and persist as an odor afterimage. *Proceedings of the National Academy of Sciences* **110**, (2013).
- 367. Zelano, C., Montag, J., Khan, R. & Sobel, N. A Specialized Odor Memory Buffer in Primary Olfactory Cortex. *PLoS One* **4**, e4965 (2009).
- 368. Zhu, J. *et al.* Transient Delay-Period Activity of Agranular Insular Cortex Controls Working Memory Maintenance in Learning Novel Tasks. *Neuron* **105**, 934-946.e5 (2020).

- 369. Liu, D. *et al.* Medial prefrontal activity during delay period contributes to learning of a working memory task. *Science* (1979) **346**, (2014).
- 370. Wolff, M. & Halassa, M. M. The mediodorsal thalamus in executive control. *Neuron* **112**, 893–908 (2024).
- 371. Parnaudeau, S., Bolkan, S. S. & Kellendonk, C. The Mediodorsal Thalamus: An Essential Partner of the Prefrontal Cortex for Cognition. *Biol Psychiatry* **83**, 648–656 (2018).
- 372. Bolkan, S. S. *et al.* Thalamic projections sustain prefrontal activity during working memory maintenance. *Nat Neurosci* **20**, 987–996 (2017).
- 373. Daume, J. *et al.* Persistent activity during working memory maintenance predicts long-term memory formation in the human hippocampus. *Neuron* (2024) doi:10.1016/j.neuron.2024.09.013.
- 374. Huang, G.-D. *et al.* A novel paradigm for assessing olfactory working memory capacity in mice. *Transl Psychiatry* **10**, (2020).
- 375. Pignatelli, A. & Belluzzi, O. Neurogenesis in the Adult Olfactory Bulb. in *The neurobiology of olfaction* (ed. Menini, A.) 267–304 (CRC Press, 2010).
- 376. Lemasson, M., Saghatelyan, A., Olivo-Marin, J. C. & Lledo, P. M. Neonatal and adult neurogenesis provide two distinct populations of newborn neurons to the mouse olfactory bulb. *Journal of Neuroscience* **25**, 6816–6825 (2005).
- 377. Mouret, A. *et al.* Learning and survival of newly generated neurons: When time matters. *Journal of Neuroscience* **28**, 11511–11516 (2008).
- 378. Abraham, N. M. *et al.* Synaptic Inhibition in the Olfactory Bulb Accelerates Odor Discrimination in Mice. *Neuron* **65**, 399–411 (2010).
- 379. Marathe, S. D. & Abraham, N. M. Synaptic inhibition in the accessory olfactory bulb regulates pheromone location learning and memory. Preprint at https://doi.org/10.1101/2024.09.08.611942 (2024).
- 380. Zhang, X. *et al.* Active information maintenance in working memory by a sensory cortex. *Elife* **8**, (2019).
- 381. Herzog, N. *et al.* Balancing excitation and inhibition: The role of neural network dynamics in working memory gating. *Imaging Neuroscience* **2**, 1–20 (2024).
- 382. Isaac, J. T. R., Ashby, M. C. & McBain, C. J. The Role of the GluR2 Subunit in AMPA Receptor Function and Synaptic Plasticity. *Neuron* **54**, 859–871 (2007).
- 383. Kim, H., Kim, M., Im, S.-K. & Fang, S. Mouse Cre-LoxP system: general principles to determine tissue-specific roles of target genes. *Lab Anim Res* **34**, 147 (2018).
- 384. Paoletti, P., Bellone, C. & Zhou, Q. NMDA receptor subunit diversity: impact on receptor properties, synaptic plasticity and disease. *Nat Rev Neurosci* **14**, 383–400 (2013).
- 385. Cull-Candy, S., Brickley, S. & Farrant, M. NMDA receptor subunits: diversity, development and disease. *Curr Opin Neurobiol* **11**, 327–335 (2001).
- 386. Zhu, J. et al. Transient Delay-Period Activity of Agranular Insular Cortex Controls Working Memory Maintenance in Learning Novel Tasks. *Neuron* **105**, 934-946.e5 (2020).
- 387. Kesner, R. P., Hunsaker, M. R. & Ziegler, W. The role of the dorsal and ventral hippocampus in olfactory working memory. *Neurobiol Learn Mem* **96**, 361–366 (2011).
- 388. Reuschenbach, J., Reinert, J. K., Fu, X. & Fukunaga, I. Effects of Stimulus Timing on the Acquisition of an Olfactory Working Memory Task in Head-Fixed Mice. *The Journal of Neuroscience* **43**, 3120–3130 (2023).

- 389. Athalye, V. R., Carmena, J. M. & Costa, R. M. Neural reinforcement: re-entering and refining neural dynamics leading to desirable outcomes. *Curr Opin Neurobiol* **60**, 145–154 (2020).
- 390. Abraham, N. M., Guerin, D., Bhaukaurally, K. & Carleton, A. Similar Odor Discrimination Behavior in Head-Restrained and Freely Moving Mice. *PLoS One* **7**, (2012).
- 391. Wilson, D. A. & Sullivan, R. M. Cortical Processing of Odor Objects. *Neuron* **72**, 506–519 (2011).
- 392. Chapuis, J. & Wilson, D. A. Bidirectional plasticity of cortical pattern recognition and behavioral sensory acuity. *Nat Neurosci* **15**, 155–161 (2012).
- 393. Stettler, D. D. & Axel, R. Representations of Odor in the Piriform Cortex. *Neuron* **63**, 854–864 (2009).
- 394. Wilson, D. A. Pattern Separation and Completion in Olfaction. *Ann N Y Acad Sci* **1170**, 306–312 (2009).
- 395. Thayer, J. F. On the Importance of Inhibition: Central and Peripheral Manifestations of Nonlinear Inhibitory Processes in Neural Systems. *Dose-Response* **4**, (2006).
- 396. Barzon, G., Busiello, D. M. & Nicoletti, G. Excitation-Inhibition Balance Controls Information Encoding in Neural Populations. *Phys Rev Lett* **134**, 068403 (2025).
- 397. Kirischuk, S. Keeping Excitation–Inhibition Ratio in Balance. *Int J Mol Sci* **23**, 5746 (2022).

#### General Discussion

Perception and manipulation of sensory information are crucial for survival, foraging, and mating among species. Animals, including humans, have evolved highly specialized neurocognitive systems for such tasks. A crucial memory system, often characterized as working memory (WM), can hold small amounts of information for short periods while allowing manipulation based on context, environmental stimuli and past experiences. Though WM has been studied extensively starting in the latter half of the last century for various sensory modalities, WM in the context of olfaction has remained largely unexplored. Not only from a perspective of unexplored modality-specific WM function, the recent COVID-19 pandemic has highlighted the importance of olfaction in the context of public health, as sensory loss of sense of smell was one of the characteristic symptoms in a large fraction of the infected population. This pretext puts the study on a much wider backdrop that highlights both the timely and important nature of the work.

We employed a delayed matching task, namely the odor matching (OM), to asses working memory based performance in healthy and diseased condition. For healthy subjects, OM performance declined with odor complexity and faster decisions correlated with higher accuracy. Decline in accuracy with increase in complexity of odor has been shown in both humans and mouse model. Matching between complex odors is computationally more taxing as the first and second odor (for different odor pair matching) have overlapping glomerular representations. This overlap makes pattern separation relatively more challenging for the performing human subject. Now, our finding of faster response times linearly correlating with accuracy, may seem like an exception to the monolithic dogma in the field of the neuroscience of decision-making, but can be addressed as a time-limited case of drift diffusion. In drift diffusion models, higher noise necessitates longer exposure in order to accumulate more odor-specific information. But for scenarios where strict boundary conditions, like a fixed response window, is employed, the performing subject relying on longer decision-making times doesn't necessarily improve accuracy. Moreover, limited decision-making time may result in rushed decisions

as the time limit approaches, which in turn, increases the likelihood of errors. So, for a temporally constrained decision-making window, trials where the subjects try to optimize decision-making with reasonable swiftness tend to perform better.

As we optimized the odor matching paradigm in mice, we could show that bidirectional modulation of the E/I balance at the level of olfactory bulb (OB) affects WM performance. Inhibiting the projection neurons improved OWM learning while a decline in learning followed for the group with reduced inhibition on OB projection neurons. Improved learning in the GluA2 KO group would translate to increased inhibition on M/T cells<sup>6</sup> resulting lower mean excitatory stimulus reaching the piriform cortex. Now, piriform cortex has been shown to compensate for poor signal to noise ratio for familiar odors.<sup>7</sup> We should keep in mind that mice had been familiarized and trained over hundreds of trials. This allowed for even a reduced incoming signal to be compensated at the level of olfactory cortex via pattern completion. While for the NR1KO group, reduced inhibition on M/T cells<sup>6</sup> would likely result in a deteriorated signal to noise ratio, resulting in poorer matching performance. The circuit level dynamics that underplay odor matching at the level of OB and olfactory cortex needs to be further looked at before any stricter conclusion can be drawn.

Our translational effort to use OAM as a diagnostic tool in determining neurocognitive health in symptomatic and recovered COVID-19 subjects had shown great promise.8 We observed marked deficiency in odor matching and odor learning in symptomatic COVID-19 patients that persisted long after recovery. Recent studies have indicated role of hyperactive immune system and early neurodegeneration as plausible causes for such observation.9,1 Further research is necessary for a detailed understanding of the causal factors and develop therapeutic interventions.

#### References

1. Baddeley, A. D. & Hitch, G. Working Memory. in Psychology of Learning and Motivation (ed. Bower, G. H.) vol. 8 47–89 (Academic Press, 1974).

- 2. Rebholz, H. et al. Loss of Olfactory Function—Early Indicator for Covid-19, Other Viral Infections and Neurodegenerative Disorders. Frontiers in Neurology vol. 11 Preprint at https://doi.org/10.3389/fneur.2020.569333 (2020).
- 3. Bhowmik, R. et al. Uncertainty revealed by delayed responses during olfactory matching. bioRxiv 2022.09.11.507462 (2022) doi:10.1101/2022.09.11.507462.
- 4. Bhattacharjee, A. S., Konakamchi, S., Carleton, A., Kuner, T. & Abraham, N. M. Similarity and Strength of Glomerular Odor Representations Define a Neural Metric of Sniff-Invariant Discrimination Time In Brief. CellReports 28, 2966-2978.e5 (2019).
- 5. Myers, C. E., Interian, A. & Moustafa, A. A. A practical introduction to using the drift diffusion model of decision-making in cognitive psychology, neuroscience, and health sciences. Front Psychol 13, (2022).
- 6. Abraham, N. M. et al. Synaptic Inhibition in the Olfactory Bulb Accelerates Odor Discrimination in Mice. Neuron 65, 399–411 (2010).
- 7. Wilson, D. A. Pattern Separation and Completion in Olfaction. Ann N Y Acad Sci 1170, 306–312 (2009).
- 8. Bhowmik, R. et al. Persistent olfactory learning deficits during and post-COVID-19 infection. Current Research in Neurobiology 4, 100081 (2023).
- 9. Pandey, S., Bapat, V., Abraham, J. N. & Abraham, N. M. Long COVID: From olfactory dysfunctions to viral Parkinsonism. World J Otorhinolaryngol Head Neck Surg (2024) doi:10.1002/wjo2.175.
- 10. Duindam, H. B. et al. Systemic inflammation relates to neuroaxonal damage associated with long-term cognitive dysfunction in COVID-19 patients. Brain Behav Immun 117, 510–520 (2024).

#### List of Publications

- Rajdeep Bhowmik, Meenakshi Pardasani, Sarang Mahajan, Rahul Magar, Samir V. Joshi, Ganesh Ashish Nair, Anindya S. Bhattacharjee, Nixon M. Abraham\*\*, Persistent olfactory learning deficits during and post-COVID-19 infection, Current Research in Neurobiology, Volume 4, 100081 (2023)
- Rajdeep Bhowmik\*, Meenakshi Pardasani\*, Sarang Mahajan\*, Anindya S. Bhattacharjee, Sasank Konakamchi, Shambhavi Phadnis, Thasneem Mustafa, Eleanor McGowan, Priyadarshini Srikanth, Shruti D. Marathe and Nixon M. Abraham\*\*, Olfactory matching reveals optimized time for accurate decisions, http://dx.doi.org/10.1101/2022.09.11.507462 (Under review)
- 3. **Rajdeep Bhowmik**, Nixon M. Abraham, Bidirectional modulation of E/I balance in the olfactory bulb regulates olfactory working memory (Manuscript under preparation)
- 4. **Rajdeep Bhowmik**, Jancy Abraham, Nixon M. Abraham, Nanopolymers as Therapeutic Agents in Parkinson's Disease (Opinion Piece, Under Preparation)

<sup>\*</sup>Equal contribution

<sup>\*\*</sup>Corresponding author



## Current Research in Neurobiology

Open access

2.2

CiteScore

Submit your article 7

Guide for authors

Menu

Q

Search in this journal

## Open access information

Compare journals 7

#### Introduction

#### **Open Access Licences**

- User rights
- Creative Commons Attribution (CC BY)
- Creative Commons Attribution-NonCommercial (CC BY-NC)
- Creative Commons Attribution-NonCommercial-NoDerivs (CC BY-NC-ND)

#### **Article Publishing Charge (APC)**

#### **Policies**

- Research4Life
- Best price promise
- Open access agreements
- Funding arrangements
- Author rights
- Responsible sharing

#### **Author Resources and Support**

- Learn more about
- Contact details

#### Introduction

Current Research in Neurobiology is a peer reviewed, open access journal.

### **Open Access Licences**

#### **User rights**

All articles published gold open access will be immediately and permanently free for everyone to read and download, copy and distribute. We offer authors a choice of user licenses, which define the permitted reuse of articles. We currently offer the following license(s) for this journal:

### **Creative Commons Attribution (CC BY)**

Allows users to: distribute and copy the article; create extracts, abstracts, and other revised versions, adaptations or derivative works of or from an article (such as a translation); include in a collective work (such as an anthology); and text or data mine the article. These uses are permitted even for commercial purposes, provided the user: gives appropriate credit to the author(s) (with a link to the formal publication through the relevant DOI); includes a link to the license; indicates if changes were made; and does not represent the author(s) as endorsing the adaptation of the article or modify the article in such a way as to damage the authors' honor or reputation.

#### Creative Commons Attribution-NonCommercial (CC BY-NC)

Allows users to: distribute and copy the article; create extracts, abstracts, and other revised versions, adaptations or derivative works of or from an article (such as a translation); include in a collective work (such as an anthology); and text or data mine the article. These uses are permitted only for non-commercial purposes, and provided the user: gives appropriate credit to the author(s) (with a link to the formal publication through the relevant DOI); includes a link to the license; indicates if changes were made; and does not represent the author(s) as endorsing the adaptation of the article or modify the article in such a way as to damage the authors' honor or reputation.

## Creative Commons Attribution-NonCommercial-NoDerivs (CC BY-NC-ND)

Allows users to: distribute and copy the article; and include in a collective work (such as an anthology). These uses are permitted only for non-commercial purposes, and provided the user: gives appropriate credit to the author(s) (with a link to the formal publication through the relevant DOI); provides a link to the license; and does not alter or modify the article.

If you need to comply with your funding body policy you can apply for a CC BY license after your manuscript is accepted for publication.

## **Article Publishing Charge (APC)**

As an open access journal with no subscription charges, a fee (Article Publishing Charge, APC) is payable by